

Editor-in-Chief B.E.Paton

Editorial board:

Yu.S.Borisov V.F.Grabin
Yu.Ya.Gretskii A.Ya.Ishchenko
B.V.Khitrovskaya V.F.Khorunov
I.V.Krivtsun
S.I.Kuchuk-Yatsenko
Yu.N.Lankin V.K.Lebedev
V.N.Lipodaev L.M.Lobanov
V.I.Makhnenko A.A.Mazur
V.F.Moshkin O.K.Nazarenko
I.K.Pokhodnya I.A.Ryabtsev
Yu.A.Sterenbogen N.M.Voropai
K.A.Yushchenko
A.T.Zelnichenko

International editorial council:

N.P.Alyoshin (Russia)
B.Braithwaite (UK)
C.Boucher (France)
Guan Qiao (China)
U.Diltey (Germany)
P.Seyffarth (Germany)
A.S.Zubchenko (Russia)
T.Eagar (USA)
K.Inoue (Japan)
N.I.Nikiforov (Russia)
B.E.Paton (Ukraine)
Ya.Pilarczyk (Poland)
D. von Hofe (Germany)
Zhang Yanmin (China)
V.K.Sheleg (Belarus)

Promotion group:

V.N.Lipodaev, V.I.Lokteva
A.T.Zelnichenko (exec. director)

Translators:

I.N.Kutianova, V.N.Mironenko,
T.K.Vasilenko, N.V.Yalanskaya

Editor

N.A.Dmitrieva

Electron galley:

I.S.Batasheva, T.Yu.Snegiryova

Address:

E.O. Paton Electric Welding Institute,
International Association «Welding»,
11, Bozhenko str., 03680, Kyiv, Ukraine

Tel.: (38044) 287 67 57

Fax: (38044) 528 04 86

E-mail: journal@paton.kiev.ua

http://www.nas.gov.ua/pwj

State Registration Certificate

KV 4790 of 09.01.2001

Subscriptions:

\$324, 12 issues per year,
postage and packaging included.
Back issues available.

All rights reserved.

This publication and each of the articles
contained herein are protected by copyright.
Permission to reproduce material contained in
this journal must be obtained in writing from
the Publisher.

Copies of individual articles may be obtained
from the Publisher.

CONTENTS

WELDING DEPARTMENT OF PSTU IS 35

Razmyshlyayev A.D. and Shaferovskiy V.A. Personnel
training at the PSTU Welding Department 2

Royanov V.A. The Chair of Welding Equipment and
Technology is 60 years 4

Chigarev V.V., Belik A.G. and Sergienko Yu.V.
Design-experimental assessment of the features of electrode
melting and transfer process 7

Razmyshlyayev A.D., Deli A.A. and Mironova M.V.
Calculation of induction of controlling longitudinal magnetic
field with consideration for magnetic properties of core, wire
and workpiece as applied to arc surfacing 10

**Chigarev V.V., Shchetinina V.I., Shchetinin S.V. and Fedun
V.I.** Regularities of the impact of item shape on
electromagnetic field of welding current 14

**Royanov V.A., Matvienko V.N., Stepnov K.K., Semyonov
V.P., Zavarika N.G., Zakharova I.V. and Klimanchuk V.V.**
Flux-cored wire for electric-arc metallizing of the surface of
working rolls of the cold rolling mill tempering stand 19

Matvienko V.N. Flux-cored wire for strengthening the necks
and fillets of mill rolls 21

Malinov V.L. Sparsely alloyed consumables providing in the
deposited metal deformation hardening in operation 25

SCIENTIFIC AND TECHNICAL

**Yushchenko K.A., Zadery B.A., Kotenko S.S.,
Polishchuk E.P. and Karasevskaya O.P.** Structure of
welded joints in tungsten single crystals 29

**Zhadkevich M.L., Tyurin Yu.N., Kolisnichenko O.V. and
Mazin V.M.** Effect of parameters of plasma detonation unit
discharge circuit on gas-dynamic characteristics of pulsed
plasma flows 37

INDUSTRIAL

**Kuchuk-Yatsenko V.S., Lozovskaya A.V., Nakonechny A.A.
and Sakhatsky A.G.** Resistance welding of aluminum-steel
transition pieces using deformable composite interlayers 40

Zhudra A.P., Krivchikov S.Yu. and Petrov V.V. Effect of
silicon on properties of low-alloy carbon deposited metal 43

Sidoruk V.S. «Know-how» and how to use it 45
Developed at PWI 28, 36, 42, 50

The E.O. Paton Electric Welding Institute of the NAS of Ukraine and Editorial Board of «Avtomaticheskaya Svarka» journal cordially congratulate the staff and students on the occasion of 60th anniversary since the day of establishment of the Chair of Equipment and Technology of Welding Production (ETWP) and 35 anniversary of the Priazovsky State Technical University Welding Department.

Establishment of ETWP Chair in 1946 and organization of Welding Department at the end of 1971 were of great importance for training specialists in welding and related technologies for industrial enterprises of the South and South-East of Ukraine and first of all Donbass, as well as for quickly developing metallurgical and machine-building giants in Mariupol, Donetsk, Kramatorsk, Kharkov, Lugansk. Over the last 60 years more than 5500 specialists were trained at the Chair, many of them are in charge of the major constructions, enterprises, are at the head of a number of higher educational institutions. More than 110 graduates of the Chair and the Department became Candidates of Science, 10 are Doctors of Science and 11 Professors. Mariupol welding school obtained the recognition far beyond the bounds of Ukraine.

For all these years the ETWP Chair and Welding Department have collaborated with leading scientific and training centers of Ukraine, China, Poland, Hungary, Czechia, Germany, and take an active part in the work of International Association «Welding».

A selection of articles is published below, which enables the readers of the journal to get some idea on the directions and level of scientific research carried out at Priazovsky STU.

PERSONNEL TRAINING AT THE PSTU WELDING DEPARTMENT

A.D. RAZMYSHLYAEV and V.A. SHAFEROVSKY
Priazovsky State Technical University, Mariupol, Ukraine

The features of implementation of a multilevel system of education and training of specialists at Priazovsky STU and organizational structure of the Welding Department and Chair facilities are described. Application of module-rating system for assessment of student knowledge allows facilitating the transition to the credit-modular system of Bologna Convention.

Keywords: welding engineering, higher education, bachelors, specialists, masters

Welding Department of Priazovsky State Technical University (PSTU) is 35 years. Assistant Prof. D.P. Antonets (1971) was its first dean. Ass. Prof. A.D. Korneev (1974), Prof. L.K. Leshchinsky (1975), Prof. A.N. Serenko (1989), Ass. Prof. Yu.V. Belousov (1990), Prof. A.D. Razmyshlyayev (1999) headed it at different times. M.V. Vereskun, Cand. of Sci (Econ.), has been the dean of the Department since 2006. Outstanding scientists such as V.K. Bagryansky, A.I. Gedrovich, G.V. Kuzmin, V.N. Kalianov worked at the Department in different years, and at present the staff includes A.D. Chepurnoj, V.A. Royanov, V.V. Chigarev, V.Ya. Zusin, L.S.

Malinov, S.V. Gulakov, S.S. Samotugin, V.I. Shchetinina, and others.

Highly qualified lecturers are engaged in the training process, pedagogical and scientific research activity at the Department: academicians of the Academy of Sciences of Higher School of Ukraine, 3 academicians of the Academy of Engineering Sciences, 4 academicians of foreign Academies of Sciences, 11 Doctors, 12 Professors, 37 Assistant Professors, Candidates of Technical Sciences, more than 30 senior lecturers, lecturers and assistants.

At present the Department consists of five Chairs: Equipment and Technology of Welding Production (Prof. V.A. Royanov, Chair Person); Metallurgy and Technology of Welding Production (Prof. V.V. Chigarev); Materials Science (Prof. L.S. Malinov); Physics (V.I. Zhuk, Ass. Prof.); Descriptive Geometry and Engineering Graphics (I.A. Kovalevsky, Ass. Prof.).

Since 1998 the first three specialized Chairs have trained and graduated bachelors, specialists and masters of the following specialties: Welding Technology and Equipment; Welding Systems; Technology and Equipment for Restoration and Improvement of Wear Resistance of Mechanisms and Structures.

The programs that are basic for all Ukrainian institutes are taken as the basis of the concept of multilevel system of higher education. Some differences are allowed only in the subjects of the optional module, the structure and content of which are determined by corresponding graduating chair of the Welding Department. This stage of bachelors training in the above-mentioned specialties is completed by state examinations.

Realization of the program for masters training in welding specialties started in 1995 by special curricula. Since 1999 masters training has been performed at the Department on the basis of bachelor and specialist qualification. The main tasks that are solved when training masters are as follows: profound and special study of problems in the respective branch of science; narrow specialization in the corresponding field of knowledge; state training for scientific-pedagogical activity in the institute and so on.

Masters training is carried out at the Department on the basis of state budget after bachelor qualification has been obtained during one academic year (two terms). In case if the Bachelor continues his education and receives the qualification of a Specialist (Engineer), he also has the possibility to get the qualification and degree of Master during one academic year (two terms), but mainly on contract basis and by individual curricula. In both cases the applicants should have a favorable recommendation from the graduating chairs and department and university scientific boards for entering the Masters course. Masters training is completed by writing and defending the qualification work to a State Examining Board.

For realization of a multilevel system of higher education at PSTU since 2000 it is envisaged to enroll technical college graduates into the second and the third year of study and vice versa to perform back rotation of junior students to technical colleges at PSTU in case of poor progress. The curricula for all specialties of the Department for the first and the second terms, as well as PSTU technical college curricula were finally coordinated in 2000 with the aim of eliminating a number of subjects and facilitating the initial stage of training at the higher education institute for students, who join the university after graduation from the technical college.

The quality of personnel training under the conditions of a multilevel system of higher education is directly connected to solving the following tasks: raising the level of school leavers training; including technical college graduates into the membership of PSTU students and back rotation of students to technical colleges at PSTU; ensuring specialist training process compliance to European and international standards;

raising the scientific-pedagogical level of professor-lecturers staff; improving the training process by applying modern technical training aids, including computer systems; perfecting language training and improvement of economic education of graduates and so on.

Department chairs are fitted with modern equipment that is used not only for student training, but also for carrying out scientific research. A considerable part of scientific R&D has been applied in industry at a number of enterprises of our country and CIS. The main R&D directions are as follows: reconditioning of technological equipment by different methods of spraying; rolling mill roll hardfacing; electric arc surfacing and welding, applying controlled magnetic fields; mechanized submerged-arc welding of plate metal with programmed operating conditions; improvement of methods for increasing the welded joint and structure performance; evaluation of stressed state in welded joints and components with protective coatings; wear-resistant cladding of metallurgical equipment components; development of sparsely-alloyed high-strength and wear-resistant steels, cast irons, surfacing consumables and strengthening technologies on the basis of self-hardening principle at cooling and loading; investigation of physical phenomena on solid surfaces and processes of heat mass transfer on macro and micro levels; formation of powerful plasma flows and study of their interaction with condensed media.

Students of senior years and post-graduates take an active part in research performance. Department chairs have long-standing creative contacts with such leading educational institutions and scientific organizations of Ukraine as NTUU «Kiev Polytechnic Institute», the E.O. Paton Electric Welding Institute (Kiev), Institute of Welding (Gliwice, Poland), Miskolc University (Hungary), Harbin Institute of Technology (China) and with many related chairs of higher educational institutions of Ukraine, as well as CIS countries that help raising the level of specialist training at the Department. Such contacts permit organizing different production practice sessions, joint scientific and methodological conferences or seminars with subsequent publication of theses materials in different journals and collections of scientific works. More than 1100 scientific works, including more than 15 monographs and school books, are published by the results of faculty research, and more than 110 authors' certificates are granted.

A computer class of the Welding Department for 16 work places, equipped with modern computers, was set up in 1995. Thanks to Azovmash Company sponsorship, 2 more computer classes, equipped with modern computers for 8 work places in each class, were set up at the Welding Chairs in 2006.

Module-rating system for assessment of student knowledge, tried out at the Department and at the higher education institute in 1980s, is used for step-by-step evaluation of the knowledge and the level of subject learning. It was introduced into the training

process in all the courses of the Department and is rather effective. Its application in the training process facilitates the transition to the new credit-modular system in the context of Bologna Convention.

In 2006 the second round of All Ukrainian Competition on specialty «Technology and Equipment for Welding» was organized at the Chair of Equipment and Technology of Welding Production, in which student teams from ten Ukrainian higher education institutes took part.

Specialized Council for defending Candidate's theses has been functioning at PSTU since 1998, and

Council for defending theses for Doctor's degree of specialty «Welding and Related Technologies» since 2005.

The Department maintains business and creative relations with the graduates, who work in different industrial organizations, commercial bodies, enterprises and educational institutions that permits establishing the demand for specialists-graduates of PSTU Welding Department, allowing for the increasing demands to their training quality, as well as improving employment assistance for young specialists after graduating from the university.

THE CHAIR OF WELDING EQUIPMENT AND TECHNOLOGY IS 60 YEARS

V.A. ROYANOV

Priazovsky State Technical University, Mariupol, Ukraine

The work of the Welding Equipment and Technology Chair over a period of 60 years is analysed. Tasks of the Chair in training specialists in metal welding and cutting are considered.

Keywords: welding engineering, higher education, specialisation, scientific developments

The Welding Equipment and Technology Chair (WET) was founded in 1946 at the Zhdanov Metallurgical Institute (since 1993 — Priazovsky State Technical University (PSTU), Mariupol). The goal of the Chair was to train specialists in metal welding and cutting, as well as engineers to be involved in a new production of electric welded pipes for construction of main pipelines. At that time, the Ilych Metallurgical Works completed preparation of pipe welding workshop #1 for commissioning, which was founded at the initiative and with direct participation of Prof. E.O. Paton.

Engineer A.Ya. Shadrin was appointed an acting head of the Chair. That same year he was replaced by Associate Professor, Dr. P.S. Elistratov. From the very first days the Chair started the work on establishing the training-laboratory base, arranging and developing research in the field of welding of structures and repair of metallurgical equipment parts by surfacing. The first graduation diplomas in a new speciality were defended in 1947. The first five graduates (D.P. Antonets, A.A. Filchakov, K.I. Korotkov, Yu.N. Grishchenko, and D.A. Rogovin) became leading specialists and organisers of welding production, and two of them (D.P. Antonets and D.A. Rogovin) defended theses for a candidate of technical sciences degree.

In August 1952, K.V. Bagryansky was elected the head of the Chair. Restructuring of the education process, improvement of the laboratory base, widening and strengthening of contacts of the Chair with the

E.O. Paton Electric Welding Institute, N.E. Bauman Moscow State Technical University, Kiev Polytechnic Institute and many enterprises of the city and country began with his coming. A new building of welding was constructed with the assistance of Prof. B.E. Paton. This made it possible, as early as in the 1960s, to markedly improve training of specialists and helped the Chair to become one of the leading chairs in welding. Talented educators and scientists were working together with K.V. Bagryansky: associate professors Z.A. Dobrotina, D.S. Kassov and G.S. Kuzmin, and teachers P.F. Lavrik, A.A. Filchakov, V.A. Muratov and V.T. Sopin.

Based on ingenious education-methodical developments of its specialists, in 1968 the Chair initiated training of welding engineers in a new speciality — «Metallurgy and Processes of Welding Engineering». A Department was arranged in 1971, which included general-engineering and general-education chairs, in addition to the two welding chairs. The first dean of the Welding Department was Associate Professor, Dr. D.P. Antonets, who had been working for many years as a chief welder of the «Azovmash» Plant.

In the 1960s, the Chair headed by K.V. Bagryansky considerably activated its research efforts aimed at development of welding and surfacing using ceramic fluxes, and investigation of properties of welded and surfaced parts. During that period, submerged arc welding of nickel using ceramic flux came into wide use at the «Bolshevik» Plant in Kiev (the work was headed by Associate Professor, Dr. G.S. Kuzmin). The method of submerged arc welding and surfacing of copper alloys using ceramic fluxes, which found wide application at metallurgical factories of Ukraine, was developed under the leadership of D.S. Kassov.



Team of the Welding Equipment and Technology Chair of the Priazovsky State Technical University

K.V. Bagryansky with an active participation of V. Ya. Zusin and A.D. Korneev developed the method for submerged arc welding of aluminium using flux, which was widely applied for welding elements of current-conducting bus lines at the Bratsk Hydroelectric Power Station. Submerged arc surfacing using ceramic flux gained wide acceptance for repair of rolls and machine parts at the Metallurgical Plant in Rustavi (Georgia), Ilych Metallurgical Works and «Azovstal» in Mariupol, Enakievo Metallurgical Works, and Ust-Kamenogorsk Ore Mining and Processing Enterprise (Kazakhstan). Associate Professor A.A. Filchakov was at the head of research, development and application of new grades of electrodes at «Azovmash». Associate Professor, Dr. K.A. Olejnikhenko developed a procedure for quantitative evaluation of harmful emissions during welding. In addition, they suggested recommendations for improvement of working conditions of welders.

30 theses for a candidate of technical sciences degree and 1 theses for a doctor's degree were defended, manual «Theory of Welding Processes» (K.V. Bagryansky, Z.A. Dobrotina, K.K. Khrenov) was prepared and re-published three times, textbook «Calculation and Design of Welded Structures» (A.N. Serenko, M.N. Krumbolt, K.V. Bagryansky), monographs «Welding of Nickel and Its Alloys» (K.V. Bagryansky, G.S. Kuzmin) and «Ceramic Fluxes for Welding and Surfacing» (K.V. Bargyansky) were published during a period of 1955–1980.

The Branch Research Laboratory (BRL) on surfacing was established at the Chair in 1971. The goal of the laboratory was to study and develop new designs of rolls and rollers for continuous steel casting machines, surfacing technologies and surfacing consumables, as well as related automated equipment. At present the Laboratory is headed by Associate Professor, Dr. V.N. Matvienko.

The Chair and BRL made a great contribution to investigation of sensitivity of welds to hot cracking.

The work was performed under the leadership of K.V. Bagryansky, Ya.Ya. Grigoriev and V.E. Saenko. As a result, a new test procedure was suggested, and a number of author's certificates were granted. Also, much consideration was given to investigation of properties of deposited metal at normal and high temperatures (V.N. Kalianov, B.I. Nosovsky).

From 1973 till 1979 the Chair was headed by Prof. A.N. Serenko. During that period the Chair was involved in studies of static and dynamic strength of welded joints and structures, and started the work on investigation of one-pass welding of steels with thickness of 40 mm or more by programming the welding process. Results of the investigations were summarised in V.A. Shaferovsky's and A.Skzypcik's (Poland) theses for a candidate of technical sciences degree, and found practical application at «Azovmash» and shipyard «Zaliv».

L.K. Leshchinsky became the head of the Chair in 1980. Together with BRL, the Chair developed new ceramic fluxes and flux-cored wires for electric arc surfacing of rolls and metallurgical equipment parts, and studied the processes of submerged arc surfacing and welding using strip electrodes. Results of these efforts were applied at machine-building and metal-



Students of Welding Department in Fusion Welding Laboratory

lurgical enterprises, and were summarised in candidate's theses of Yu.V. Belousov, V.I. Shchetinina, V.N. Matvienko, V.P. Lavrik and A.V. Zarechensky. The Chair was active in upgrading of automatic surfacing equipment and control of quality of deposited metal. Results of this work were presented in a doctor's thesis of S.V. Gulakov. Wide acceptance was received by investigations in the field of plasma hardening of parts, including after surfacing. This subject is covered in monograph «Plasma Surface Hardening» (L.K. Leshchinsky, S.S. Samotugin, I.I. Pirch, V.I. Komar).

Since 1985 the Chair has been headed by Prof. V.A. Royanov. He participated in widening and strengthening of the resource base, in including disciplines on robotisation of welding production into the education process, as well as application of computers and new information technologies (for preparation of term papers and graduation diplomas). At present the Chair is involved in investigations in the field of thermal spraying of corrosion- and wear-resistant coatings. Flux-cored wires were developed for electric arc metallising, which found application at the Kiev Association «Kievtraktordetal», vehicle repair enterprises of Poltava, Tashkent and other cities. The investigation results were summarised in the E.V. Vojtsekhovskiy's thesis for a candidate of technical sciences degree and V.A. Royanov's theses for a doctor's degree. Now the Chair is active in including elements of the Bologna education process into its education procedure, implementation of the credit-modular education system, development and publication of training aids for students, and improvement of curricula.

During a period of 1998–2001 the doctor's thesis were defended by S.V. Gulakov, V.A. Royanov, L.K. Leshchinsky, A.D. Razmyshlyayev, S.S. Samotugin, and A.N. Serenko, who were granted the academic status of professors. The courses for doctor's degrees were opened, where two persons are working for a doctor's degree. A specialised council on defence of candidate's and doctor's degrees in speciality «Welding and Related Technology» is functioning at the Chair.

The following manuals were prepared and published during the last three years «Welding. Introduction into Speciality» (A.N. Serenko, V.A. Royanov), «Formation of Defects in Welding and Related Processes» (V.A. Royanov, V.Ya. Zusin, S.S. Samotugin),

«Welding and Surfacing of Aluminium and Its Alloys» (V.Ya. Zusin, V.A. Serenko), «Repair of Machines Using Welding and Related Technologies» (V.A. Royanov, G.G. Psaras, V.K. Rubajlo), as well as books: «Magnetic Control of Arc Weld Formation» (A.D. Razmyshlyayev), «Natural Theory of Fine Scale Energy of Quantum Space» (Yu.V. Belousov).

Within the framework of multi-stage training of specialists, the Chair actively co-operates with industrial and machine-building secondary schools of Mariupol.

During a period of 60 years the team of the Chair trained about 5000 engineers, including for the European, Asian, African and Latin American countries, more than 40 candidates of technical sciences and 8 doctors of technical sciences. It published more than 30 manuals and monographs, and 650 scientific papers. Over 250 developments were covered by author's certificates and foreign patents.

The Chair graduates A.D. Chepurnoj, T.G. Kravtsov, V.Ya. Zusin, V.I. Shchetinina and V.N. Kallianov successfully defended their doctor's theses. Many graduates became noted specialists in the field of welding engineering, and now they are at the head of industrial enterprises of Ukraine, Russia and other CIS countries.

At present the staff of the Chair comprises 3 professors, doctors of technical sciences, 10 associate professors, candidates of technical sciences, 1 senior teacher, and 1 assistant. The Chair has been accredited and granted level IV by the Commission of the Ministry of Education and Sciences of Ukraine. The Chair trains specialists in «Welding Equipment and Technology» and «Welding Units».

Specialists of the Chair participate in the work of the International Association «Welding». Along with traditional co-operation with welding chairs of colleges of Moscow, St.-Petersburg, Chelyabinsk, Ekaterinburg, Tbilisi, Minsk, Mogilev and other CIS cities, the Chair established contacts with colleges and institutions of the so-called far-foreign countries, such as the Institute of Welding in Gliwice (Poland), Miskolc University (Hungary), Harbin Institute of Technology (China), etc.

The Chair meets its sixtieth anniversary with willingness to further upgrade the education-methodical process and improve the quality of training of specialists.

DESIGN-EXPERIMENTAL ASSESSMENT OF THE FEATURES OF ELECTRODE MELTING AND TRANSFER PROCESS

V.V. CHIGAREV, A.G. BELIK and Yu.V. SERGIENKO
Priazovsky State Technical University, Mariupol, Ukraine

An estimate is given of the degree of interaction of molten metal of the sheath and core of flux-cored surfacing strip. Factors and energy characteristics are considered, which influence the nature of its melting.

Keywords: arc surfacing, flux-cored strip, core, sheath, drop, complex master alloys, uniformity

In surfacing with flux-cored strips, a separate melting of the strip sheath and core occurs, which may lead to chemical inhomogeneity of the deposited metal layer, and later on may affect its performance and welding-technological properties. Level of homogeneity of the deposited metal is ensured, depending on the proportion of interaction of molten metal of the sheath and core.

It does not seem possible to conduct theoretical calculations or direct measurement of the reacting mass of the core at the drop stage, because of a lack of knowledge of all the factors, influencing the process of flux-cored strip melting, and mechanisms of transformations at the electrode tip. Several works [1–4] describe the features of metal alloying in surfacing or welding with different electrode materials, and propose analytical dependencies for quantitative assessment of component interaction at different stages of electrode material melting. In view of the considerable influence of geometrical parameters of the flux-cored strip, relative weight of its core and its composition, as well as occurrence of thermoderformational phenomena and separate melting of the sheath and core, the most acceptable is the design-experimental method of determination of mass transfer in flux-cored strip melting. This problem can be solved at determination of energy characteristics of flux-cored strip melting, and application of available and characteristic procedures of obtaining the required experimental data.

The procedure of calculation of the process of flux-cored strip melting is based on N.N. Rykalin equation [5]:

$$q_e = vF_e\gamma(S_d - S_1), \quad (1)$$

where q_e is the thermal energy contributed by the arc to the electrode in a unit of time; v is the electrode melting rate; F_e is the electrode cross-sectional area; γ is the electrode metal density; S_d is the heat content of electrode metal drop or specific energy consumption for electrode melting; S_1 is the heat content of electrode metal at heating by passing current.

For the case of flux-cored electrodes, analytical dependence (1) was corrected allowing for the following assumptions:

- values of thermal energy q_{melt} evolved by the arc on the electrode, and specific power consumption S_{sh} for sheath melting remain constant, independent on the weight and composition of the flux-cored electrode core;
- their change results in just redistribution of the heat between the sheath and core, which leads to a change of the electrode melting rate;
- energy evolved in the electrode is spent only for melting of the core and sheath, and we ignore the losses for evaporation;
- part of the core interacting with the sheath metal in melting of the flux-cored electrode, is presented as a certain effective layer, which is equal to fraction ϵ of its overall thickness.

Allowing for the taken assumptions, the equation of the process of flux-cored strip melting can be presented as follows:

$$q_{\text{melt}} = v\delta\dot{\Gamma}\gamma S_{\text{sh}} + v\epsilon hbaS_c \text{ [J/s]}, \quad (2)$$

where δ is the sheath thickness; Π is the sheath perimeter; h , b are the thickness and width of the core, respectively; a is the bulk weight of the core components; S_c is the heat content or specific power consumption for core melting.

In equation (2) the left-hand part expresses the amount of the heat contributed by the arc into the flux-cored strip, and the right-hand part is the total heat consumption for melting of the sheath and the core.

Let us present the instant efficiency of the process of sheath melting in the form of the dependence

$$g_{\text{sh}} = v\delta\dot{\Gamma}\gamma. \quad (3)$$

Efficiency of the core melting is equal to

$$g_c = v\epsilon hba. \quad (4)$$

Considering that the relative mass of the flux-cored strip core is defined as

$$K_f = g_c / g_{\text{sh}}, \quad (5)$$

we will transform equation (2), allowing for (3)–(5), as follows:

$$g_{\text{melt}} = g_{\text{sh}}S_{\text{sh}} + \varepsilon g_{\text{c}}K_{\text{f}}S_{\text{c}}. \quad (6)$$

Having analyzed equation (6), it should be noted that at $K_{\text{f}} = 0$ (in case of absence of the core), the dependence characterizes melting of the flux-cored strip (1)

$$g_{\text{e}} = g_{\text{sh}}S_{\text{sh}}. \quad (7)$$

Allowing for the taken assumptions $g_{\text{melt}} = g_{\text{e}}$, and substituting the calculation results of (6) in (7), we get the following relationship:

$$g_{\text{sh}}S_{\text{sh}} = g_{\text{sh}}S_{\text{sh}} + \varepsilon g_{\text{c}}K_{\text{f}}S_{\text{c}}. \quad (8)$$

Energy conditions on the electrode at its melting can be the most completely expressed through the coefficient of melting, which is determined using the known equations. Allowing for the transition from q_{sh} , q_{melt} , q_{c} , K_{f} values through the coefficients of melting of the sheath and flux-cored strip, $\alpha_{\text{m}}^{\text{sh}}$ and α_{m} , respectively, i.e. $g_{\text{sh}} = \alpha_{\text{m}}^{\text{sh}}I$, expression (8) after transformation becomes

$$\alpha_{\text{m}}^{\text{sh}} = \alpha_{\text{m}} \left(1 + \varepsilon K_{\text{f}} \frac{S_{\text{c}}}{S_{\text{sh}}} \right) \quad (9)$$

Value ε is taken as the quantitative criterion, which is used to evaluate the fraction of the flux-cored strip core, melted together with the metal sheath at the drop stage. Process of flux-cored strip melting, characterizing the complete transition of its sheath and core through the drop stage, meets condition $\varepsilon = 1$.

Solving equation (9) for ε , we get

$$\varepsilon = \frac{(\alpha_{\text{m}}^{\text{sh}}/\alpha_{\text{m}} - 1)S_{\text{sh}}}{K_{\text{f}}S_{\text{c}}}. \quad (10)$$

Equation (10) correlates in the general form the main parameters of the flux-cored strip and degree of transition of its components through the drop stage at melting. From (10) it follows that at the known power consumption for melting of sheath S_{sh} , the main parameters determining the fraction of interaction ε with the flux-cored strip, core and sheath at melting of the latter, are the refractoriness S_{c} of the core and its relative weight K_{f} , which is found from the following relationship

$$K_{\text{f}} = K_{\text{fil}} / (1 - K_{\text{fil}}). \quad (11)$$

Value $\alpha_{\text{m}}^{\text{sh}}/\alpha_{\text{m}} - 1$ is determined experimentally. It characterizes the ratio of energies consumed in melting of the core and sheath of the flux-cored strip at the drop stage as follows:

$$\mu = \frac{\alpha_{\text{m}}^{\text{sh}}}{\alpha_{\text{m}}}, \quad (12)$$

where μ is the coefficient of energy distribution at the drop stage in melting of the flux-cored strip.

Substituting the results of calculations of equations (11) and (12) into (10), and considering the degree of interaction of the core and sheath at the drop stage in melting of the flux-cored strip, let us find

$$\varepsilon = \frac{\mu S_{\text{sh}}(1 - K_{\text{fil}})}{K_{\text{fil}}S_{\text{c}}}. \quad (13)$$

At analysis of equation (13) it should be noted that lowering of the values of the coefficients of filling K_{fil} of the flux-cored strip, power consumption for core melting and distribution of energy μ promotes an increase of the degree of interaction of the sheath and core metal at their melting.

To obtain ε values, it is necessary to determine μ , S_{sh} , S_{c} and K_{fil} . Coefficient of energy distribution μ at melting of flux-cored strip is obtained by calculation-experimental method through the parameters of flux-cored strip melting. For this purpose the values of the coefficient of melting α_{m} of flux-cored strip (in the presence of the core) and $\alpha_{\text{m}}^{\text{sh}}$ of the sheath (in the absence of the core) are found, i.e. coefficient of filling $K_{\text{fil}} = 0$. In the calculations the value of specific power consumption for sheath melting S_{sh} is taken to be constant and independent on the parameters of flux-cored electrode and surfacing modes. Proceeding from the results of numerous studies for a sheath of flux-cored electrode from low-carbon steel $S_{\text{sh}} = 2095 \text{ J/g}$ [5–9].

Specific power consumption S_{c} for melting of the components of the flux-cored strip can be determined by calculation-experimental method from equation (13) at $\varepsilon = 1$ or its other obtained values:

$$S_{\text{c}} = \frac{\mu S_{\text{sh}}(1 - K_{\text{fil}})}{K_{\text{fil}}}. \quad (14)$$

To determine the influence of S_{c} value on ε experiments were conducted, in which the applied flux-cored electrode strips had an alloying charge consisting of a mechanical mixture of components and complex alloy, and, therefore, had different specific energy content. Coefficient of filling of flux-cored strips was from 0.30 to 0.53. The above flux-cored strips were used to perform surfacing to determine α_{m} , $\alpha_{\text{m}}^{\text{sh}}$, and the «no-pool method» was used to select electrode metal drops by a procedure described in [7, 10].

Fraction of interaction ε in surfacing with a flux-cored strip was determined from the conditions of energy balance, equations (10) and (13) and ratio of nickel content in the electrode metal drop Ni^{d} to its content in the core Ni^{c} . Nickel content in the drops was determined by chemical analysis.

We will perform calculation from the condition of material balance using equation

$$\varepsilon = \frac{\text{Ni}^{\text{d}}(1 - K_{\text{fil}})}{(\text{Ni}^{\text{c}} - \text{Ni}^{\text{d}})K_{\text{fil}}}. \quad (15)$$

Experimental and calculation data are given in Table 1. As shown by investigation results, calcula-

Table 1. Calculation-experimental data on characteristics of flux-cored strip melting

Core composition	K_{fil}	α_m , g/(Å·h)	μ	S_c , J/g	Ni ^c , %	Ni ^d , %	ϵ	
							Acc. to (13)	Acc. to (15)
Complex alloy	0.30	16.5	0.37	1851.98	6.2	1.82	0.94	1.00
	0.36	15.2	0.48	1822.65	6.2	2.22	0.90	0.90
	0.40	14.1	0.58	1772.37	6.2	2.52	0.90	0.93
	0.48	12.2	0.85	--	6.2	2.90	0.95	0.92
	0.57	11.3	0.93	--	6.2	2.98	0.78	0.78
	0.58	11.2	0.96	--	6.2	2.99	0.70	0.65
	0.57	11.0	1.06	--	6.2	2.97	0.78	0.72
Mechanical mixture of components	0.29	15.9	0.42	2241.65	6.0	1.24	0.90	0.95
	0.34	14.7	0.55	2208.13	6.0	1.85	0.93	0.87
	0.40	13.2	0.71	2220.70	6.0	2.30	0.91	0.95
	0.45	14.2	0.82	2157.85	6.0	2.52	0.89	0.85
	0.50	11.6	0.95	--	6.0	2.70	0.83	0.79
	0.53	10.9	1.08	--	6.0	2.60	0.84	0.79
	0.55	10.7	1.00	--	6.0	2.60	0.70	0.65

Note. $\alpha_m^{sh} = 22.6$ g/(Å·h).

tion-experimental method of ϵ determination ensures a good agreement with the experimental data on the core composition. Note that the refractoriness of the flux-cored strip core has an essential influence on the completion of the alloying process at the drop stage. For flux-cored strips using a core from a mechanical mixture of the components $\epsilon = 0.65$ is ensured at the coefficient of filling $K_{fil} = 0.58$ and $S_c = 2191.37$ J/g, and in flux-cored strips with a core from a complex alloy $\epsilon = 0.78$ at $K_{fil} = 0.57$ and $S_c = 1814.27$ J/g.

It should be noted that ϵ is influenced by the filling coefficient. With increase of its value, the quantity of components going through the drop stage decreases, which is in agreement with the results of work [2].

Investigations have been conducted on determination of the influence of sheath thickness δ on the

Table 2. Dependence of the fraction of interaction ϵ of the metal of the core and sheath on sheath thickness δ and its filling coefficient K_{fil} in flux-cored strip melting

δ , mm	K_{fil}	μ	S_c , J/g	ϵ
0.2	0.52	0.58	1822.65	0.57
	0.55	0.53	1969.30	0.50
	0.62	0.54	1998.63	0.38
0.4	0.50	0.97	2053.10	1.00
	0.56	1.03	1780.75	0.85
	0.61	0.95	1801.70	0.66

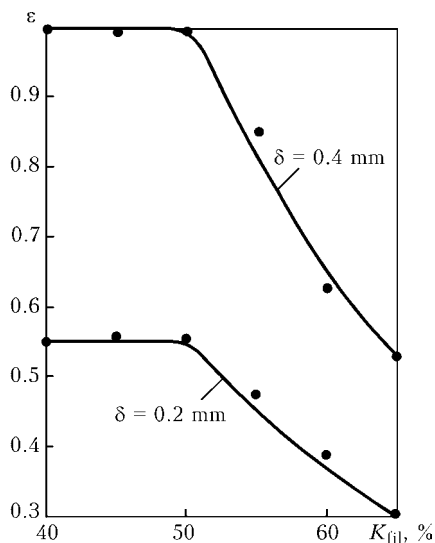


Figure 1. Influence of sheath thickness δ on the fraction of its interaction ϵ with the core at flux-cored strip melting

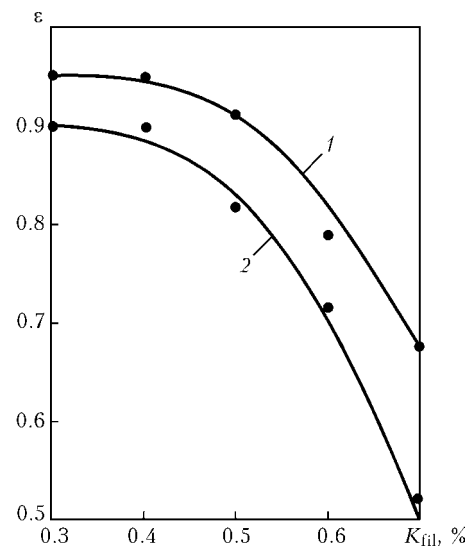


Figure 2. Influence of the coefficient of filling K_{fil} of the core from a complex alloy (1) and mechanical mixture of components (2) on the fraction of interaction ϵ with the sheath in melting of flux-cored strip

fraction of interaction ε of flux-cored strip core at the drop stage. For this purpose, flux-cored strips with a sheath from low-carbon steel of different thicknesses were made, and a complex alloy, containing chromium, carbon, silicon, nickel, manganese with addition of 1 % (from the total weight of the core) of aluminium-magnesium powder was used as the core. Power content of the core was $S_c = 1722.09 \text{ J/g}$. The above composition of the flux-cored strip was achieved due to the presence of sormite-1 alloy in the deposited layer. As the core material has constant thermal power characteristics, this allows evaluation of the influence of the sheath thickness and relative weight of the core on ε . Deposition was performed on plates of St3 in a constant mode. Calculation of ε values was performed by equation (13). Calculation results are given in Table 2 and in Figures 1 and 2.

From the above data it follows that the maximum fraction of interaction of the core and the sheath in flux-cored strip melting is provided in the case of using a core from a complex alloy.

Thus, the design-experimental method can be used to evaluate the fraction of interaction of the core and the sheath at the drop stage in flux-cored strip melting.

1. Zarechensky, A.V., Kolechko, A.A., Muratov, V.A. (1980) Increase of efficiency of flux-cored strip electrode melting. *Avtomatch. Svarka*, **7**, 72–73.
2. Patskevich, I.R., Khejsets, L.A. (1970) Specifics of metal alloying in flux-cored strip surfacing. *Ibid.*, **2**, 13–15.
3. Erokhin, A.A., Kotov, G.N. (1968) Main electrode parameters determining the degree of chemical macroheterogeneity of deposited metal in alloying through a coating. *Fizika i Khimiya Obrab. Materialov*, **1**, 54–60.
4. Kotov, G.N., Erokhin, A.A. (1968) Effect of thickness of coating and metal additives in it on electrode melting rate. *Avtomatch. Svarka*, **8**, 16–17.
5. Rykalin, N.N. (1951) *Calculations of thermal processes in welding*. Moscow: Mashgiz.
6. Erokhin, A.A. (1973) *Principles of fusion welding*. Moscow: Mashinostroenie.
7. Erokhin, A.A. (1964) *Kinematics of metallurgical processes in arc welding*. Moscow: Mashinostroenie.
8. Bezbakh, D.K., Benua, F.F. (1971) Heat content and grain composition of electrode metal drops in some welding methods. *Svaroch. Proizvodstvo*, **10**, 12–14.
9. Pokhodnya, I.K., Suptel, A.M. (1967) Heat content of electrode metal drops in shielded-gas arc welding. *Avtomatch. Svarka*, **2**, 13–18.
10. Erokhin, A.A. (1949) Procedure for determination of the main controls of electrode fusion in electric arc welding. *Avtogen. Delo*, **10**, 1–11.

CALCULATION OF INDUCTION OF CONTROLLING LONGITUDINAL MAGNETIC FIELD WITH CONSIDERATION FOR MAGNETIC PROPERTIES OF CORE, WIRE AND WORKPIECE AS APPLIED TO ARC SURFACING

A.D. RAZMYSHLYAEV, A.A. DELI and M.V. MIRONOVA

Priazovsky State Technical University, Mariupol, Ukraine

Design and experimental procedures have been used to determine the influence of magnetic properties of the electrode wire, solenoid core and workpiece in arc surfacing in a longitudinal magnetic field on the nature of distribution and magnitude of magnetic field induction in the region between the electrode tip and workpiece, as well as inside the workpiece and electrode wire. These data allow outlining the methods to improve the efficiency of a longitudinal magnetic field application in arc surfacing.

Keywords: arc surfacing, longitudinal magnetic field, solenoid with core, ferromagnetics, magnetic properties, calculation of magnetic field, longitudinal component of magnetic induction

Use of the controlling longitudinal magnetic field (CLMF) in submerged arc surfacing allows reduction of participation share of the base metal in the deposited one, raise of process productivity, improving formation of deposited bead [1, 2]. However complexity of physical processes in the welding arc and liquid metal of the welding pool, occurring under the effect of CLMF, and their inadequate investigation, retard practical employment of this method of surfacing. Besides, now there is no reliable device of inputting the

magnetic fields as applied to industrial conditions of surfacing the workpieces.

In surfacing under the effect of CLMF, the workpiece and the electrode wire in most cases are ferromagnets, as is the solenoid core. The design of the latter and its size should be such that in the welding arc zone the longitudinal induction component is maximal.

The system of ferromagnetic bodies (solenoid core, welding wire and the workpiece (a plate)) in the presence of non-ferromagnetic (air) gap between the tip of the welding wire and the workpiece, causes complex distribution pattern of the magnetic field in space. The longitudinal induction component B_z in said gap is determined not only by the geometric dimensions of the ferromagnetic bodies and their relative

positioning, but also by their magnetic properties (magnetic permeability μ). It is known that μ essentially depends on the chemical composition of the alloys on the basis of iron, microstructure, grain size and is in nonlinear dependence on the field intensity H .

In determining the values of induction in the gap between the tip of the electrode and the workpiece (a flat plate), either by calculation or by experiment [2, 3], magnetization of these bodies, governed by the magnetizing force of the solenoid winding (level of H) and by μ value of the material, also by the dependence of μ on H , is usually not taken into account.

The objective of this work was the establishment of the distribution pattern of the magnetic field induction in ferromagnetic areas of the magnetic circuit, from the winding with current up to the workpiece subject for surfacing, in order to achieve maximal values of longitudinal components of induction B_z of the magnetic field in the welding arc zone (gap between the tip of the electrode and the workpiece).

Values of induction B_z were obtained by way of calculations by the technique of [3] which essence consists in the following. The equation of distribution of magnetic vector potential in stationary plane-meridian magnetic fields after inputting of the flux function $\psi = r\dot{A}$, was used as the initial one:

$$\frac{\partial}{\partial r} \left(\frac{v_a}{r} \frac{\partial \psi}{\partial r} \right) + \frac{\partial}{\partial z} \left(\frac{v_a}{r} \frac{\partial \psi}{\partial z} \right) = -J, \quad (1)$$

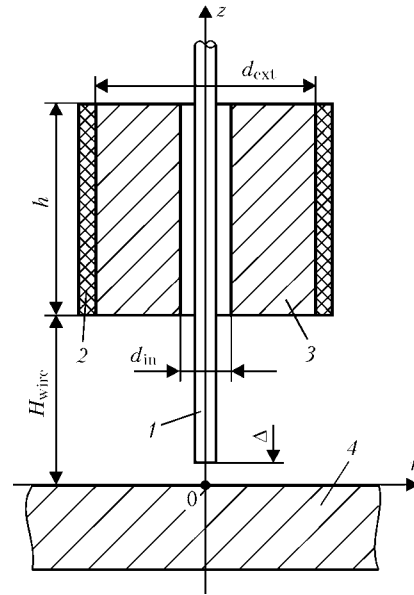


Figure 1. Schematic of arrangement of system of bodies for studying distribution of magnetic field induction: 1 — electrode wire; 2 — winding; 3 — solenoid core; 4 — workpiece (plate)

where J is the current density in a point with coordinates (r, z) ; v_a is the inverse value of absolute magnetic permeability of the medium.

Calculation of components of magnetic induction using the flux function ψ is carried out by the formula

$$B_r = -\frac{1}{r} \frac{\partial \psi}{\partial z}; \quad (2)$$

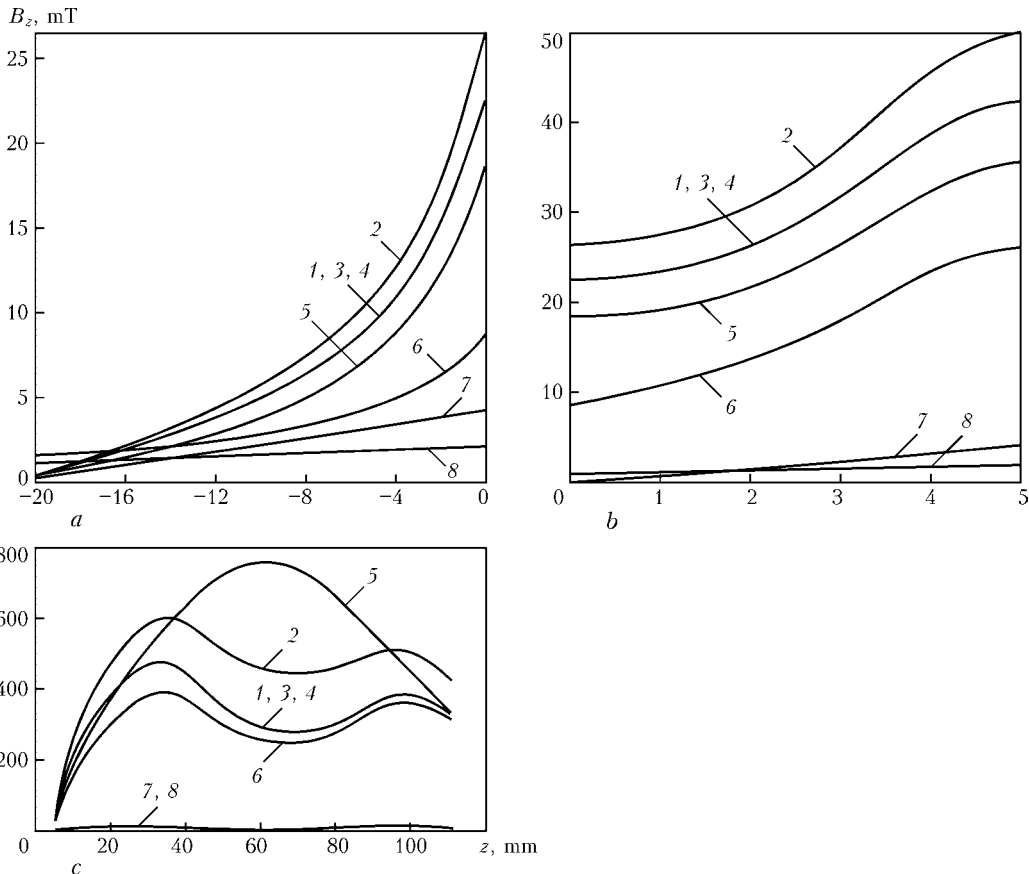


Figure 2. Distribution of longitudinal component of induction B_z along axis Oz in plate (a), gap between plate and electrode tip (b) and electrode wire (c): 1–8 — magnetic permeability of system elements (see the Table)

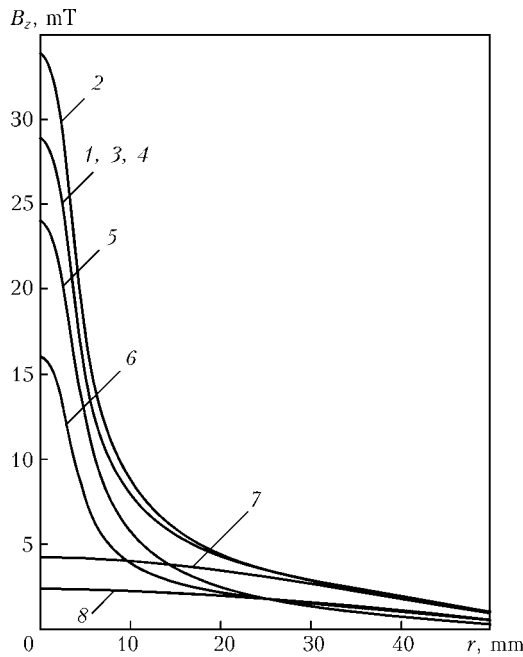


Figure 3. Radial distribution of induction components B_z at $z = 2.5$ mm (1–8 see in the Table)

$$B_z = \frac{1}{r} \frac{\partial \psi}{\partial r}; \tag{3}$$

$$|B| = \sqrt{B_r^2 + B_z^2}. \tag{4}$$

On the borders of the estimated area considered as a cylinder, the following boundary conditions are set:

on the top and bottom borders

$$\frac{\partial A}{\partial z} = \frac{\partial \psi}{\partial z} = 0; \tag{5}$$

on the external border (maximal values of r)

$$\left. \frac{\partial \psi}{\partial n} \right|_S = 0; \tag{6}$$

(surface S is assumed being parallel to the system axis);

on the system axis

$$\psi = 0. \tag{7}$$

Equation (1) was solved by finite difference method. Solution of the difference equation was carried out applying the iterations method of [4].

Figure 1 shows schematic of the system of bodies standing on the way of the magnetic flux created by the direct current running in the winding (welding wire having 5 mm diameter; plate 20 mm thick; gap between the electrode tip and the plate $\Delta = 5$ mm). In calculations the following dimensions of the solenoid were assumed: internal diameter of the ferromagnetic core $d_{in} = 12$ mm; external $d_{ext} = 50$ mm; height of the core $h = 50$ mm; electrode wire extension $H_{wire} = 40$ mm.

For estimation of the influence of the magnetic permeability μ on the magnitude and pattern of distribution of the longitudinal component of induction

Values of magnetic permeability μ assumed in the calculations

Curve No.	μ values for		
	core	plate	welding wire
1	250	250	250
2	250	250	500
3	500	250	250
4	250	500	250
5	1	250	250
6	250	1	250
7	250	250	1
8	250	1	1

of the magnetic field B_z , in the specified areas of the system of bodies, μ magnitudes were set stepwise ($\mu = 1; 250; 500$). Magnetizing force of the solenoid coil IW was restricted to 400 Ampere-turns. Such restrictions ($\mu = 500$ and IW = 400 Ampere-turns) are necessary, so that in said ferromagnetic bodies saturation did not occur. The Table shows values of the magnetic permeability μ , assumed in calculations.

Distribution pattern of induction B_z along the system axis (at $r = 0$) in the plate (Figure 2, a), the air gap between the electrode tip and the plate (Figure 2, b) and in the welding wire (Figure 2, c), does not change on the borders of these bodies, which corresponds with theoretical postulations. In the area of the welding wire located in the middle of its length (inside the ferromagnetic core), the level of induction B_z is maximal and depends on the level of the values of magnetic permeability μ assumed in calculations for all components of the magnetic system: the workpiece (plate), the welding wire (electrode) and the ferromagnetic core.

If the welding wire is a ferromagnet, so the value of B_z essentially depends on the values μ assumed in calculations for the wire (Figure 2, c, curves 1, 2, 7). Thus the value of μ assumed in calculations for the ferromagnetic core ($\mu = 1; 250; 500$), does not influence the level of induction B_z in this area of the wire (at constant value $\mu = 250$) (Figure 2, c, curves 1, 3). For the non-magnetic wire ($\mu = 1$), the level of values B_z in it is close to zero (curves 7, 8). Comparison of curves 1 and 5 shows that at the absence of the ferromagnetic core the welding wire of $\mu = 250$ is magnetized on this area more than at its presence. Presence or absence of the ferromagnetic plate (workpiece) practically has not affected the process of magnetization of the wire on this area (Figure 2, c, curves 4, 6). From here follows that presence of the ferromagnetic wire inside of the solenoid and value of its magnetic permeability are a major factor defining the value of the induction in the gap between the tip of the welding wire and the workpiece (in welding arc zone). The data shown in Figure 2, b, as well as distribution B_z along radius r near the surface of the workpiece, testify to this (Figure 3). From here follows that in calculating the induction B_z in the weld-

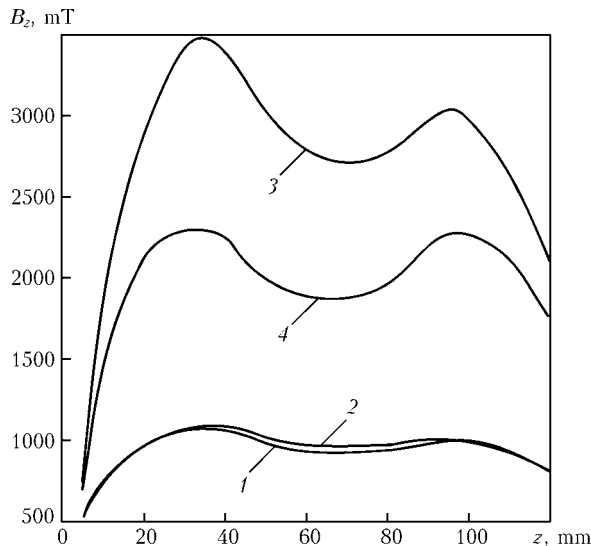


Figure 4. Distribution of longitudinal component of induction B_z in wire along axis Oz : 1, 2 — IW = 400; 3, 4 — 2000 Ampere-turns; 1, 3 — at constant values $\mu = 500$ for ferromagnetic components of system; 2, 4 — with consideration for dependence $\mu = f(H)$ for specified components of system

ing arc zone, it is necessary to take into account real values of magnetic permeability for the welding wire, which testifies also to the necessity of obtaining real data on dependences $B = f(H)$ and $\mu = f(H)$ for welding wires, which are presently unavailable.

It is pertinent to note that the above results were obtained at magnetizing force of the solenoid core of 400 Ampere-turns, however, to obtaining the level of B_z in the welding arc zone, necessary for controlling the geometric dimensions of the bead in arc surfacing, the magnetizing force should be of the order of 2000 Ampere-turns [2]. Thus saturation of ferromagnets of the considered system of bodies (first of all welding wire) is possible.

With consideration for dependences $B = f(H)$ and $\mu = f(H)$, assumed according to data of [5], calculation for low-carbon steel with carbon content of 0.1 %, was made. Results of calculation (Figure 4) have shown that at small magnetizing force of the solenoid (400 Ampere-turns), the account of the dependences $B = f(H)$ and $\mu = f(H)$ for the welding wire material, has not led to the change of the induction along the wire (Figure 4, curves 1, 2). For significant magnetizing force of the solenoid (2000 Ampere-turns), with account of the real data on dependences $B = f(H)$ and $\mu = f(H)$, calculated values of B_z in the wire are much lower than by the use in calculations of constant value $\mu = 500$ (Figure 4, curves 3, 4).

It is worth noting that the radial component of the magnetic field induction B_r , as evidenced by the calculations, for sections $z = 35, 60$ and 90 mm, are two orders less than the longitudinal component B_z . Only on the end of the electrode ($z \approx 10$ mm) at the distance $r = 0.1$ – 2.5 mm, value of B_r is comparable with B_z (reaches half of the values of induction component B_z).

Data on the distribution B_z along the radius near the surface of the ferromagnetic plate (Figure 5, curves

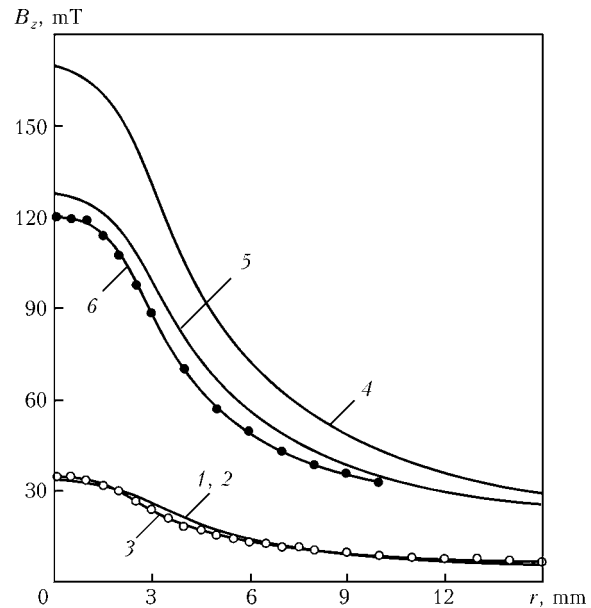


Figure 5. Radial distribution of component of induction B_r at $z = 2.5$ mm: 1–3 — IW = 400; 4–6 — 2000 Ampere-turns; 1, 4 — calculated data at constant values $\mu = 500$ for ferromagnetic components of system; 2, 5 — with consideration for dependence $\mu = f(H)$ for specified components of system; 3, 6 — experimental data

1, 3) show that at magnetizing force of the solenoid of 400 Ampere-turns, calculated data closely match experimental, both at constant value $\mu = 500$, and by the account in calculations of dependence $B = f(H)$ for the wire material. At magnetizing force of the solenoid of 2000 Ampere-turns, in connection with saturation of the ferromagnetic material, of which the welding wire is made, coincidence of calculated data with experimental is reached in the event if in calculations account is taken of the dependence $B = f(H)$ for the wire material (Figure 5, curves 4–6).

CONCLUSIONS

1. In arc surfacing in CLMF, the basic influence on the value and pattern of distribution of the longitudinal component of the induction of field near the surface of the ferromagnetic workpiece, comes from ferromagnetic properties of the electrode wire.

2. At significant magnetizing force of the solenoid, calculated values of the longitudinal component of the induction of CLMF near the surface of the ferromagnetic workpieces (plate) adequately matches the experimental data, if in calculations is taken into account of dependence $B = f(H)$ of the electrode wire material.

1. Chernysh, V.P., Kuznetsov, V.D., Briskman, A.N. et al. (1983) *Electromagnetic stir welding*. Kiev: Tekhnika.
2. Razmyshlyayev, A.D. (2000) *Magnetic control of weld formation in arc welding*. Mariupol: PGTU.
3. Lazarenko, M.A., Razmyshlyayev, A.D., Chichkarev, E.A. (1999) Computer-aided calculations of controlling magnetic fields for welding and surfacing processes. *Vestnik PGTU*, Issue 8, 147–150.
4. Demirchyan, K.S., Chechurin, V.L. (1986) *Machine computations of electromagnetic fields*. Moscow: Vysshaya Shkola.
5. Preobrazhensky, A.A., Bishard, E.G. (1986) *Magnetic materials and elements*. Moscow: Vysshaya Shkola.

REGULARITIES OF THE IMPACT OF ITEM SHAPE ON ELECTROMAGNETIC FIELD OF WELDING CURRENT

V.V. CHIGAREV, V.I. SHCHETININA, S.V. SHCHETININ and V.I. FEDUN
Priazovsky State Technical University, Mariupol, Ukraine

Equations have been derived for calculation of the electromagnetic field induction in welding of plates and pipes. Calculation and experimental procedures have been used to establish the influence of the part shape on the electromagnetic field of welding current, and a method has been developed to prevent magnetic blow in pipe welding.

Keywords: arc welding, pipe, plate, electromagnetic field, induction, electromagnetic force, electromagnetic pressure, magnetic blow, two-sided current supply

In one-sided high-speed arc welding the quality of weld formation is determined by process stability, which becomes lower at magnetic blow. Closed contour of the pipes intensifies the magnetic blow, which results in disturbance of the welding process and deterioration of weld formation quality. In order to avoid it, the magnetic blow should be reduced.

A great contribution to investigation and use of electromagnetic field and magnetohydrodynamic phenomena in pipe welding was made by B.E. Paton, V.K. Lebedev, and S.L. Mandelberg [1–3].

Electromagnetic field arising at current flowing through the conductor was studied by R.M. White [4], D. Mattis [5], W. Gilbert [6], and J. Maxwell [7]. Electromagnetic field is used for containment of hot plasma, in charged particle accelerators, in the regular and quantum electronics, power generation, solid physics, chemistry, biology, etc. [4]. Of special interest is investigation and use of electromagnetic fields in welding.

Electromagnetic field of the welding circuit is created by current flowing through the electrode, arc and item being welded. Electromagnetic field of current flowing through the electrode and the arc, creates a pinch-effect, which induces powerful plasma flows and welding arc pressure [8–10], ensuring the specified depth of penetration. Electromagnetic field of current, flowing through the item, is the transverse field and it induces the Ampere force, which makes the plasma deviate towards the field with a lower intensity, and it also induces magnetic blow. It should be noted that the electromagnetic field in welding is insufficiently well-studied [1–3, 11].

The purpose of the conducted research is studying the impact of the item shape on the electromagnetic field of welding current and development of a method of magnetic blow prevention in one-sided high-speed welding of pipes.

Measurement of the electromagnetic field of welding current in the near-arc space is made difficult by the presence of high temperature here: when moving closer to the arc and weld pool to a distance less than

$16 \cdot 10^{-3}$ m, the quartz-insulated probe of magnetic induction measuring unit Sh1-7 burns down. In this connection, it is rational to study the distribution of the electromagnetic field of welding current in the near-arc space by calculation.

At calculation of induction B of the electromagnetic field of current in an infinitely long small-section rectilinear conductor [12, 13] the influence of the conductor shape on the electromagnetic field is ignored. In welding the current runs through larger section conductors, the shape of which influences the induction of the welding current electromagnetic field and nature of its distribution. As the panels of boilers and pipes are widely used welded structures, equations were derived to determine the induction of the electromagnetic field of current flowing exactly in the plates and pipe.

Calculation of the electromagnetic field of current flowing through an item is performed on the basis of Biot-Savart–Laplace law and principle of superposition of magnetic fields [12–14]. To determine the electromagnetic field in the gap between the plates (without allowing for the edge effects), let us divide them into infinitely long thin conductors of $dx dy$ section.

Induction B of the electromagnetic field generated by an element of an infinitely long current conductor, flowing through an area with coordinates x , y of $dx dy$ section, in point (x_0, y_0) (Figure 1) is equal to

$$dB = \mu \mu_0 \frac{I dx dy}{2\pi \sqrt{[(x - x_0)^2 + (y - y_0)^2] 4\delta b}} [T],$$

where μ is the relative magnetic permeability of the ferromagnetic; μ_0 is the magnetic constant equal to $4 \cdot 10^{-7}$ H/m; I is the current flowing along two plates (or along a pipe), A; δ is half of the plate thickness, m; b is the plate width, m.

Induction of the electromagnetic field

$$dB = \sqrt{dB_x^2 + dB_y^2} [T],$$

where $dB_x = dB \frac{y - y_0}{r}$ is the transverse component;

$dB_y = dB \frac{x - x_0}{r}$ is the longitudinal component; r is

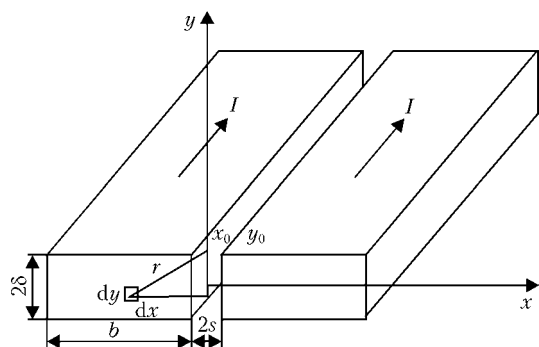


Figure 1. Schematic of induction calculation at current flowing through the plates

the distance from the measurement point to current element, m.

Induction of the transverse electromagnetic field

$$dB_x = \mu\mu_0 \frac{I(y - y_0)dx dy}{8\pi\delta b(x - x_0)^2 + (y_0 - y)^2} \text{ [T]}. \quad (1)$$

Induction of the longitudinal electromagnetic field

$$dB_y = \mu\mu_0 \frac{I(x - x_0)dx dy}{8\pi\delta b(x - x_0)^2 + (y_0 - y)^2} \text{ [T]}. \quad (2)$$

Induction of the transverse and longitudinal electromagnetic fields in point (x_0, y_0) is determined by integration of equations (1) and (2), respectively:

$$B_x = \mu\mu_0 \frac{I}{8\pi\delta b} \times \int_{-\delta}^{\delta} \left(\int_{-\delta-s}^{-s} \frac{(y - y_0)dy}{(y_0 - y)^2 + (x - x_0)^2} + \int_s^{s+b} \frac{(y - y_0)dy}{(y_0 - y)^2 + (x - x_0)^2} \right) dx \text{ [T]};$$

$$B_y = \mu\mu_0 \frac{I}{8\pi\delta b} \times \int_{-\delta}^{\delta} \left(\int_{-\delta-s}^{-s} \frac{(x - x_0)dy}{(x - x_0)^2 + (y_0 - y)^2} + \int_s^{s+b} \frac{(x - x_0)dx}{(x - x_0)^2 + (y_0 - y)^2} \right) dy \text{ [T]}.$$

Induction was calculated in the personal computer. Its calculated values agree well with the experimental ones obtained at simulation of the welding process (Figure 2) and measurement of magnetic induction in gap s of the butt across its entire thickness and at a distance from the item by teslameter F 4355, which uses the Hall effect. To achieve the model adequacy to the actual conditions, induction measurements were performed when passing 2100 A current through the item, as in the case of welding by a composite electrode. VMG-5000 welding rectifier was used as the power source.

As a result of calculation of dependence $B_x(y)$ at $x = 0$ and conducted studies, it was established that in the case of current flowing through the plates, the electromagnetic induction is zero in the plate mid-thickness, it rises closer to the surface, and reaches its maximum value on the very surface of the plate (Figure 3). Farther away from the surface, the electromagnetic field induction first decreases abruptly as a result of the low magnetic permeability of the air,

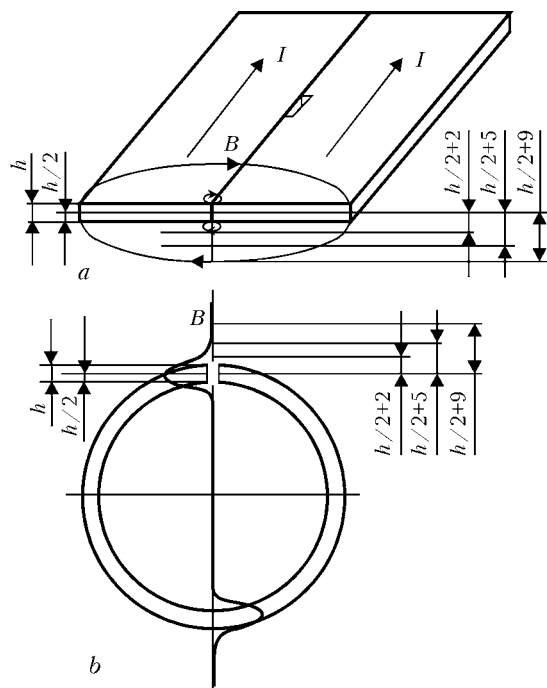


Figure 2. Simulation of the welding process at current flowing through the plates (a) and pipe (b)

and then changes only slightly. In keeping with the direction of the force lines of the electromagnetic field at transition from the middle to the lower part of the plate surface, the direction of induction changes to the opposite one.

Induction distribution in the gap between the plates is the result of a uniform distribution of current across the item section. According to the superposition principle, the magnetic field induced by several currents, is equal to the sum of the fields, induced by each current separately. According to Biot-Savart's law,

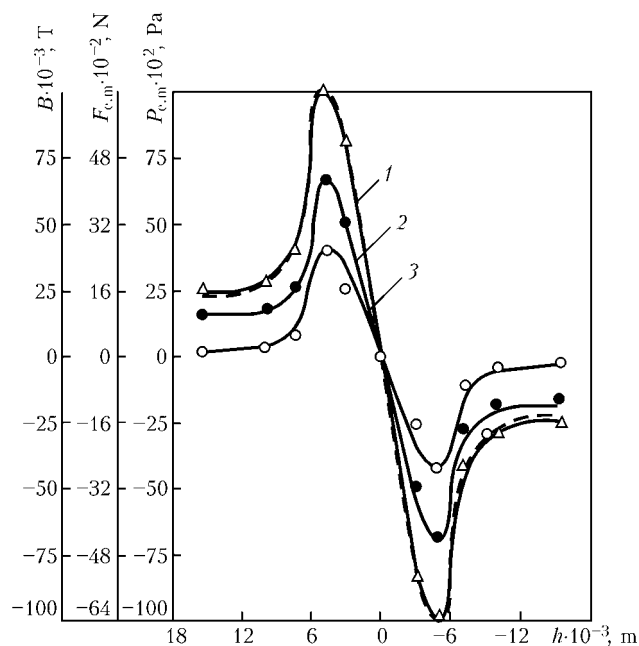


Figure 3. Distribution of electromagnetic field at flowing of current $I = 2100$ A along a plate of size $10 \times 40 \times 300$ mm and 2 mm gap in the butt: 1 — electromagnetic field induction B ; 2 — electromagnetic force $F_{e,m}$; 3 — electromagnetic pressure $P_{e,m}$; dash curve — calculated values of induction; h — measurement point

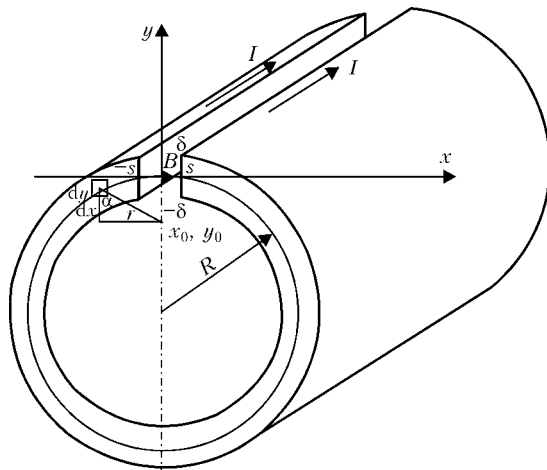


Figure 4. Schematic of induction calculation at current flowing along the pipe (for designations see the text)

the magnetic field induced by direct current of an infinite conductor is directly proportional to current and inversely proportional to the distance from the conductor with current.

In the plate mid-thickness the currents flowing along its upper and lower surfaces induce electromagnetic fields of equal magnitude but opposite direction, which are mutually annihilated. Therefore, the induction here is zero.

In case of approaching the plate surface, the distance from its other surface increases, which results in weakening of the compensating action of currents, and rising of the values of electromagnetic field induction. Presence of maximum induction on the plate surface shows that the welded joint strength is determined by the maximum electromagnetic forces of interatomic interaction.

Good agreement of the design and experimental data obtained at simulation of the welding process, confirms the validity of the equations for determination of the induction of the electromagnetic field of current flowing through the plates.

It is known that at current flowing through the pipe without a gap, the electromagnetic field inside it is zero [14]. Pipes are welded with a gap in the butt which influences the electromagnetic field of welding current. Calculation formulas for determination of the regularities of induction distribution in the gap of the pipe butt are based on the following assumptions.

As in welding of thick-walled pipes their thickness 2δ is greater than the gap in the butt $2s$ (Figure 4), it may be assumed that there is no distortion of force lines of the electromagnetic field. Therefore, electromagnetic induction in the pipe and the gap on the ferromagnetic-air boundary is equal. Then induction of the electromagnetic field in the butt gap is determined from the circulation theorem [13]:

$$\oint_L \mathbf{H} d\mathbf{l} = \frac{B}{\mu_0 \mu} l + \frac{B}{\mu_0} l_g = \sum I_{el},$$

where $l = 2\pi R - 2s$ is the ferromagnetic length, m; $l_g = 2s$ is the gap in the butt, m; R is the pipe radius,

m; I_{el} is the elementary current flowing along the pipe, A.

Sum of elementary currents flowing inside the contour, which is enclosed by a circumference with a center falling on the pipe axis, which runs through point $(0, y)$, is equal to

$$\sum I_{el} = \frac{I}{2\delta} (\delta + y) \text{ [A]},$$

where 2δ is the pipe wall thickness; y is the ordinate $-\delta \leq y \leq \delta$.

Then induction of electromagnetic field in the pipe butt gap is equal to

$$B = \frac{\mu_0 \sum I_{el}}{l/\mu + l_g} = \frac{\mu_0 \frac{I}{2\delta} (\delta + y)}{\frac{2\pi R - s}{\mu} + 2s} \text{ [T]},$$

and after transformations we obtain

$$B = \frac{\mu_0 I (\delta + y)}{4\delta \left(\frac{\pi R - s}{\mu} + s \right)} \text{ [T].} \quad (3)$$

Using equation (3) induction of electromagnetic field of welding current in the near-arc space can be calculated at different gaps equal to the width of Curie isotherm, welding modes and current supply to the item.

Validity of equation (3) is confirmed by experimental data, obtained at simulation of the welding process by passing current along the pipe and induction measurement in the butt gap across the metal thickness and at a distance from the pipe surface.

Model adequacy to the actual conditions is confirmed at measurement of induction of the electromagnetic field of welding current under production conditions in welding pipes of $426 \cdot 10^{-3}$ m diameter for the main gas and oil pipelines.

It is established that at current flowing along a pipe, the maximum value of induction rises from 0.35 T, compared with 0.1 T at current flowing along plates (Figure 5).

It is experimentally established that the relative magnetic permeability μ of a ferromagnetic pipe applied in simulation of the welding process, depends on intensity H of the electromagnetic field (Figure 6). In the case of small H values, μ rises up to 1300 with their increase. At increase of H value μ values first drop abruptly to 158, and then drop less significantly (to 10).

Without allowing for μ dependence on H , the maximum value of induction is observed on the pipe surface according to calculation data. On the inner surface of the pipe wall the induction is equal to zero. Allowing for the dependence of μ on H , the maximum induction is found in the middle of the pipe wall, which agrees well with experimental data.

Calculation and experimental procedures were used to establish that at current flowing along a pipe

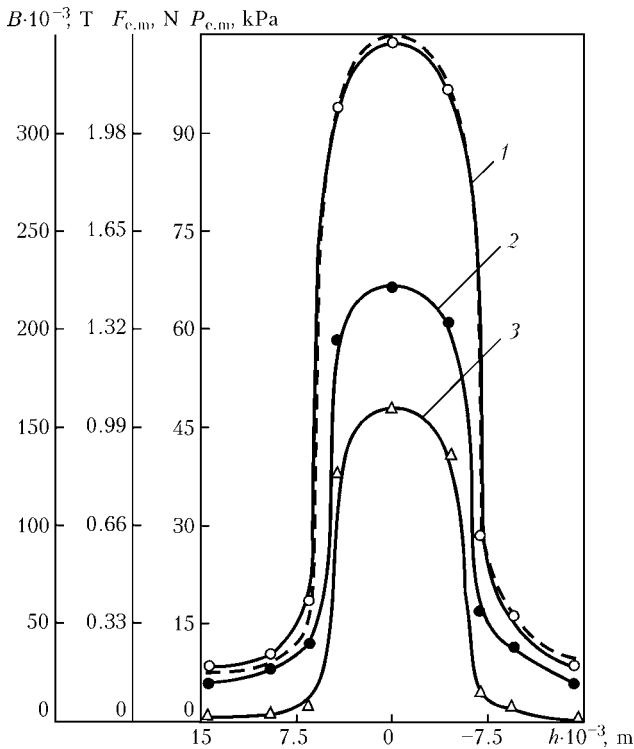


Figure 5. Distribution of electromagnetic field at flowing of current $I = 2100$ A along a pipe of size $10 \times 60 \times 300$ mm and 2 mm gap in the butt: 1-3 — see Figure 4; hatched line — calculated values of induction, considering the dependence of magnetic permeability on intensity of electromagnetic field

the maximum value of induction increases abruptly, being π times greater than the values of induction in plate welding. Direction of induction in the butt does not change, and it reaches the maximum value in the pipe wall mid-thickness. Induction and its distribution change as a result of the fact that the electromagnetic field force lines concentrate in a closed ferromagnetic body of the pipe, the contour of which coincides with the electromagnetic field force lines. Beyond the ferromagnetic body of the pipe the magnetic permeability decreases and the electromagnetic field induction drops abruptly. Value of induction on the pipe axis is not equal to zero, and its direction is opposite in the lower wall region.

Item shape also influences the maximum electromagnetic Ampere force $F = IB_l a$ (here I_a is the arc length), acting on the arc and liquid metal of the weld pool, and in the quadratic dependence — on electromagnetic pressure $P_{e.m} = B^2 / 2\mu$ [15], which rises almost 10 times at current flowing along the pipe. Therefore, in pipe welding the magnetic blow and influence of electromagnetic field on weld formation become stronger.

As a result of magnetic blow in welding of straight seam pipes from the current supply, the electromagnetic force deflects the arc forward so that its length periodically increases up to the moment of a natural breaking of the arc, which is re-excited at electrode shorting to the item. The welding mode becomes unstable and influences the quality of weld formation. In pipe welding to the current supply the arc deflects backwards, is immersed into the base metal and stabilized, but the weld forms with undercuts.

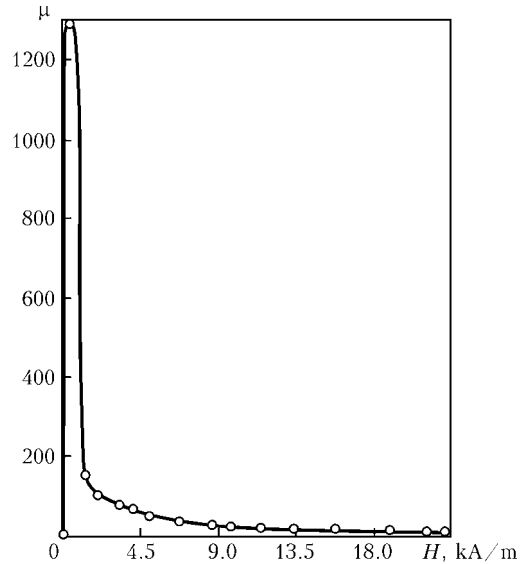


Figure 6. Dependence of relative magnetic permeability μ of ferromagnetic on intensity H of electromagnetic field

For a thin-walled pipe, the induction of the electromagnetic field generated by current flowing through a pipe (Figure 7) was determined according to the principle of superposition of the fields formed by infinitely long rectilinear conductors, through which currents flow

$$dI = \frac{Id\varphi}{2(\pi - \alpha)}$$

where φ is the angle determining the position of an elementary section with current; α is the angle depending on the gap in the butt.

Currents symmetrical relative to y axis induce in point y_0 a summary field directed along axis x :

$$dB = 2\mu\mu_0 \frac{Id\varphi}{2(\pi - \alpha)} \frac{1}{2\pi r} \frac{y - y_0}{r}$$

where $r = \sqrt{(y_0 - y)^2 + x^2}$; y is the ordinate of an elementary section with current; y_0 is the ordinate of a point, in which induction is measured.

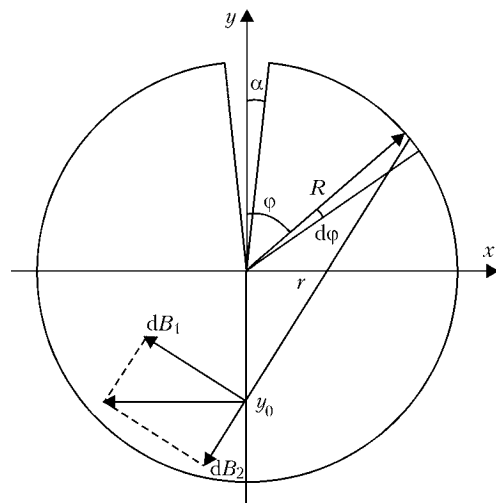


Figure 7. Schematic of induction calculation at current flowing along a thin-walled pipe: B_1, B_2 — induction components; for other designations see the text

Going over to polar coordinates, we obtain

$$dB = \mu\mu_0 \frac{Id\varphi}{\pi - \alpha} \frac{1}{2\pi} \frac{y_0 - R \cos \varphi}{R^2 \sin^2 \varphi + (y_0 - R \cos \varphi)^2} =$$

$$= \mu\mu_0 \frac{I}{2\pi(\pi - \alpha)} \frac{y_0 - R \cos \varphi}{R^2 + y_0^2 - 2Ry_0 \cos \varphi} d\varphi,$$

where $x = R \sin \varphi$; $y = R \cos \varphi$.

Induction of the electromagnetic field of current flowing along a pipe was determined by integration:

$$B(0, y_0) = \int_{\alpha}^{\pi} \mu\mu_0 \frac{I}{2\pi(\pi - \alpha)} \frac{y_0 - R \cos \varphi}{R^2 + y_0^2 - 2Ry_0 \cos \varphi} d\varphi =$$

$$= \int_{\alpha}^{\pi} \mu\mu_0 \frac{I}{2\pi(\pi - \alpha)} \frac{1}{2y_0} \frac{2y_0^2 - 2Ry_0 \cos \varphi + R^2 - R^2}{R^2 + y_0^2 - 2Ry_0 \cos \varphi} d\varphi =$$

$$= \mu\mu_0 \frac{I}{4\pi(\pi - \alpha)y_0} \int_{\alpha}^{\pi} \left(1 + \frac{y_0^2 - R^2}{R^2 + y_0^2 - 2Ry_0 \cos \varphi} \right) d\varphi =$$

$$= \mu\mu_0 \frac{I}{4\pi(\pi - \alpha)y_0} \left\{ \int_{\alpha}^{\pi} d\varphi + \frac{y_0^2 - R^2}{R^2 + y_0^2} \int_{\alpha}^{\pi} \frac{d\varphi}{1 - \frac{2Ry_0}{R^2 + y_0^2} \cos \varphi} \right\}$$

As $\int_{\alpha}^{\pi} d\varphi = \pi - \alpha$, after integration and transformations we obtain

$$B(0, y_0) = \mu\mu_0 \frac{I}{4\pi(\pi - \alpha)y_0} \times$$

$$\times \left[\pi - \alpha + \frac{y_0^2 - R^2}{R^2 - y_0^2} \left(\pi - 2 \arctg \frac{R^2 - y_0^2}{(R - y_0)^2} \operatorname{tg} \frac{\alpha}{2} \right) \right].$$

Inside the pipe at $y_0 \leq R$ the electromagnetic field induction is equal to

$$B(0, y_0) = \mu_0 \frac{I}{4\pi(\pi - \alpha)y_0} \times$$

$$\times \left[-\alpha + 2 \arctg \left(\frac{R^2 - y_0^2}{(R - y_0)^2} \operatorname{tg} \frac{\alpha}{2} \right) \right]. \quad (4)$$

Beyond the pipe the induction of the electromagnetic field is

$$B(0, y_0) = \mu_0 \frac{I}{4\pi(\pi - \alpha)y_0} \times$$

$$\times \left[\pi - \alpha + \left(\pi - 2 \arctg \frac{R^2 - y_0^2}{(R - y_0)^2} \operatorname{tg} \frac{\alpha}{2} \right) \right].$$

Induction of the electromagnetic field at a considerable distance from the pipe at $y_0 \gg R$ is

$$B(0, y_0) = \mu_0 \frac{I}{4\pi(\pi - \alpha)y_0} \times$$

$$\times \left[2\pi - \alpha - 2 \arctg \left(\frac{y_0^2}{(y_0^2)^2} \operatorname{tg} \frac{\alpha}{2} \right) \right] =$$

$$= \mu_0 \frac{I}{4\pi(\pi - \alpha)y_0} 2\pi = \mu_0 \frac{I}{2(\pi - \alpha)y_0}.$$

Neglecting α in view of its low value, we obtain the induction of the electromagnetic field at a greater distance from the pipe:

$$B(0, y_0) = \mu_0 \frac{I}{2\pi y_0} [\text{T}],$$

which is the classical expression for a straight linear inductor and confirms the validity of the derived formula.

From equation (4) on the pipe axis at $y_0 = 0$ the induction is equal to

$$B(0, y_0) = \mu_0 \frac{I \sin \alpha}{2\pi R(\pi - \alpha)} [\text{T}]. \quad (5)$$

As follows from (5), at current flowing through a pipe with a gap, the induction of the electromagnetic field on the pipe axis is not zero, and rises with the increase of the gap in the butt.

Validity of the obtained equations is confirmed by good agreement with the experimental and published data [14].

To prevent magnetic blow, a process of electric arc welding of pipes with a two-sided current supply has been developed, in which the electromagnetic force acting on the arc and the liquid metal of the pool is regulated by passing current of different magnitudes ahead of and behind the arc [16].

Developed process of one-sided high-speed welding of pipes with two-sided current supply is characterized by a stable and sound weld formation, lower material and power content.

CONCLUSIONS

1. Equations were derived for calculation of induction of the electromagnetic field in welding of plates and pipes. Calculation and experimental methods were used to establish the influence of item shape on magnetic permeability, distribution of the electromagnetic field in the butt gap and values of induction, which in pipe welding are π times higher than in plate welding.

2. In the plate butt induction is maximum on the plate surface, is equal to zero in the plate middle and changes its direction to the opposite one on pipe lower surface. In the pipe butt induction reaches its maximum value in the pipe wall mid-thickness and changes its direction in the region of its lower wall.

3. Magnetic blow in pipe welding rises as a result of presence of a closed circuit, increase of magnetic permeability, force line concentration in the ferromagnetic pipe, characterized by greater magnetic permeability, increase of induction of electromagnetic force, acting on the arc and electromagnetic pressure.

4. A welding process was developed with two-sided current supply, which provides regulation of the electromagnetic force acting on the arc and the liquid metal of the weld pool, stability of the process of one-sided high-speed welding of pipes and sound weld formation.

1. Paton, B.E., Mandelberg, S.L. (1968) Submerged-arc welding in manufacturing of large diameter pipes. *Avtomatich. Svarka*, 3, 41-46.

2. Paton, B.E., Lebedev, V.K. (1964) Magneto-hydrodynamic phenomena in electric welding and their application. In: *New problems of welding engineering*. Kiev.
3. Lebedev, V.K. (1965) Magneto-hydrodynamic phenomena in arc welding. In: *Technical electromagnetic hydrodynamics*. Moscow: Metallurgiya.
4. White, R.M. (1972) *Quantum theory of magnetism*. Moscow: Mir.
5. Mattis, D. (1967) *Theory of magnetism*. Moscow: Mir.
6. Gilbert, W. (1956) *About magnet, magnetic fields and large magnet — the Earth*. Moscow: AN SSSR.
7. Maxwell, J. (1954) *Selected works on theory of electromagnetic field*. Moscow: AN SSSR.
8. Lebedev, V.K. (1981) Power effect of electric arc. *Avtomatich. Svarka*, **1**, 7–14.
9. Finkelburg, W., Mekker, G. (1961) *Electric arcs and thermal plasma*. Moscow: Inostr. Literatura.
10. Leskov, G.I. (1970) *Electric welding arc*. Moscow: Mashinostroenie.
11. Gagen, Yu.G., Taran, V.D. (1970) *Magnetically-controlled arc welding*. Moscow: Mashinostroenie.
12. Govorkov, V.A. (1968) *Electric and magnetic fields*. Moscow: Energiya.
13. Zilberman, G.E. (1970) *Electricity and magnetism*. Moscow: Nauka.
14. Bessonov, L.A. (2001) *Theoretical principles of electrical engineering. Electromagnetic field*. Moscow: Gardariki.
15. Abramovich, G.P. (1969) *Applied gas dynamics*. Moscow: Nauka.
16. Shchetinina, V.I., Akulov, A.I. *Arc welding method*. USSR author's cert. 1524981. Int. Cl. B 23 K 31/06, 9/18. Publ. 30.11.89.

FLUX-CORED WIRE FOR ELECTRIC-ARC METALLIZING OF THE SURFACE OF WORKING ROLLS OF THE COLD ROLLING MILL TEMPERING STAND

V.A. ROYANOV, V.N. MATVIENKO¹, K.K. STEPNOV¹, V.P. SEMYONOV¹, N.G. ZAVARIKA¹,
I.V. ZAKHAROVA¹ and V.V. KLIMANCHUK²

¹Priazovsky State Technical University, Mariupol, Ukraine

²Open Joint-Stock Society «Ilyich MMK», Mariupol, Ukraine

Flux-cored wire for the process of electric-arc metallizing of the surface of working rolls of a tempering stand of the cold rolling mill and coating technology have been developed. Shown is the possibility of applying finely dispersed wear-resistant materials with provision of a high adhesion resistance of the coating to delamination in the technological process of temper rolling with reduction of 0.5–2.0 %.

Keywords: electric-arc metallizing, flux-cored wire, finely dispersed materials, coating, working rolls, tempering stand

Improvement of the quality of cold-rolled sheets and diversification of products assortment, are among the primary objectives of the sheet-rolling industry. In recent years special attention is paid to the quality of cold-rolled sheet surface.

The way of chromium-plating of working rolls of tempering stands by electrolytic depositing using an electrolytic conductor on the basis of pure chromium in a special set-up with vertical arrangement of the roll was reported in [1, 2]. However it is not void of drawbacks.

In Priazovsky State Technical University, at the Chair of Equipment and Technology for Welding Engineering, was developed and is extensively used the technology of thermal spraying and electric-arc metallizing with flux-cored and electrode wires of various compositions and properties [3, 4].

At request of Ilyich MMK company, Priazovsky State Technical University carried out a research aimed at assessing the feasibility of using electric-arc metallizing process for coating application on the roll barrels of tempering stands of cold rolling mills.

Research has been carried out aimed at working out the composition of the flux-cored wire providing for the obtaining of wear-resistant electric-arc metallization coatings. Thus alloying with non-critical al-

loys was used, whereas into the composition of the core were added aluminium and ferrochromium powders with the purpose of obtaining by metallization of carbide and hard oxide phases (including in the form of spinels). Fe–Cr system was selected as a basic alloying component of the wear-resistant coating.

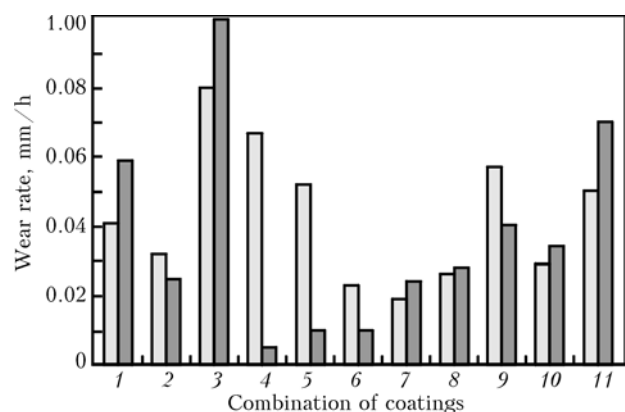


Figure 1. Diagram of values of average rates of wear for various combinations of friction pairs of detonation coatings (1, 2), electric-arc metallization coatings with flux-cored (3–8) and solid-drawn wires (9–11): 1 — PS-12NVK-01 and PN-80Kh13S2r; 2 — PS-12NVK-01 and PN-65Kh25S3R3; 3 — St3 and PP-MM-63; 4 — St3 and PP-MM065; 5 — steel 20GFL and PP-MM-63; 6 — PP-MM-63 and PP-MM-63; 7 — PP-MM-65 and PP-MM-63; 8 — PP-MM-65 and PP-MM-65; 9 — 95G and 65G; 10 — Kh2-N80 and 65G; 11 — 10Kh16N25A1 and 65G



Figure 2. Working roll of the tempering stand after metallization

In view of the noted, a series of compositions of flux-cored wires was developed for producing of wear-resistant coatings, namely PP-MM-2, PP-MM-6, PP-MM-63, PP-MM-65, etc. which provide cohesive strength of the coatings in normal tear or shear of not less than 50 MPa, and under the combined loading conditions (tear with shear) of not less than 39 MPa. The developed compositions of flux-cored wires provide coatings containing 1–2 % C; 4–10 % Cr.

Comparative tests for wear resistance of coatings at friction of metal pairs were conducted at dry friction of cylindrical specimens with coating applied to their end-faces. Testing conditions were the following: unit pressure of 50 kgf/cm², sliding speed of 3.8–7.3 cm/s, surface roughness of the coatings before testing $R_z = 80$.

During testing, time and changing of thickness of the coatings were noted. The developed compositions of flux-cored wires provide wear resistance of coatings (Figure 1) comparable to that of expensive metal powder and detonation coatings, and have significantly better wear resistance than the coatings obtained using solid wires from alloys types Kh20N80, 10Kh16N25Al, provide high cohesion of the coating with the substrate (adhesion strength).

Technological process of electric-arc metallizing includes shotblasting of the surface, metallization, and quality control.

Preparation of the roll surface was carried out by shotblasting, at which the desirable degree of roughness was simultaneously imparted to the surface, while removing the oxide film and grease, which promotes better cohesion of the coating. Thus time between the end of surface preparation process and the beginning of metallization should not exceed 1.5–2.0 h.

Based upon the experience of promoting the previous developments, the following key parameters of the metallizing conditions for the flux-cored wire having diameter 2.6 mm are recommended: arc current $I_a = 280\text{--}300$ A, arc voltage $U_a = 34\text{--}36$ V, metallizing distance $L = 140$ mm, pressure of spraying air $P_{\text{air}} = 0.50\text{--}0.55$ MPa. Travel speed of the metallizing unit can be chosen within the range of 2–6 rpm and peripheral velocity of 10–40 m/min.

Pilot research metallization of surfaces of tempering stand rolls (2 pieces: No. 115 and 116) is carried out in cold rolling shop of MMK company, using a previously developed technique (Figure 2).

The rolls were first subject to form-grinding for +0.09 (top), +0.15 (bottom), and to shotblasting. Compressed air for the metallizing unit EM-17 came from a separate compressor unit, with pressure at the input of the spraying nozzle of not less than 0.50–0.55 MPa. The air used for metallization and shotblasting, was passed through oil and water separators placed by the compressor or right at the workplace. After metallizing layer 80–200 μm thick, polishing, followed by shotblasting on «Gopstop» plant was carried out. Residual thickness of the deposited metal ranged from 15 to 25 μm . Measurements of the roughness gave values from 3.76 to 6.86 μm .

Thus prepared and assembled rolls were mounted in the mill. A preliminary running-in of the rolls «as in operation» conditions, without loading, was carried out; they made 15–20 turns. At temper rolling of the first coil, roughness of the strip exceeding the requirements ÖU 227-P-02–2004 was noted. Measurements on the top and bottom planes of the strip, using device «Sutronik» have shown the following values: bottom --- 2.00; 3.76; 2.20 μm ; top --- 2.64; 2.76; 1.68 μm .

After rolling half of the coil, the mill was stopped, and another running-in «as in operation» conditions, without loading, during 8–10 min was carried out. Then tempering was resumed. The first sample of the strip was taken. After rolling of about 20 t of the strip, roughness of the top roll was measured (top back-up was lifted by 120–130 mm). The following values for roll body generatrix were obtained (at 250 mm intervals): 2.42; 1.50; 1.82; 1.96; 2.88; 1.74 μm . These data testify to the running-in of the surface layers of the roll during strip tempering. Still another running-in «as in operation» conditions, without loading, during not less than 15 min, with washing the rolls with a liquid under pressure, and then tempering was resumed again. Mill operators have noticed an appreciable improvement of the quality of the strip surface, and its meeting the requirements of technical specifications on tempering. The second sample from the coil was taken. During the testing neither delaminations nor spalling of the deposited layer were noted.

Results of the research have shown a possibility in principle of applying finely dispersed wear-resistant materials on the working surface, and their adhesion resistance to delamination in the technological process of tempering cold-rolled strips with reduction of 0.5–2.0 %.

1. Kolpakov, S.S., Kapnin, V.V., Mukhin, Yu.A. et al. (1995) Chrome-plating of tempering mill working rolls. *Stal*, **8**, 48–50.
2. Mukhin, Yu.A., Soloviov, V.N., Bobkov, E.B. et al. (2002) Examination of strip quality in temper rolling using the chrome-plated rolls. *Ibid.*, **6**, 50–52.
3. Royanov, V.A. (1990) Fusion of electrodes in arc metallizing. *Svarochn. Proizvodstvo*, **2**, 35–38.
4. Royanov, V.A., Semyonov, V.P. (1995) Sparsely alloyed flux-cored wire for arc spraying of wear-resistant coatings. *Vestnik PGTU*, Issue 1, 157–160.

FLUX-CORED WIRE FOR STRENGTHENING THE NECKS AND FILLETS OF MILL ROLLS

V.N. MATVIENKO

Priazovsky State Technical University, Mariupol, Ukraine

Composition of a surfacing consumable in the form of flux-cored wire is developed, which provides improved service properties of the rolls of Slabbing-1150 mill. Resistance of roll necks is on the level of that of the working surface of roll barrel.

Keywords: electric arc surfacing, flux-cored wire, deposited metal, necks and fillets of mill rolls

The problem of preservation of a sufficiently high level of technical and economic parameters of operation of Slabbing-1150 rolling mill at OJSC «Ilyich MMW» first of all envisages reaching the main objective --- extension of the service life of its main operating tool --- the mill rolls. The first part of this problem is being successfully solved under the conditions of the surfacing section of Slabbing-1150 shop [1], namely strengthening of the working surface of the roll barrels by the method of arc surfacing of a layer of metal using materials and technologies developed by Industrial Research Laboratory of PSTU.

Analysis of roll resistance shows that in most of the cases their failure, including their breaking up, runs along the necks, particularly in the place of transition from the neck to barrel, i.e. along the fillet (Figure 1). In this connection, it is necessary to develop a surfacing consumable and technology, providing an improvement of the neck resistance to the level of that of the roll barrel working surface.

Surface of roll necks of Slabbing-1150 mill operates under the heavy temperature-force conditions of hydroabrasive wear in combination with considerable shock bending alternating loads and torques. Conditions of the impact of the abrasive and corrosive media on the metal, the nature of its surface damage predetermine the required composition, microstructure, phase condition and properties of the deposited metal. To increase the operating resistance of the necks and fillets, their working surface should be surfaced with

consumables, ensuring a sufficiently high strength and ductility both at normal and elevated temperatures, high wear and heat resistance of the deposited layer alongside the corrosion resistance. Material development should provide both its high performance meeting the above-mentioned requirements, and technological capabilities of its deposition on the surface of the neck and fillets by electric arc surfacing.

To be able to resist the destroying impact of the abrasive medium under the conditions of metal friction against metal, the deposited metal should have a hard component (carbides, borides, nitrides, intermetallic compounds), and hard particles of carbides and other compounds should be firmly held by the matrix, which is the alloy base. Martensite, ferrite, austenite and ledeburite can play the role of the matrix in steels and alloys. Accordingly, the classification of wear-resistant deposited metal by structural features [2] includes the following classes: martensite, martensite-carbide (here, other hard particles can be present in addition to carbides, namely borides, carbonitrides, intermetallics, etc.), ferrite-carbide, austenite-carbide, ledeburite-carbide. Table 1 gives the characteristics of the deposited metal of different classes.

In view of the above, as well as generally accepted recommendations [2, 3], surfacing consumables were selected at the preliminary stage of investigations, which provide the deposited metal of martensite, martensite-carbide and austenite-carbide classes. Metallographic examinations, testing for wear and heat resistance, hardness at normal and elevated temperatures, and resistance to solidification cracking at surfacing were conducted.

Table 1. Characteristic of the deposited metal of different classes

No.	Type of deposited metal	Structural class	Relative labour consumption of machining
1	30KhGSA	Martensite	1.0
2	18Kh6GMFS	Martensite-carbide	1.6
3	25Kh7GMFS	Same	1.7
4	12Kh12G12SF	Austenite-carbide	1.7
5	Kh20N10G6	Same	1.7

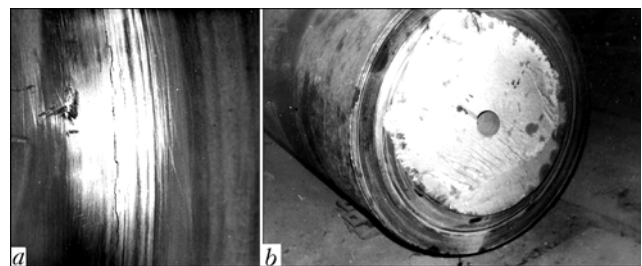


Figure 1. Appearance of the fillet part of the mill roll with a crack on the surface (a) and zone of fracture of the horizontal roll of Slabbing-1150 mill along the fillet (b)

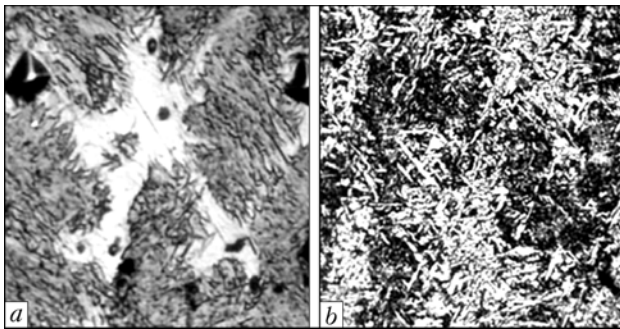


Figure 2. Microstructure of 30KhGSA deposited metal: a --- multipass surfacing with wire electrode (ferrite + pearlite, *HV* 200); b --- single-pass surfacing with strip electrode (martensite, troostite, bainite, *HV* 400) ($\times 320$)

To prepare the samples, four- and five-layer deposits were performed on 40 mm thick plates from steel 50 with preheating up to the temperature of 300–350 °C*. Wear resistance of the deposited metal was evaluated in a unit with reciprocal motion of the friction body from steel R18. Temperature of the friction body was equal to 400 °C, specific pressure was 14.7 MPa, velocity of the friction body movement was 11.2 m/min, testing time was 1 h [4]. Metal hardness at elevated temperatures was measured on samples of 6 × 3 × 40 mm size, cut out of the deposited metal at current flowing through it. Sample temperature during heating and cooling was measured by a chromel-copel thermocouple welded to the sample [4]. Heat resistance of the deposited metal was determined by short-time passing of current through a section of the deposited metal with its subsequent fast cooling by flowing water jet [4]. Number of heating-cooling cycles was recorded up to appearance of a visible crack. Deposited metal testing for solidification crack resistance was conducted by a procedure envisaging forced bending of a flat sample (by pure bending schematic) during surfacing, which leads to tensile stresses in the solidifying deposited metal [4]. Maximum critical deformation rate, at which the deposited metal still has no cracks, was a criterion of technological resistance to solidification crack formation. Results of deposited metal testing are shown in Table 2.

Metal of martensite class can be obtained in surfacing with medium- or high-carbon steel (for instance

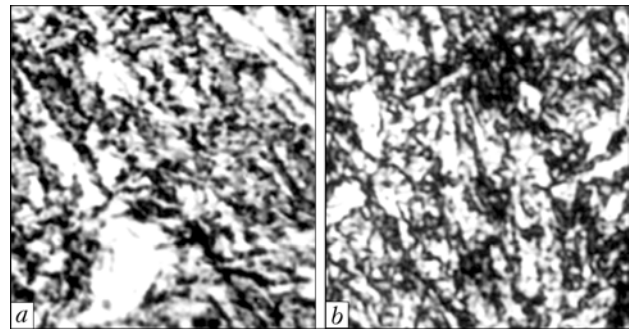


Figure 3. Microstructure of Fe-C-Cr-Mo-V system alloy of the deposited metal: a ---18Kh6GMFS; b ---25Kh7GMFS ($\times 500$)

with Np-35, Np-65G, Np-30KhGSA wires, etc.). The final structure and properties of such a metal are mainly determined by its content of carbon and temperature-time conditions (mode and technology) of surfacing. 30KhGSA metal, the structure of which is shown in Figure 2, became the most widely accepted of the low- and medium-carbon materials for surfacing roll necks. Such a metal is quite readily adaptable to fabrication --- it is practically not prone to cracking in a wide range of variation of the mode parameters, having a sufficiently high index of technological strength (see Table 2), it is readily machinable, and has a good resistance to impact loads due to a high ductility. However, in view of a relatively low hardness (because of a low content of carbon) and absence of hard strengthening particles (carbides) in the structure, the wear resistance of medium-carbon deposited metal of the martensite class is low (see Table 2), and is on the level of wear resistance of heat-hardened structural steels. Therefore, 30KhGSA metal is mainly used only as intermediate layers (so-called underlayers), when surfacing mill rolls.

Metal of martensite-carbide class has a higher hardness and wear resistance compared to metal of the martensite class. Known are modifications of sparsely-alloyed alloys of Fe-C-Cr-Mo-V system of Kh5MF --- 25Kh5FMS type obtained by surfacing with flux-cored wire [5], and 18Kh6GMFS, 20Kh7GFM, 25Kh7GMFS alloys obtained by surfacing with low-carbon wires or strips using alloying ceramic flux ZhSN-5 [6]. In multi-pass surfacing with

Table 2. Results of testing the deposited metal

Test	30KhGSA	18Kh6GMFS	25Kh7GMFS	12Kh12G12SF	Kh20N10G6
Wear resistance, mg	85.6–90.2	42.4–46.3	28.6–32.1	25.2–28.9	33.7–35.4
Heat resistance, cycle number	1710–1830	1850–1980	1320–1450	1510–1640	840–970
Hardness (<i>HRC</i>) of metal at the temperature, °C:					
20	26–30	40–44	47–50	33–36	30–34
500	18–21	28–31	33–36	29–32	24–27
Technological strength (deformation rate), mm/min	17.6–18.2	8.6–9.3	7.1–7.5	10.8–12.4	9.5–10.1

Note. Tables 2 and 3 give the results of 3–5 tests or measurements.

* K.K. Stepanov and A.I. Oldakovsky took part in this work.

preheating such metal has the structure of high-tempered martensite --- sorbite + carbides (Figure 3). It is characterized by a combination of quite high values of hardness, wear, heat and crack resistance (see Table 2) that predetermined a wide application of these sparsely-alloyed consumables for strengthening the working surface of the roll barrel in hot rolling mills.

On the other hand, these alloys, similar to those described above, are not corrosion- or cavitation-resistant under the conditions of hydroabrasive wear, characteristic for operation of roll necks of Slabbing-1150 mill. Therefore, application of these materials for neck surfacing is not rational. From this viewpoint, it is highly advantageous to apply the deposited metal of austenite-carbide class.

Austenite matrix has several advantages compared to the martensite or ferrite one. First of all, martensite has a higher toughness and strength than ferrite, this promoting, on the one hand, a better containment of the solid phase particles, and on the other --- an overall increase of wear resistance, particularly at impact-abrasive wear. In addition, austenite can be completely or partially unstable, and during plastic deformation it may undergo martensite transformation (so-called deformation martensite), this leading to an additional increase of wear resistance. Another important service property of the austenitic deposited metal is a higher corrosion resistance compared to all other structural classes.

Cr-Mn-V alloy 12Kh12G12SF [3, 4] the structure of which is shown in Figure 4, and testing results are given in Table 2, is successfully used as a wear-resistant deposited metal of the austenite-carbide class for surfacing mill rolls and rollers of continuous casting machines. Austenitic wires (Sv-08Kh21N10G6, Sv-08Kh20N9G7T, Sv-07Kh25N13, Sv-10KhN15, etc.) with up to 18–20 % nickel content, making these materials expensive and deficit, are also used for deposition of a corrosion-resistant metal layer. It is cost-effective to replace nickel in the deposited metal of the austenitic class by elements providing the required structure and combination of the metal properties. A number of Cr-Mn steels were proposed [7, 8], which are designed to replace the Cr-Ni alloys. It is established [9] that the Cr-Ni and Cr-Mn austenite are close in many of their properties, and in terms of heat resistance Cr-Mn austenite is superior to Cr-Ni one. A higher ability of Cr-Mn austenite to strengthening is manifested stronger at elevated temperatures (if the latter do not exceed the recrystallization threshold). In this connection, manganese content in such alloys is limited to 10–15 %, i.e. the minimum quantity which provides a stable austenitic structure [7, 9].

The optimum content of chromium in the above Cr-Mn alloys is 10–13 %, this providing high wear and heat resistance of the alloy due to precipitation of high-melting and hard chromium carbides in the metal structure. This element prevents the growth of alloy grain, and increases the stability of overcooled austenite. In addition, chromium content in the above

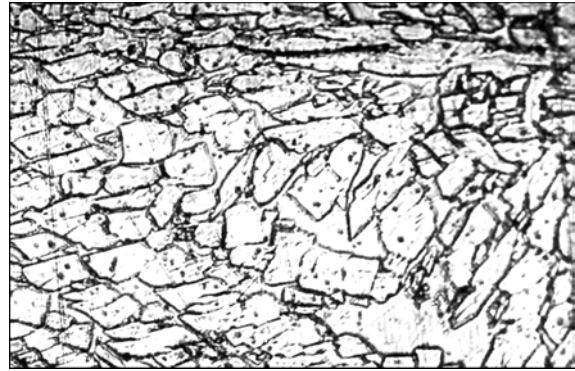


Figure 4. Microstructure of 12Kh12G12SF deposited metal of austenite-carbide class ($\times 320$)

concentrations allows preservation of the alloy high-temperature hardness at a sufficiently high level [10], and at a higher concentration of chromium (above 13 %) the alloy becomes sensitive to temper brittleness, that may lead to spallation of the deposited layer in service.

Carbon content should be not more than 0.10 %, otherwise there is the risk of formation of the brittle component of σ -phase during long-term operation of the item at high temperatures [7–10].

It is recommended [11] to alloy the Cr-Mn alloys designed for hardsurfacing steel parts, operating under the conditions of elevated temperatures, thermal cycling in combination with high specific pressures, by vanadium and titanium, strengthening the solid solution and influencing the dispersity and rate of carbide particle strengthening at long-term thermal soaking. Forming stable carbides and reducing their solubility in the alloy, these elements promote an increase of thermal stability, heat and wear resistance of the alloy, values of critical points, this being highly important for the metal, operating under the conditions of multiple thermal cycles. In addition, such high-melting carbide compounds play the role of modifiers, effectively refining the primary structure of the alloy, and thus increasing the technological strength of the metal during its solidification [12]. Titanium further provides a good deoxidation and degassing of the alloy, producing a dense and fine primary microstructure and fracture of the cast steel [13].

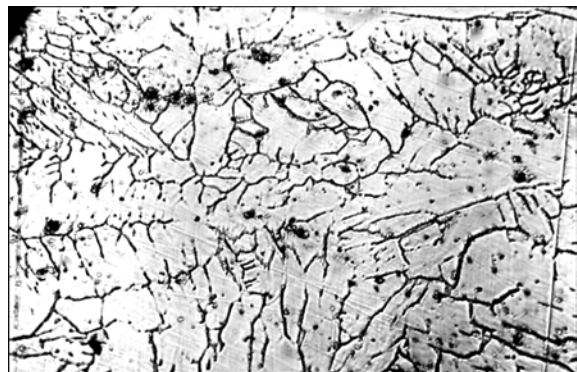


Figure 5. Microstructure of the metal deposited with test wire PP-09Kh11G12F2YuTsT ($\times 500$)

Table 3. Results of testing the metal deposited with test wire PP-09Kh11G12F2YuTsT under AN-60 flux and Sv-08GA wire under ZhSN-5 flux

Test	Surfacing material grade		
	PP-09Kh11G12F2YuTsT	Sv-08GA + ZhSN-5	
	Deposited metal type		
	09Kh11G12F2YuTsT	20Kh6GMFS	
Wear resistance, mg	20.6–24.1	37.4–41.6	
Heat resistance, cycle number	1760–1910	1670–1750	
Hardness (HRC) at the temperature, °C			
	20	32–34	39–41
	500	28–30	31–33
Technological strength (deformation rate), mm/min	15.9–16.3	9.1–10.4	

When developing the composition of the deposited metal for strengthening the mill roll necks and flux-cored wire, a low-carbon chromium-manganese alloy of 09Kh11G12 type was used as a base with additional alloying by vanadium, titanium, aluminium, as well as zirconium microadditives.

The composition of flux-cored wire PP-09Kh11G12F2YuTsT was developed to produce deposited metal of the above type. Alloying is performed by adding the respective metal powders and ferroalloys to the charge. Aluminium added to the metal in small amounts (0.10–0.20 %) essentially refines its structure due to the forming highly-dispersed particles of aluminium oxides, and thus increases the alloy resistance to formation of solidification cracks during surfacing. Metal microalloying with zirconium has the same role.

Results of laboratory testing of metal deposited by test flux-cored wire using fused flux AN-60 are given in Table 3. Composition of the metal deposited by test wire PP-09Kh11G12F2YuTsT is as follows, wt. %: 0.07–0.09 C; 10.8–11.2 Cr; 11.6–11.8 Mn; 1.9–2.1 V; 0.13–0.15 Al; 0.01 Ti; 0.01 Zr. The surfacing process was characterized by high welding-technological properties: stable arcing, satisfactory formation of the deposited metal and good separability of the slag crust, absence of cracks, pores, lacks-of-fusion and other defects. Microstructure of the deposited metal features equiaxiality and consists of austenite with carbides located along its grain boundaries (Figure 5).

For comparison, Table 3 gives the results of testing metal of 20Kh6GMFS type deposited with ZhSN-5 flux and Sv-08GA solid wire, used in surfacing mill roll barrels.

Analyzing the results of laboratory resting (see Tables 2 and 3) it may be noted that the metal produced in surfacing with test flux-cored wire has improved service properties, which was confirmed by subsequent production surfacing of the roll necks and fillets of Slabbing-1150 mill. Results of operation of the surfaced rolls showed an improvement of their performance 1.3 to 1.5 times. An increase of neck resistance to the level of that of the roll barrel working

surface was achieved. Fillet surfacing by flux-cored wire allowed eliminating cracking and mill failure in this zone.

CONCLUSIONS

1. Composition of a surfacing consumable has been developed to increase the resistance of necks and fillets of Slabbing-1150 mill rolls, and a test batch of flux-cored wire was manufactured to produce it.

2. Metal produced in surfacing by test flux-cored wire has improved service properties, which was confirmed by the results of operation of surfaced rolls of Slabbing-1150 mill, which demonstrated an increase of their performance by 1.3 to 1.5 times. An increase of neck resistance to the level of that of the working surface of the roll barrel was achieved.

1. Matvienko, V.N., Stepnov, K.K., Gulakov, S.V. et al. (2005) Increase of life of mill steel rolls at the OAO «MMK im. Ilyicha». *Metallurg. Oborudovanie*, **2**, 39–42.
2. Samotugin, S.S., Leshchinsky, L.K., Solyanik, N.Kh. (1996) *Structure and type of fracture of welded joints, deposited and strengthened materials*. Mariupol: PGTU.
3. Tylkin, M.A. (1981) *Handbook of heat-treater of repair service*. Moscow: Metallurgiya.
4. Nosovsky, B.I., Leshchinsky, L.K., Gulakov, S.V. et al. (1979) About estimation of the main properties of metal for surfacing of mill rolls. In: *Theoretical and technological principles of surfacing. Properties and tests of deposited metal*. Ed. by I.I. Frumin. Kiev: PWI.
5. Frumin, I.I., Kondratiev, I.A. (1968) Flux-cored wire PP-25Kh5FMS for surfacing of mill rolls. *Avtomatich. Svarka*, **10**, 56–58.
6. Leshchinsky, L.K., Gulakov, S.V., Nosovsky, B.I. et al. (1978) Increase of serviceability of mill rolls by deposition of a layer with varying wear resistance along the barrel length. *Ibid.*, **3**, 57–62.
7. Bogachev, I.N., Egolaev, V.F. (1973) *Structure and properties of iron-manganese alloys*. Moscow: Metallurgiya.
8. Malinov, L.S., Malinov, V.L. (2001) Manganese-containing surfacing consumables. *The Paton Welding J.*, **8**, 30–32.
9. Khimushin, F.F. (1965) Chrome-manganese steels of austenite and austenite-ferrite type. *Trudy VIAM*, **32**, 24–26.
10. Khimushin, F.F. (1964) *Heat-resistant steels and alloys*. Moscow: Metallurgiya.
11. Meskin, V.S. (1964) *Principles of steel alloying*. Moscow: Metallurgizdat.
12. Lakhtin, Yu.M., Leontieva, V.M. (1980) *Materials science*. Moscow: Mashinostroenie.
13. Kontorovich, I.E. (1950) *Heat treatment of steel and cast iron*. Moscow: Metallurgiya.

SPARSELY ALLOYED CONSUMABLES PROVIDING IN THE DEPOSITED METAL DEFORMATION HARDENING IN OPERATION

V.L. MALINOV

Priazovsky State Technical University, Mariupol, Ukraine

The paper gives the results of investigations on development of sparsely alloyed surfacing consumables ensuring an increase of the fatigue life of machine parts by producing in the deposited metal structure of a metastable austenite which undergoes deformation hardening in operation.

Keywords: arc surfacing, flux-cored strip, deposited metal, metastable austenite, martensite, wear resistance, mechanical properties, deformation hardening

Nowadays the problem of resource saving is quite urgent. One of the perspective avenues of its solving is development and active industrial introduction of sparsely-alloyed consumables with the effect of deformation hardening of the deposited metal in operation consisting of transformation of metastable austenite into martensite under the action of external loading.

First consumables which have ensured formation in the deposited metal of metastable austenite were devised under the direction of M.I. Razikov. Electrodes UPI 30Kh10G10 and flux-cored wire PP-30Kh11G120 [1] were developed. Alongside with high operational properties, a number of disadvantages are inherent to them, namely poor machinability of the deposited metal, as well as insufficient corrosion resistance and poor resistance to abrasive wear.

In this work, results of research aimed at creation of more technological consumables, including those having increased abrasive resistance, are generalized. Lines of further research were established and examples of technical solutions which can be widely used in the industry of Ukraine for increasing of service life of rapidly wearing parts of machines are shown.

In [2], data on flux-cored strip PL-Np-15Kh13AG10MFS (PLN-4) which has shown high efficiency in hard-facing parts operating under the conditions of contact loading are cited. It was applied in restoration of crane wheels, plungers of hydraulic presses and trunnions of steel-casting ladles. Deposited using this strip metal has improved machinability, which is due to the reduction of carbon content and increased austenite stability in relation to strain

martensite transformation thanks to the increase in the degree of alloying with chrome and manganese.

It is shown that the heat treatment including inverse annealing at 600–650 °C, usually carried out after surfacing for relieving the internal stresses, reduces stability of austenite to strain martensite transformation, and due to this improves its wear resistance by 30–40 % in sliding and rolling friction conditions [3].

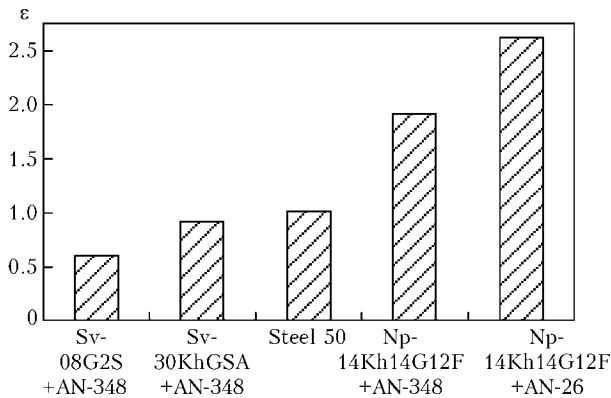
It is known that the most uniform properties of the deposited metal can be obtained by the use of solid electrode wire. For this purpose a 4 mm wire Np-14Kh14G12F [4] was developed. The present author has carried out a research of properties of the metal deposited using this wire and fluxes AN-348 and AN-26. Mechanical properties of the deposited metal are listed in the Table.

Wear tests were conducted in block-on-roller dry-friction configuration on machine MI-1M. A roller with diameter 46 mm and thickness 10 mm, was made of steel 50 having hardness *HB* 320. The studied samples of deposited metal had dimensions 10 × 10 × 25 mm. Roller rotation speed was 425 rpm, sliding speed was 0.98 m/s, and load was 100 MPa. Annealed steel 50 was used as a reference. Results of estimation of relative wear resistance after testing during 15 min, are presented in the Figure. For comparison are also cited data of comparative wear resistance of the metal deposited using wires Sv-08G2S and Np-30KhGSA and flux AN-348.

In the metal deposited using wire Np-14Kh14G12F and flux AN-26, the amount of martensite in the structure increased from approximately 5 % (as-deposited condition) up to 60 % (wearing surface). When employing flux AN-348, after deposition, the amount of

Mechanical properties of metal deposited with Np-14Kh14G12F wire

Flux brand	Yield limit $\sigma_{0.2}$, MPa	Tensile strength σ_r , MPa	Relative elongation, %	Reduction in area, %	Hardness <i>HB</i>
AN-348	580	770	6.5	9.8	50
AN-26	330	680	14.5	22.0	260



Comparative wear resistance of deposited metal ϵ in comparison with steel 50

martensite was 30 %, whereas after wearing it increased to 70 %. Higher wear resistance of the deposited metal in the former case is explained by optimum intensity of strain martensite transformation providing not only required surface hardening, but also simultaneous stress relieving, which allows involving more of external action for transformation, rather than fracture.

On the basis of the obtained data a conclusion is drawn that using for hard-facing flux AN-26 is more expedient than flux AN-348, as it provides better mechanical properties (see the Table) and wear resistance of the deposited metal, along with better separability of slag crust.

In [5] are presented data on surfacing strip PLN-6 (PL-Np-20G15SAF) which is more cost-effective in comparison with the materials considered above on Fe-Nr-Mn-C base, as it also provides formation in the deposited metal of metastable austenite structure. Comparative tests in conditions of rolling and sliding friction have shown that in terms of wear resistance, the metal deposited using strip PLN-6, as well as that obtained using strips PLN-4 and Np-14Kh14G12F, considerably surpasses the metal deposited using wire Sv-30KhGSA. Strip PLN-6 has shown high efficiency in hard-facing of crane wheels.

A specific field of application allowing the advantage of structures containing meta-stable austenite to be fully realized, is restoration and hardening of the parts exposed to wear in combination with strong impacts. Such operating conditions are characteristic for wobblers and sleeves of rolling mills, railway and tram road frogs, parts of automatic coupling of railway cars, hammers, dredger buckets, teeth of earth-moving machines, etc.

Most widely used in these conditions are cast parts from steel 110G13L. The increased wear resistance of steel 110G13L is achieved at greater static and dynamic loading causing its strong cold work hardening, but in the absence of such loading the surface layer of parts does not harden and wears out by abrasive action just as any carbon steel.

Usually hard-facing is applied for repair of the worn out cast parts, which allows their service life to be prolonged. However obtaining deposited metal corresponding in chemistry to steel 110G13L, involves

serious technological difficulties as it is susceptible to embrittlement if overheated and slowly cooled. An efficient method allowing increasing crack-resistance of the deposited metal, is the reduction of its carbon content. Retention of high wear resistance is thus due to implementation of strain martensite transformation, given optimum intensity of its development. In view of this, the surfacing wire 70G7Kh4N2I was reported [6]. In its use, the austenite formed in the structure of the deposited metal, is metastable. Investigation by X-radiography of its worn out surface has shown that in the initial austenite structure, up to 20 % of strain martensite had been formed. Use of the wire 70G7Kh4N2I for electroslag cladding of dredger buckets has provided increase of their durability by 20 %, in comparison with steel 110G13L.

In conditions of contact-impact loading it is possible to provide high wear resistance also using flux-cored wire PP-30Kh8G8S0 [7]. The structure of the deposited metal alongside with austenite contains 20--30 % of martensite. Use of this wire at Kamensk-Uralsk Factory for non-ferrous metals working, has shown that durability the hard-faced parts of spindles of rolling mills, rollers of flatteners, frogs of tram roads, etc. has increased 2--7 times.

The consumables providing in the structure of the deposited layer a significant amount of solid phases (carbides, borides, etc.), are usually applied in conditions of abrasive and impact-abrasive wear. However their presence, though necessary, is not a sufficient condition for high wear resistance. The increase in their amount over the optimum, for the given wear process conditions, leads to embrittlement and to fast deterioration of the working surface. In so doing the important role is played by the structure of the alloy metallic matrix, particularly presence of the residual austenite. In the literature inconsistent data concerning its optimum content are cited. One of the reasons of this is that in most cases by development of wear-resistant alloys, qualitative evaluation of conditions in which they operate, is only made. It complicates a rational choice of the surfacing material for specific operating conditions. In [8] it is proposed to use the factor of dynamism K_d defined as the relation of hardness of the sample from steel 110G13L after wear process in given conditions, to its initial hardness, for the characterization of various conditions of wear process. Steel 110G13L accumulates the energy of external action, being thus strengthened, and the level of its hardening allows judgment on integrated intensity of impact-abrasive effect.

In view of K_d , study of abrasive and impact-abrasive wear resistance of deposited metal of alloying systems Fe-Cr-Mn-C and Fe-Cr-Mn-V-C, with various ratios of strengthening phases and metastable austenite in the structure [9], was conducted. The research was carried out with planning of the experiment for various values of K_d in the range from 1.2 up to 3.5, which corresponds to the test conditions varying from abrasive wear process practically with-

out impacts, to wear process with very intensive impact loading. The content of alloying elements in the deposited metal changed within the following limits, %: 1–3 C, 6–12 Cr, 2–6 Mn. Properties of the deposited metal additionally alloyed with vanadium in the amount of approximately 3 % were also studied. As a result were obtained regressive dependences of impact-abrasive wear resistance ε from chemical composition of the deposited metal:

$$\varepsilon_{(K_d=1.2)} = 0.98 + 0.68C + 0.087Mn - 0.027Cr + 0.021C \cdot Cr - 0.2C^2 - 0.017Mn^2; \quad (1)$$

$$\varepsilon_{(K_d=1.4)} = 0.93 + 0.6C + 0.11Mn - 0.018Cr + 0.017C \cdot Cr - 0.18C^2 - 0.019Mn^2; \quad (2)$$

$$\varepsilon_{(K_d=1.7)} = 1.17 + 0.41C + 0.044Mn - 0.018Cr + 0.017C \cdot Cr + 0.025C \cdot Mn - 0.16C^2 - 0.015Mn^2; \quad (3)$$

$$\varepsilon_{(K_d=2.0)} = 1.19 + 0.36C + 0.023Mn - 0.015Cr + 0.017C \cdot Cr + 0.037C \cdot Mn - 0.18C^2 - 0.012Mn^2; \quad (4)$$

$$\varepsilon_{(K_d=3.5)} = 0.77 + 0.866C + 0.002Mn - 0.014Cr + 0.031C \cdot Mn + 0.01Cr \cdot Mn - 0.34C^2 - 0.017Mn^2. \quad (5)$$

At small factors of dynamism ($K_d = 1.2$ – 1.4) the greatest wear resistance in the deposited metal of the following chemical composition, %: 2–25 C, ~12 Cr, 2–3 Mn, is obtained. Its hardness is in the range *HRC* 45–50. The structure of the deposited metal was mainly martensite-carbide type, residual austenite constitutes 25–30 %. In the given conditions of impact-abrasive action alloying of the deposited metal with vanadium in the amount of up to 3 % at simultaneous increase of carbon content up to 2.5–3.0 %, increases wear resistance by 10–15 %. With increasing intensity of impact-abrasive action and accordingly growth of K_d in the deposited metal, it is necessary to reduce the carbon content and increase the amount of manganese. So, at $K_d = 3.5$, optimum is the following content of the alloying elements, %: 1.0–1.7 C, 5–6 Mn, ~12 Cr. Hardness of the deposited metal was about *HRC* 40. The structure was predominantly austenitic, with total amount of martensite and carbides in the structure of less than 40 %. In the given conditions of impact-abrasive action, alloying with vanadium is inefficient, as does not increase wear resistance.

For various impact-abrasive wear process intensities characterized by K_d , the following flux-cored strips were developed: PL-Np-230Kh12G2 and PL-Np-250Kh10G4F3 at $K_d = 1.2$ – 1.4 ; PL-Np-200Kh12G2 at $K_d = 1.7$ – 2.0 ; PL-Np-160Kh12G5 and PL-Np-100Kh6G4 at $K_d = 3.5$, and also PL-Np-200Kh12G5 for a wider range of $K_d = 1.4$ – 3.5 . Surfacing with the developed flux-cored strips of section 18×4 mm, is carried out using flux AN-26 in the following conditions: current $I = 600$ – 700 A, voltage $U = 28$ – 32 V, surfacing speed $v = 35$ – 40 m/h. The

above strips feature good welding-technological properties.

Flux-cored strip PL-Np-160Kh12G5 has passed industrial testing and has been adopted for restoration of jaw breaker plates, which has allowed increasing durability of these parts 1.5 times in comparison with those made of steel 110G13L [9].

After hard-facing, the structure and phase composition can differ from optimum (in particular, effecting adaptability to manufacturing process). In this case the effective way of their regulation is normalization, whose conditions should be selected in view of the intensity of impact-abrasive action K_d . The effect of the heating temperature on the properties of the metal deposited using flux-cored strips PL-Np-200Kh12G5 and PL-Np-250Kh10G4F3 was studied at normalization from 800 to 1100 °N for 20 min. It is established that with increasing intensity of impact-abrasive action, and accordingly K_d , it is necessary to use higher heating temperatures at normalization with the purpose of increasing the amount of austenite in the structure, also the degree of its stability due to additional alloying resulting from dissolution of some carbides. In conditions of abrasive wear with low intensity of impact effect ($K_d = 1.2$ – 1.4), increase of wear resistance of the deposited metal is provided with normalization from rather low temperatures (~800 °N). The structure obtained at this is mainly martensite-carbide type, where austenite accounts for 20–30 %. The deposited metal containing vanadium, at wear process under such conditions, has higher (15–20 %) wear resistance. At greater intensity of impact effect $K_d = 2.0$ – 3.5 , the highest wear resistance is provided with normalization from high temperatures (~1100 °N). Thus in the structure prevails austenite (> 70 %) which has the increased stability in relation to strain martensite transformation. With the increase of martensite and carbides content in the structure at the given test conditions, wear resistance decreases. At $K_d = 3.5$, after normalization, the metal deposited using flux-cored strips PL-Np-250Kh10G4F3, has about the same impact-abrasive wear resistance, as deposited with PL-Np-200Kh12G5 not containing vanadium [9].

At surfacing of high-carbon content wear-resistant alloys, formation of cracks usually occurs. An effective technological procedure allowing one to avoid this, and at the same time to obtain metastable austenite with various amounts of strengthening phases in the deposited metal, is surfacing with low-carbon alloys, with subsequent chemical-heat and heat treatments [10]. Use of this procedure allows crack formation to be avoided, while the treatments allow obtaining in the structure of the deposited metal a metastable austenite, and achieve the effect of deformation hardening at operation.

At abrasive wear of the deposited metal type 30Kh10G10, the highest wear resistance is provided after cementation and hardening from 1000 °N. This corresponded to obtaining in the structure, alongside

with martensite and carbides, of metastable austenite (> 50 %), intensely transforming into martensite under the effect of abrasive particles. Thus the increment of strain martensite reaches about 40 %. The positive effect in the increase of wear resistance is produced also by dynamic ageing with precipitation of carbides on the wear surface.

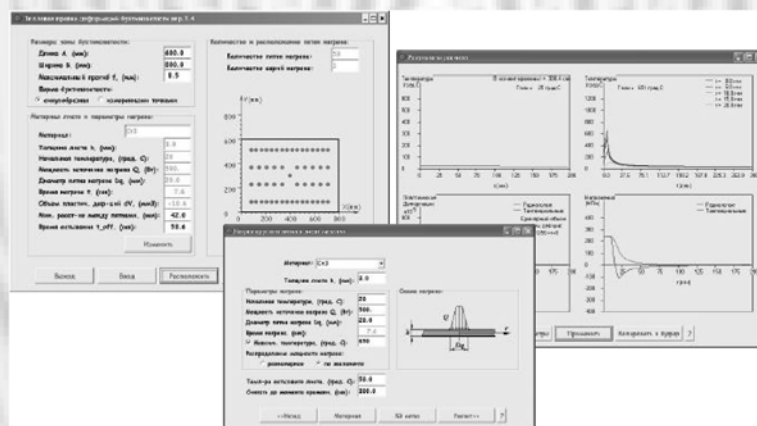
Of great interest are surfacing materials, in which at high tempering carried out after deposition for stress relieving, takes place dispersion hardening of austenite and its destabilization, which intensifies strain martensite transformation.

1. Razikov, M.I., Melnichenko, S.L., Iliin, V.P. (1964) *Welding and surfacing of cavitation steel of 30Kh10G10 grade*. Moscow: NIIMASh.
2. Malinov, L.S., Konop-Lyashko, V.I., Panin, V.D. et al. (1977) Wear resistance of dispersion-hardened steels with instable austenite. In: *Abstr. of 2nd All-Union Sci.-Techn. Conf. on Advanced Methods of Welding in Heavy Machine-Building and Surfacing in Ferrous Metallurgy*. Zhdanov: Zhd. MI.
3. Malinov, L.S., Malinov, V.L. (2001) Manganese-containing surfacing consumables. *The Paton Welding J.*, **8**, 30–32.
4. Malinov, L.S., Poleshchuk, V.M., Derkach, D.O. *Composition of wire for wear-resistant surfacing*. Pat. 23408A Ukraine. Int. Cl. C 22 C 38/38. Fill. 12.07.96. Publ. 02.05.98.
5. Malinov, L.S., Kharlanova, E.Ya., Kolechko, A.A. et al. (1988) New surfacing consumable of C-Fe-Mn-V system for increase of life of overhead crane running wheels. *Svarochn. Proizvodstvo*, **9**, 18–20.
6. Ponomarenko, V.P., Shvartsner, A.Ya., Malko, V.N. et al. (1982) High-manganese steel for electroslag cladding. *Met-allovedenie i Term. Obrab. Metallov*, **10**, 57–60.
7. Razikov, N.I., Kuleshenko, B.A. (1967) On selection of surfacing consumable resistant to cavitation-impact loading. *Svarochn. Proizvodstvo*, **7**, 10–12.
8. Petrov, I.V. (1965) *Study of wear resistance of surfacing consumables under abrasive wear and dynamic loadings*: Syn. of Thesis for Cand. of Techn. Sci. Degree. Moscow.
9. Malinov, V.L. (2000) *Development of sparsely alloyed surfacing consumables for increasing of wear resistance of parts under impact-abrasive wear conditions*: Syn. of Thesis for Cand. of Techn. Sci. Degree. Mariupol.
10. Malinov, L.S., Malinov, V.L. *Method of strengthening*. Pat. 63462 Ukraine. Int. Cl. C 21 D 1/2. Fill. 22.04.2003. Publ. 15.01.2004.

COMPUTER PROGRAM «THERMAL STRAIGHTENING OF BUCKLING DISTORTIONS»

Software «Thermal Straightening of Buckling Distortions» allows determination of parameters of a round heat spot for a definite material and thickness of metal sheet, optimum from the point of view of producing maximum residual plastic shrinkage deformations and prevention of a local buckling of the sheet during heating. The software allows also in-process estimation and arrangement of necessary amounts of such heat spots at the area of buckling zone depending on definite sizes of the zone and value of deformation. The software has been developed to automate the process of thermal straightening of thin-sheet structures with buckling distortions and contains appropriate interface for input of data by sizes of the zone and value of deformation with an automatic system of measurement. To control the process of a manual shock-free thermal straightening, the program envisages the feasibility of a quick input of data to preset the length and width of a rectangular zone of buckling distortion and value of maximum buckling in the zone center. Software gives the opportunity of selection of interface support and reference in two languages (Russian, English).

Purpose. Control of process of manual or automatic thermal straightening of buckling deformations of thin-sheet structures.



View of main window of software, window of data input and representation of results of simulation of a round heat spot

Application. Manufacture of welded thin-sheet structures in ship-, railway car building and other branches. Cost of license for a permanent use of the program is 4900 UAH.

Contacts: Prof. Lobanov L.M.
E-mail: office@paton.kiev.ua



STRUCTURE OF WELDED JOINTS IN TUNGSTEN SINGLE CRYSTALS

K.A. YUSHCHENKO¹, B.A. ZADERY¹, **S.S. KOTENKO¹**, E.P. POLISHCHUK¹ and O.P. KARASEVSKAYA²

¹E.O. Paton Electric Welding Institute, NASU, Kiev, Ukraine

²G.V. Kurdyumov Institute of Metal Physics, NASU, Kiev, Ukraine

Methods of X-ray diffraction analysis and optical metallography were used to examine structure of tungsten single crystal (99.99 wt.%) subjected to local melting (welding) by the electric beam in vacuum. Data were obtained on crystallographic orientation of different zones of a welded joint relative to the base metal. Evaluation of density and distribution of dislocations in these zones was conducted. A zonal non-uniform multi-level distribution of dislocations in the welded joint was determined. Changes revealed in parameters of the dislocation ensemble are attributable to features of thermal-deformation processes occurring in welding.

Keywords: electron beam welding, single crystal, welded joint, X-ray analysis method, crystallographic orientation, dislocation density, structural changes

Mechanical properties, performance and quality of parts comprising welded joints are determined, primarily, by structural and crystallographic processes occurring in metal under the effect of the thermal-deformation welding cycle, and are related to changes in phase composition of multi-phase materials [1, 2], character of texture and size of grains of polycrystalline objects [1–3], and formation of stray grains that violate crystallographic perfection of single crystals and their dislocation structure [4–6]. In turn, this involves formation of micro- and macrocracks in different zones of a welded joint. As follows from the majority of publications, the efforts of researchers are focused on identification of parameters and conditions of welding of a specific material, providing a minimal distortion of structure of the weld metal (WM), compared with the base metal (BM), and, hence, maintaining the level of physical-mechanical properties and performance of the material. When solving this problem, it is not always possible to reveal causes and a mechanism of phase and structural changes leading to formation of microdefects or fracture of a welded joint, which may take place in different zones of the joint, in particular, on the fusion surface, in weld or HAZ. To eliminate the disturbing effect of phase transformations and high-angle grain boundaries on the formation of structure of welded joints during welding, the first stage of investigations was conducted on a single crystal one-phase material — tungsten, which does not feature polymorphic and phase transformations over the entire temperature range.

As in production of welded joints on single crystal materials one of the most important tasks is a maximum possible maintenance of initial characteristics, and, first of all, a single crystal nature of a weldment as a whole, it was necessary to study crystallographic transformations in different zones of a welded joint. Revealing dynamic causes of restructuring of crystal-

lographic characteristics of the initial material under the effect of the thermal welding cycle makes it possible not only to understand the mechanism of formation of a welded joint with the preset crystallographic structure, but also to provide the consistency of quality and physical-mechanical characteristics of welded structures.

The use of the electron beam as a source of heating and melting allowed avoidance of the probability of ingress of active impurities into the WM from the surrounding atmosphere, and made it possible to control the processes of heating, melting and solidification of metal.

X-ray analysis method was selected as a key method for examination of structural transformations, as it is characterised by locality and informativity, and provides minimal distortions of structure during analysis.

Examination procedures. Examinations were carried out on flat specimens measuring $1 \times 10 \times 40$ mm, cut from large-size (38 mm diameter and 550 mm long) single crystals of tungsten (99.99 wt.%) of double electron beam remelting with a standard content of impurities ($1 \cdot 10^{-3}$ – $1 \cdot 10^{-5}$ C, $1 \cdot 10^{-3}$ – $1 \cdot 10^{-5}$ O, $(5$ – $8) \cdot 10^{-5}$ H). A welded joint was produced by electron beam welding (EBW) in vacuum at a residual pressure of about 6.6 MPa, the welding speed in material preheating to 300–600 °C was 22 mm/s. The method for preparation of edges (their crystallographic orientation, bevel angle, presence of cold-worked layer, etc.) exerts a considerable effect on formation and structural state of the welded joint. To exclude this effect, EBW was performed with through penetration. The results obtained can be used for development of the technology for surface treatment of single crystals. Width of the welds was 2–3 mm from the top and 1.8–2.8 mm from the root side, and the selected orientations of the top surface, fusion surface and welding direction were $[1\bar{1}0]$, $[110]$ and $[001]$, respectively (Figures 1 and 2).

Examinations of structure of different regions of welded joints were conducted on flat specimens cut

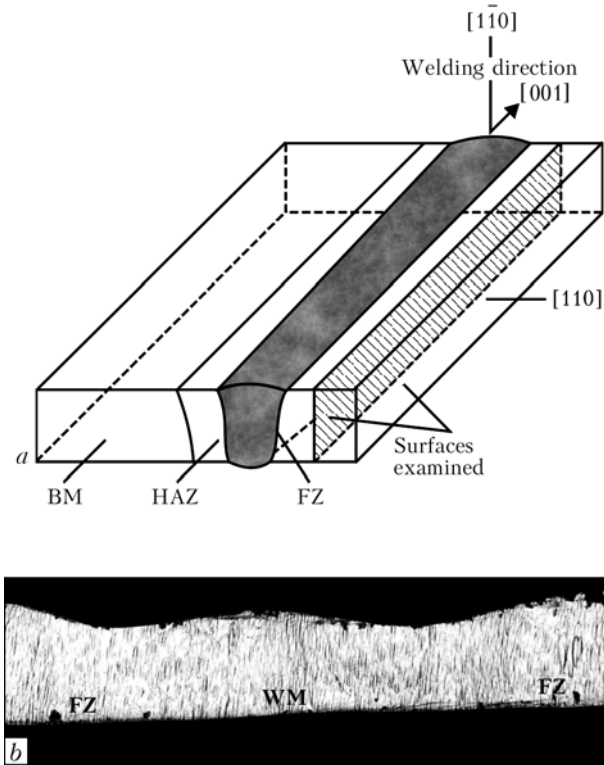


Figure 1. Schematic of cutting of welded joint specimen for metallographic and X-ray examinations (a), and its transverse macrosection (b)

by the electric spark method parallel to the conditional fusion surface (see Figure 1). The cold-worked layer was removed from the surface by electric polishing. The surfaces of the specimens were prepared for examinations according to the traditional procedure used to make microsections of tungsten. The specimens for examinations were cut from the zones of the material located at different distances both to BM and WM from the conditional fusion surface that separated molten metal from non-molten one. The following regions were examined: BM --- here the effect of the thermal-

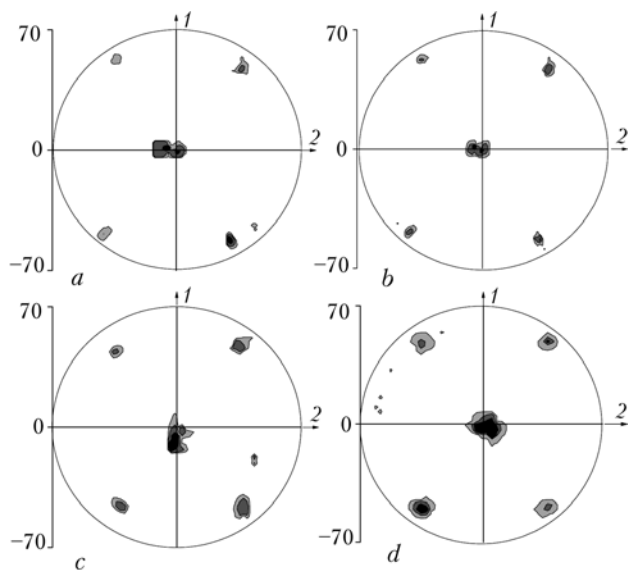


Figure 2. Pole figures {110} in different zones of welded joint: a --- BM; b --- HAZ; c --- FZ; d --- WM; 1 --- welding direction; 2 --- fusion surface

deformation welding cycle can be ignored (the specimens were cut at a distance of 2 and 3 mm from the fusion zone (FZ)); HAZ --- metal subjected to the temperature effect during the welding process (1.4, 1.2, 1.0, 0.4, and 0.1 mm from FZ); FZ --- located at a distance of ± 0.02 and ± 0.08 mm from the conditional fusion surface; WM --- metal heated above the melting point with its subsequent solidification according to the EBW process conditions (0.02, 0.50, 1.00 and 1.25 mm from the fusion surface in a direction to the cast zone).

X-ray examinations of structure of the specimens were conducted by three methods [7, 8]. The method of plotting pole figures was used to determine crystallographic orientation of the specimens before and after EBW in different zones of the welded joint (the accuracy of determination of the reflex centre is approximately 2°). The presence of high-angle boundaries was determined from stray reflexes, which did not correspond to the basic orientation of the material. Material volume V_ω separated by these boundaries from the base single crystal was estimated from the integral value of the intensity under stray reflections.

The shape and width of the Debye lines, i.e. distribution of the intensity of reflections along diffraction vector $I_{q\parallel}$, were studied using the θ - 2θ method.

The X-ray diffraction method [9-11] was used to study the intensity of scattered X-ray radiation in the vicinity of points of the reciprocal lattice in the azimuthal plane normal to diffraction vector $I_{q\perp}$. This method makes it possible to determine $I_{q\perp}$ in any direction in the azimuthal plane, and is similar to the method of rocking curves or ω -scanning with marking out of the $I_{q\perp}$ distribution in one of the azimuthal directions.

$CuK\alpha$ -radiation with a graphite monochromator was used for X-ray analysis. The area of the irradiated region was varied from 0.1 to 2.0 mm², depending upon the character of an experiment. Diffractometer DRON-3M with a texture attachment was employed in the experiments, which provided a four-circle equatorial geometry of an experiment with movement of a specimen about three mutually perpendicular axes, and movement of a detector about axis 2θ . The course of an experiment was controlled using PC. Photographing was performed in a stepwise mode. PC stored data on the intensity of scattered radiation at preset positions of a specimen (points of reciprocal space). Pole figures of $I_{q\parallel}$ and $I_{q\perp}$ distributions were plotted following the programs developed. The same X-ray reflections (110), (020), (200), (211), (21 $\bar{1}$), (121) and (12 $\bar{1}$) were studied in all the specimens, and shape and width ($\delta_{q\parallel}$, $\delta_{q\perp}$) of experimental X-ray reflections were analysed for each of the X-ray reflections. In addition, the values of width of X-ray reflections, averaged over all reflexes, were determined in a direction of maximal, $\delta_{q\perp \max}$, and minimal, $\delta_{q\perp \min}$, broadening for each of the specimens. Experimental (total physical and instrumental) values of broadening of reflexes are considered below. Metallographic ex-



aminations were conducted using microscope OLYMPUS IX70.

Examination results. As seen from Figure 3, *a*, the top surface of a welded joint along the welding direction comprises bands of an inhomogeneous dislocation structure; the same inhomogeneous zonal structure was revealed also on the surface normal to the welding direction (see Figure 1, *b*). Alternating light and dark bands of a fragmented structure comprise finer and coarser sub-grains. The zones of dislocation structure differ from each other in etchability, size and clearness of the fragment and sub-grain boundaries. The coarsest fragments and sub-grains are seen at the centre of WM at the junction of the solidification fronts. Transition from the zone of the material not subjected to melting to WM (Figure 3) takes place within a region less than 0.1 mm wide, the more correct term of which is the fusion zone, rather than the fusion surface.

As shown in Figure 2, coarse main and fine stray reflexes are seen at pole figures in all the zones. Positions of the coarse main reflections {110} are similar to those taking place in BM, HAZ, FZ and WM. Crystallographic orientation of the specimens cut from these zones corresponds to orientation of the top surface (110), fusion surface (110) and welding direction [001]. Therefore, the welding process parameters selected on the basis of earlier studies [6] do provide a single crystal welded joint. Stray, fine and low-intensity reflexes, which do not coincide with positions of main reflexes, are caused partially by incomplete perfection of the single crystal investigated. The volume of imperfections in the material, affecting formation of stray reflections, is approximately 0.01 % of the total volume of the BM single crystal. In HAZ and on the fusion surface (see Figure 2, *b*, *c*), the volume of the material causing such reflections is approximately 0.01 %, which corresponds to the data generated for BM. At the centre of WM (Figure 2, *d*), there is an increase in volume of imperfect regions of the single crystal (0.03–0.05 % of the total volume of the material), which may be related to inheritance by the WM of structure of regions with stray orientation of the material located in the FZ.

Diffraction profiles $I_{q\parallel}$ of reflections (110) are shown in Figure 4. For BM, HAZ and FZ, the shape of the $I_{q\parallel}$ distribution (curves 1–3 in Figure 4) is close to that of the Gaussian curve. Averaged half-width of reflections $I_{q\parallel}$ in HAZ grows to some extent (approximately 1.1 times) compared with BM, and to a more substantial extent (approximately 2.5–3 times) compared with FZ. The shape of reflexes obtained at the centre of WM (curve 4 in Figure 4) varies: there is an increase in the intensity at «tails» of the diffraction profile, and the $I_{q\parallel}$ distribution becomes close to the Lorentz one. Half-width of the $I_{q\parallel}$ distributions in WM (0.5 mm from FZ) and FZ is almost identical (the difference being less than 6 %).

Characteristics of the $I_{q\perp}$ distributions are considered by an example of reflections (110) and (200).

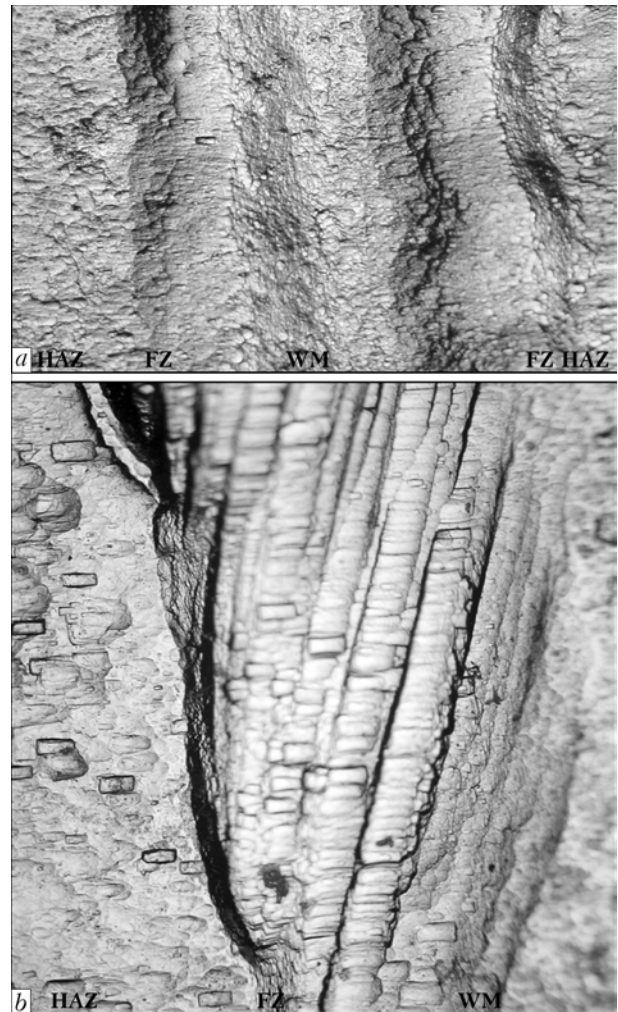


Figure 3. Macrostructure of top surface of welded joint: *a* — $\times 20$; *b* — $\times 50$

Iso-intensive (reflection (110)) and spatial (reflection (200)) $I_{q\perp}$ distributions for these reflexes in different zones of a welded joint are shown in Figure 5. Values of width of the reflexes in the azimuthal plane for a direction of their maximal broadening in all zones of the welded joint are given in the Table. In Figure 6, curves 3 and 4 were plotted on the basis of the data on variations in the reflection width averaged over all reflexes in a direction of maximal, $\delta_{q\perp \max}$, and minimal, $\delta_{q\perp \min}$, azimuthal broadening.

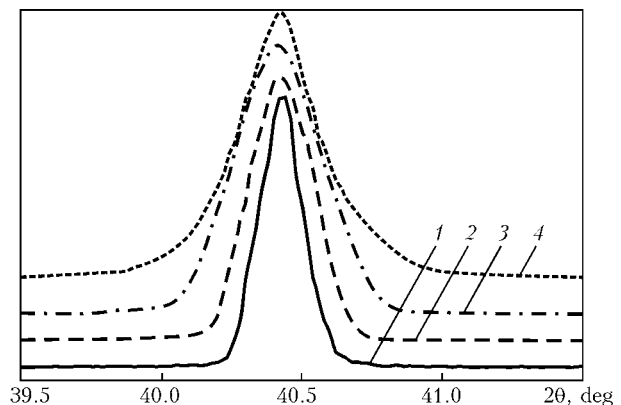


Figure 4. Diffraction profiles $I_{q\parallel}$ of reflections (110) in BM (1), HAZ (2), FZ (3) and WM (4)

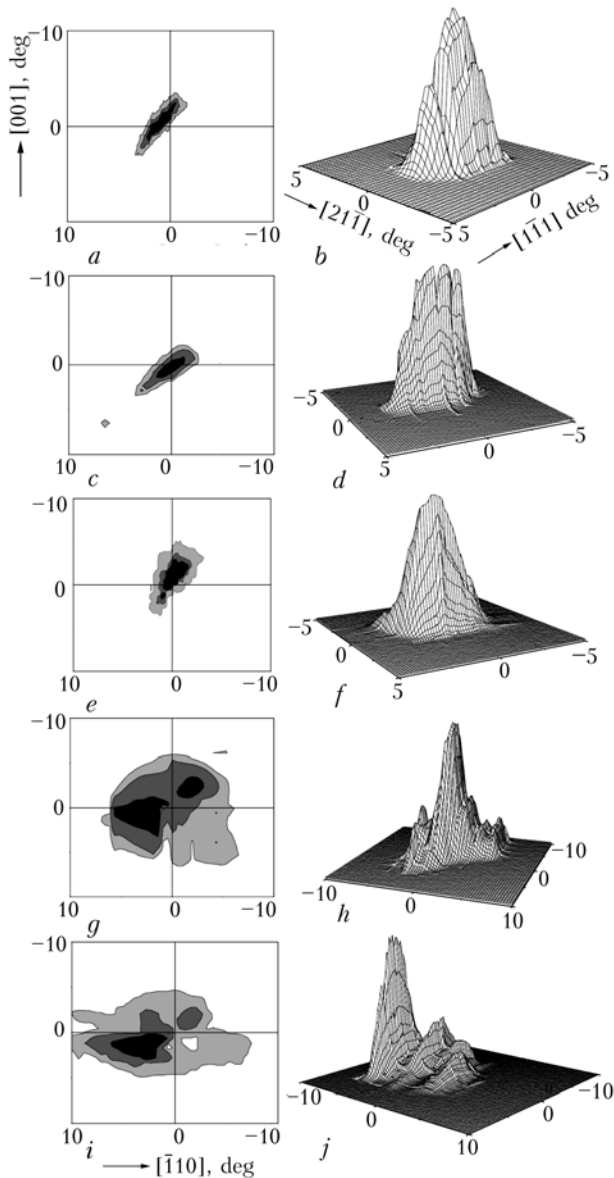


Figure 5. Distribution of intensity $I_{q\perp}$ of reflections (110) (a, c, e, g, i) and (200) (b, d, f, h, j) in BM (a, b), HAZ with increased (c, d) and decreased (e, f) dislocation density ρ , FZ (g, h), and WM (i, j)

In BM (Figure 5, a, b), the iso-intensive curves of $I_{q\perp}$ in the azimuthal plane are close to the elliptic ones for all reflections investigated. Each reflection has directions of maximal and minimal broadening. Crystallographic analysis of the direction of broadening for all reflexes showed that disorientation of substructure elements in single crystal occurred primarily around a direction close to $[1\bar{1}1]$ ($[\bar{1}1\bar{1}]$). The $I_{q\perp\max}$ and $I_{q\perp\min}$ distributions for reflection (110), similar to the rolling curves in two different azimuthal directions and typical of BM, are shown in Figure 7, a. The shape of the $I_{q\perp\max}$ and $I_{q\perp\min}$ distributions for all reflexes is close to that of the Gaussian curve. Besides, in a direction of minimal broadening the shape of the $I_{q\perp\min}$ distribution (Figures 5, b, and 7, curves 2) is smooth, whereas insignificant peaks of the intensity with a 4–12 % decrease in its values from the maximal value are observed sometimes in a direc-

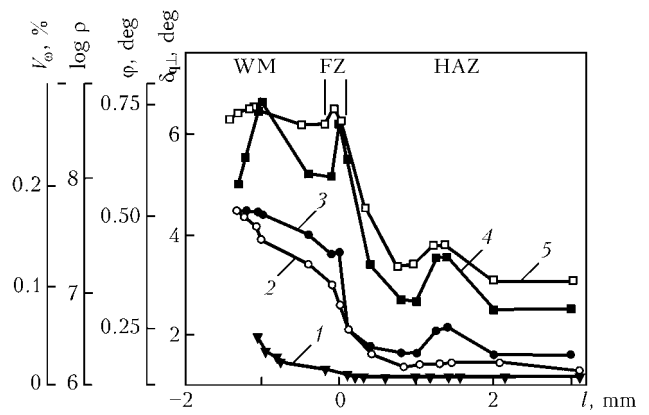


Figure 6. Variations in experimental (V_{ω} , $\delta_{q\perp\min}$, $\delta_{q\perp\max}$) and calculated (ρ , φ) characteristics of dislocation ensemble in different zones of welded joint: 1 — metal volume V_{ω} of stray orientations; 2 — mean angle φ of disorientation of fragments; 3, 4 — averaged values of broadening in a direction of minimal, $\delta_{q\perp\min}$, and maximal, $\delta_{q\perp\max}$, broadening, respectively; 5 — dislocation density ρ ; l — distance from fusion surface

tion of maximal broadening $I_{q\perp\max}$ (Figures 5, a, and 7, curves 1). The quantity of the intensity peaks varies in different reflections and specimens from 3 to 6, while disorientation between them is 0.05–0.12°.

As seen from Figure 5, c–f, the iso-intensive curves of $I_{q\perp}$ in HAZ remain close to the elliptic ones, like in BM. Anisotropy of half-width of the $I_{q\perp}$ distributions in different directions of the azimuthal plane, and in a direction about which the maximal turn of X-ray reflections takes place, persists. It can be seen from the Table and Figure 6 that half-width of reflexes in HAZ depends upon the distance to BM. The entire HAZ can be conditionally subdivided in this parameter into three regions. In the HAZ first region that follows the BM zone in a direction to FZ, half-width of the $I_{q\perp\max}$ distributions increases (growth of the averaged values is approximately 2°), increase in $\delta_{q\perp\min}$ being less intensive (growth of the averaged values is about 1.2°). In the second region, where the examination zone moves closer to FZ, there is a decrease in the above characteristics of the intensity distributions to the values that correspond to BM, or even lower for some reflexes. There is a probability of decrease in $\delta_{q\perp}$ to the lower values than in BM, which is attributable to heterogeneity of structure under examination. Near FZ, in the third region of HAZ, half-width of reflections $I_{q\perp\max}$ and $I_{q\perp\min}$ again grows, and most intensively for $I_{q\perp\max}$. Changes in values of the half-width of reflections in the azimuthal plane are accompanied by transformations of shape of the $I_{q\perp}$ distributions (see Figure 5). The Gaussian shape of the $I_{q\perp\min}$ distributions persists, and variations in the intensity in a direction of maximal broadening of reflexes become stronger for the first region of HAZ with an increased width of reflections. For reflection (200), the angle range comprises the intensity peaks amounting to about 1° (see Figure 5, d). Drop of the intensity between the peaks is 3–19 % of the maximal intensity, the disorientation angles are 0.05–0.24°, and quantity of peaks in a direction of maximal broadening grows 3–5 times, compared with BM. The difference in width



of reflexes in directions of maximal and minimal broadening persists. For the second region of HAZ with a decreased half-width of reflections, the $I_{q\perp}$ distributions again acquire a smooth shape in all azimuthal directions (see Figure 5, *f*). Drop of the intensity between rarely seen peaks is 2–10 %. Their quantity decreases compared with the first region of HAZ and varies from 2 to 5 in different reflections. The difference in width of reflexes in directions of maximal and minimal broadening of $I_{q\perp}$ persists. In the third region of HAZ, directly adjoining FZ, variations in the intensity of the $I_{q\perp}$ distributions aggravate for all reflexes.

In FZ, half-width of the $I_{q\perp}$ distributions (see Figure 5, *g, h*, and Figure 6, curves 3 and 4) considerably grows in all azimuthal directions, which leads to decrease in difference between its values in a direction of minimal and maximal broadening. The $I_{q\perp \max}$ and $I_{q\perp \min}$ distributions of reflection (110) in two different azimuthal directions are shown in Figure 7, *b*. In FZ, the shape of the $I_{q\perp}$ distributions is characterised by clearly defined variations of the intensity. The $I_{q\perp}$ distributions feature a comparatively small number (4–12) of high intensity maxima, caused by a fall of values between peaks by 10–80 % of its maximal value. High intensity peaks are quite smooth, and variations of the intensity in them are insignificant (4–10 %). The iso-intensive lines for high peaks take the form close to circumferences, which makes them substantially different from similar characteristics of the zones of BM and HAZ.

Peculiarity of the WM zone is growth of half-width of reflections $I_{q\perp}$ (see Figure 5, *i* and *j*, and Figure 6, curves 3 and 4) in a direction of minimal broadening, whereas WM can be subdivided into three regions by a change in half-width of reflections in a direction of maximal broadening. The first region of WM, located next to FZ, features decrease in the maximal half-width of the reflection, the second region is characterised by its growth, and the third region corresponding to the central part of the weld is again characterised by decrease in half-width of $I_{q\perp \max}$. The shape of reflection in WM features substantial variations of

the intensity. The fall of the intensity between high peaks is 50–80 % of its maximal value, and the disorientation angle is 0.2–1.4°. In turn, high peaks of the $I_{q\perp}$ distribution are broken down into the lower ones (intensity variations are 5–15 %) with disorientation angles of 0.10–0.25°.

Results and discussions. Positions of main X-ray reflexes in pole figures of different regions of a welded joint are indicative of the fact that the above EBW process conditions result in formation of a single crystal welded joint. The volume of metal, wherein violation of the single crystal structure occurs, is no more than 0.05 % of the total volume of an investigated region of the welded joint. As seen from X-ray and metallographic examinations, the dislocation structure of the welded joint is of a banded zonal character. The X-ray examination results (variations in profile and width of X-ray reflexes of $I_{q\parallel}$ and $I_{q\perp}$) can be interpreted in terms of the theory of scattering of X-rays by the dislocation containing crystals. As follows from study [10], the form of the $I_{q\perp}$ and $I_{q\parallel}$ distributions is determined by parameters of the dislocation ensembles. The Gaussian distribution of the intensity of X-ray reflection along the diffraction vector and in the azimuthal plane occurs in a case where the dislocation ensembles form no long-range stress fields. The width of the reflections is determined by the following expressions:

$$\delta_{q\perp} \sim \varphi_1(\mathbf{b}, \mathbf{t}, \mathbf{q})\sqrt{\rho} \text{ and } \delta_{q\parallel} \sim \psi_1\sqrt{\rho} \text{ tg } \theta,$$

where θ is the Bragg angle; φ and ψ are the orientation factors reflecting relative positions of dislocations with Burgers vector direction \mathbf{b} , dislocation line \mathbf{t} , and diffraction vector \mathbf{G} ($\mathbf{q} = \mathbf{G}/|\mathbf{G}|$).

Orientation factor φ sets the width of reflexes in the azimuthal plane, and determines their possible anisotropy. For example, for crystals containing screw dislocations the iso-intensive curves in the azimuthal plane have the form of circumferences, while for crystals containing edge dislocations these curves have the form of ellipses, the φ factor determining width of these distributions. Structures with Gaussian $I_{q\parallel}$ and $I_{q\perp}$ distributions are characterised by an equal prob-

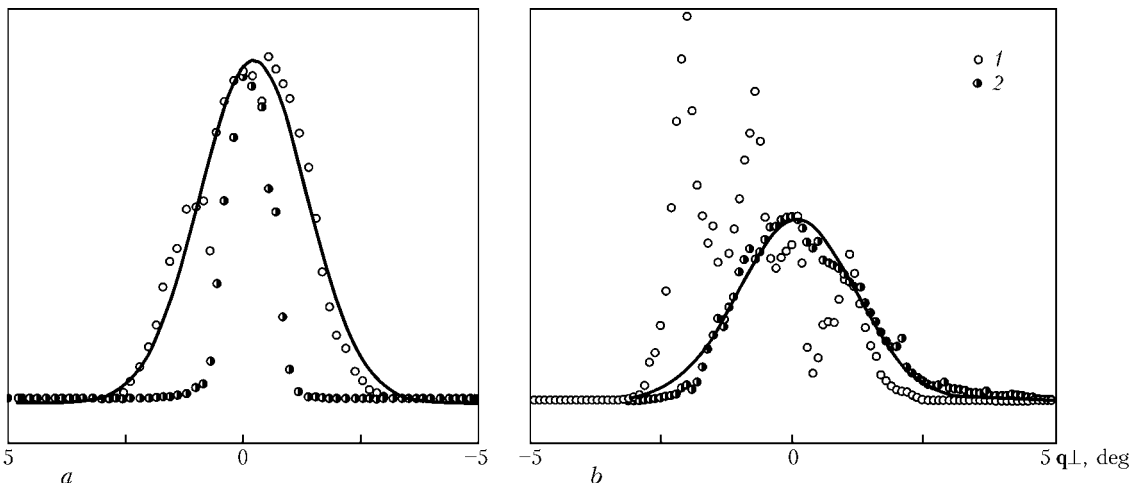


Figure 7. Distribution of intensities $I_{q\perp \max}$ (1) and $I_{q\perp \min}$ (2) of reflection (200) in BM (a) and FZ (b) (solid line — Gaussian curve)



Plane indices	$\delta_{q\perp \max}$ in different zones of welded joint, deg								
	BM	HAZ at distance from FZ, mm			FZ	WM at distance from FZ, mm			
		1.2	1.0	0.4		0.1	0.5	1.0	1.25
(110)	2.20	3.75	2.35	3.51	5.05	5.00	8.00	7.90	5.70
(020)	2.81	4.00	3.10	3.40	6.94	5.95	5.84	6.05	5.29
(200)	3.32	3.97	2.25	3.72	6.45	5.57	5.40	5.55	5.25
(211)	2.30	3.53	2.24	3.34	6.36	5.38	8.15	6.45	6.56
(211)	2.25	3.10	2.31	3.30	4.67	4.24	6.76	4.88	5.54
(121)	2.21	3.56	2.25	3.41	5.86	5.16	5.36	5.37	5.20
(121)	2.25	3.14	2.42	4.02	4.71	4.67	5.70	5.41	4.93

ability of dislocations with opposite (+**b** and -**b**) Burgers vectors, as well as by their chaotic distribution or grouping in walls by the type of the cellular ones.

Dislocation structures with long-range stress fields lead to the Lorentz shape of curves, $I_{q\parallel}$, and Gaussian shape, $I_{q\perp}$, ($\delta_{q\perp} \sim \varphi_2(\mathbf{b}, \mathbf{t}, \mathbf{q})\varpi/D$), $\delta_{q\parallel} \sim \psi_2 D \sec \theta$ (where ϖ is the angle of disorientation of the dislocation wall, and D is the mean distance between the walls). Structures with polygonal walls are an example of such dislocation ensembles. Distribution of the $I_{q\perp}$ intensity has a constant value in the case where the crystal has an excess of dislocations of one sign ($\rho+$) (i.e. the quantity of dislocations with the Burgers vector, +**b** and -**b**, is not equal):

$$\delta_{q\perp} \sim \varphi_3(\mathbf{b}, \mathbf{t}, \mathbf{q})\rho+, \quad \delta_{q\parallel} \sim \varphi_3\sqrt{\rho} \operatorname{tg} \theta.$$

Multi-peak or asymmetric curves $I_{q\perp}$ are formed in the case where the dislocation ensemble has a substantially inhomogeneous, disoriented and multi-level structure, e.g. consisting of coarse fragments separated by the boundaries that contain finer blocks and/or dislocations, and sizes of the fragments are commensurable with an area of the irradiated region (e.g. classical model [12–14]). A condition of averaging over all parameters of a statistic dislocation ensemble, as required in study [15], is not met in such multi-level dislocation structures, which causes peaks (asymmetry) of the intensity in $I_{q\perp}$ (and, sometimes, $I_{q\parallel}$) distributions. The shape of the $I_{q\perp}$ distribution strongly depends upon the ratio of sizes and angles of disorientation of coarse fragments and blocks. In this case, numerical methods are used to estimate parameters of structure of the dislocation ensemble [16–20].

Based on the above theoretical premises, and allowing for the presence in BM of the Gaussian $I_{q\parallel}$ and $I_{q\perp}$ distributions with insignificant intensity peaks in one of the azimuthal directions, as well as results of optical metallography, it can be concluded that the dislocation structure of an initial single crystal consists mostly of chaotically located edge dislocations with Burgers vector directions $[\bar{1}\bar{1}\bar{1}]$ ($[\bar{1}\bar{1}\bar{1}]$). The averaged half-width of a distribution (about 2.5°) under the experimental conditions corresponds to a dislocation density of about $1 \cdot 10^7 \text{ cm}^{-2}$, while the insignificant intensity peaks correspond to sub-boundaries

with a mean disorientation angle of about 0.1°. Individual high-angle boundaries are found in the BM structure. Thus, BM has a structure characteristic of large metal single crystals produced by double electron beam remelting.

In HAZ, the first maximum of the $\delta I_{q\parallel}$ and $\delta I_{q\perp}$ values is formed at a distance of 1.1–1.6 mm from FZ. The Gaussian shape of the $I_{q\parallel}$ and $I_{q\perp \min}$ distributions, increase in the number of peaks, insignificant variations in the $I_{q\perp \max}$ intensity, and microstructure examinations suggest that dislocation boundaries of the cellular type, free from long-range stress fields, the disorientation of which is caused by interlacing dislocations of a different sign, are formed in this region of HAZ. Compared with BM, the averaged half-width of reflections increases by 1.1°, whereas the dislocation density grows 4–5 times, the mean angle of disorientation of sub-boundaries being approximately 0.151°. At a distance of 0.4–0.9 mm from FZ, i.e. closer to WM, the dislocation density decreases to its initial value, and the character of distribution of dislocations in a single crystal structure is close to chaotic. Decrease of the dislocation density in HAZ and its subsequent decrease in a region located both farther from and closer to FZ, are related to peculiarities of the stress-strain state of HAZ. Figure 8 shows results of the calculation of variations in temperature and distribution of welding stresses in different zones of a welded joint*. FZ divides the welded joint into comparatively low-temperature (HAZ) and high-temperature (WM) regions of structure formation, compressive stresses being dominant in the low-temperature region, and tensile stresses ---- in the high-temperature region. Relationship of values of these stresses and sizes of the above regions depends upon the welding conditions. HAZ comprises a region with stresses the values of which are close zero. Here compressive stresses are transformed into tensile ones. Rapid heating of a narrow zone in the welding location to melting point T_{melt} with subsequent levelling of the latter to about $0.4T_{\text{melt}}$ over the entire section of the joint provides relaxation of stresses in the transition region

* Calculations were made by Dr. E.A. Velikoivanenko, the E.O. Paton Electric Welding Institute.



and formation of a dislocation ensemble, the parameters of which are close to those of BM.

The next maximum of $\delta_{q\parallel}$ and $\delta_{q\perp}$ is seen in FZ. Growth of the $\delta_{q\parallel}$ and $\delta_{q\perp}$ values is accompanied by decrease in anisotropy of width of the $I_{q\perp}$ distributions. According to the effect of the orientation factor on the character of iso-intensive lines in the azimuthal plane, decrease in anisotropy of broadening of reflexes with increase in their half-width is related to growth of the dislocation density of a number of slip systems with Burgers vectors ([111], $\bar{1}\bar{1}\bar{1}$). In other words, a change in shape of the $I_{q\perp}$ iso-intensive lines is caused by a change in the stressed state of FZ, compared with HAZ, this leading to growth of values of the Schmidt factor [21] in a larger quantity of the slip systems than in HAZ. Increase of the dislocation density in a number of slip systems with no predominance of any of them is indicative of symmetry of the stressed state. Multi-peak $I_{q\perp}$ distributions and microscopic examinations showed formation of a sub-grain structure with mean disorientation angles of about 0.3° . The average value of $\delta_{q\perp \max}$ grew by about 3.3° compared with BM, and the total dislocation density in FZ increased about 50 times ($5 \cdot 10^8 \text{ cm}^{-2}$) compared with BM.

In WM, the dislocation structure retains its heterogeneous banded character. Heterogeneity of its structure, like in other zones of the welded joint, is seen in a direction normal to FZ. The EBW conditions determining the character of the stress-strain state and time of dwelling of different WM regions in a high-temperature range are the factors that determine the banded character of the dislocation structure. Outside FZ, $\delta_{q\perp}$ first decreases (averaged value --- approximately 1°), and then increases by about 1.3° , after which it again decreases at the WM centre approximately by 2.3° , compared with FZ. In WM, anisotropy of broadening in different azimuthal directions is even lower than in FZ, whereas at the WM centre the averaged values of broadenings in different azimuthal directions are equal, which implies closeness of the values of longitudinal and transverse stresses. The shape of the $I_{q\perp}$ distributions corresponds to a structure with clearly defined sub-boundaries. The mean disorientation angle between coarse fragments of the sub-structure is about 0.50° , and between sub-grains --- about 0.15° . The shape of the $I_{q\parallel}$ distributions has the form of the Lorentz curve, which also reflects a change in character of the dislocation ensemble compared with HAZ and FZ. Considerable fragmentation of X-ray reflexes in the azimuthal plane and results of microscopic examinations allow classification of the dislocation structure at the WM centre as a well polygonised one. Sub-grains with long-range stress fields of the type of polygonal walls prevail in it. This part of the weld is characterised by dominant relaxation processes, while the dislocation density decreases.

It is probable that the revealed peculiarities of sub-structure of a welded joint result in a wavy char-

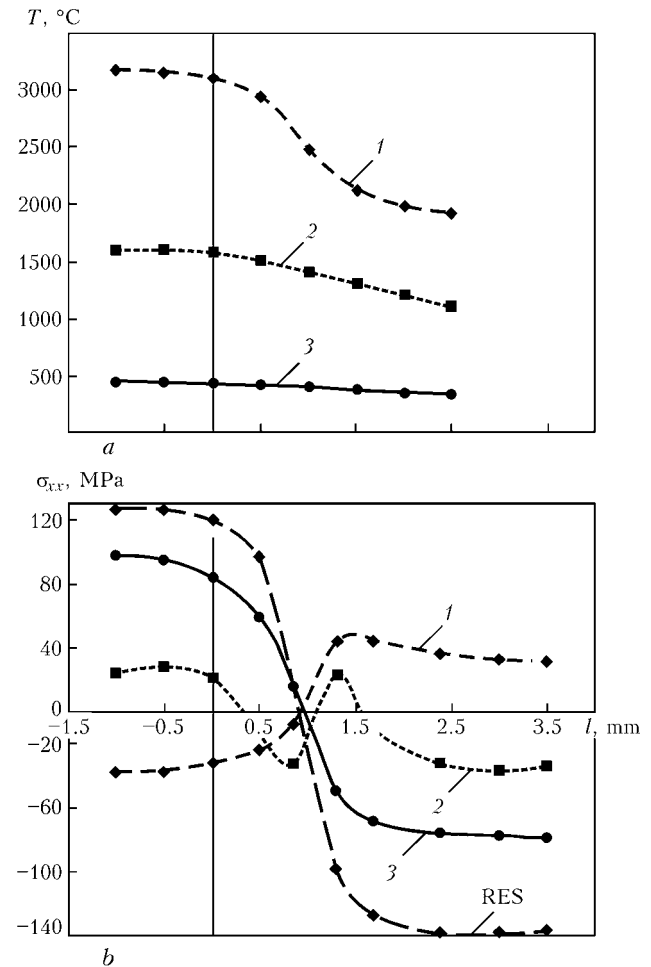


Figure 8. Calculated evaluation of variations in temperature T (a) and distribution of stresses σ_{xx} (b) in cross section of welded joint in tungsten single crystal 1 mm thick after propagation of a melting source for 1 (1), 3 (2) and 15 (3) s

acter of distribution of interstitial inclusions, which was earlier investigated by the authors [19].

It should be noted in conclusion that distributions of the intensity of X-ray reflexes, $I_{q\perp}$ and $I_{q\parallel}$, which depend upon the density of dislocations, character of their location and other parameters of the dislocation ensemble, allow evaluation of the relaxation processes occurring in different zones of a welded joint, as well as prediction of the quality of zones of welded joints in single crystals.

CONCLUSIONS

1. Perfection of structure of different zones of welded joints in tungsten single crystals was examined by X-ray and metallography methods. It is shown that EBW can provide welded joints retaining a single crystal structure of the base metal.

2. Single crystal welded joints are characterised by a banded inhomogeneous dislocation structure, where the dislocation density non-uniformly varies from BM to the centre of WM, this being related to heterogeneity of welding thermal-deformation fields. In HAZ, FZ and WM there are regions with a higher dislocation density than in the neighbouring regions



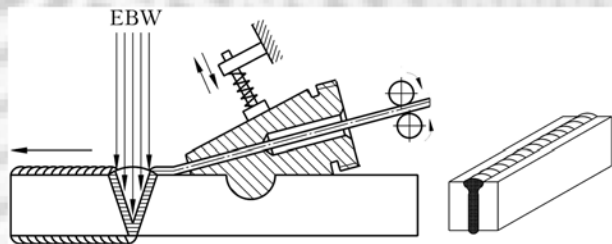
of a welded joint. Values of the dislocation density in these regions depend upon the EBW conditions.

3. Single crystal structure of a welded joint is characterised by isotropic broadening of X-ray reflexes in the azimuthal plane, which is indicative of the presence of the stress-strain state. A multi-level dislocation structure is formed in this case, the main indicator of which is formation of polygonal boundaries.

- Petrov, G.L., Tumarev, A.S. (1977) *Theory of welding processes*. Moscow: Vysshaya Shkola.
- Trefilov, V.I., Milman, Yu.V., Ivanenko, R.K. et al. (1983) *Structure, texture and mechanical properties of wrought molybdenum alloys*. Ed. by V.I. Trefilov. Kiev: Naukova Dumka.
- Nerodenko, M.M., Polishchuk, E.P., Milman, Yu.V. et al. (1978) Bonding of crystallographic textures of base and weld metals on high molybdenum alloys. *Avtomatich. Svarka*, **12**, 12–16.
- Nerodenko, M.M., Polishchuk, E.P., Robnina, M.D. et al. (1979) Peculiarities of solidification and fracture of welded joints in thin-sheet molybdenum and niobium alloys. *Ibid.*, **11**, 14–18.
- Park, J.-W., Babu, S.S., Vitek, J.M. et al. (2003) Stray grain formation in single crystal Ni-base superalloy welds. *J. Appl. Phys.*, **94**(6), 4203–4209.
- Zadery, B.A., Kotenko, S.S., Polishchuk, E.P. et al. (2003) Peculiarities of crystalline structure of welded joints in single crystals. *The Paton Welding J.*, **5**, 13–20.
- Gorelik, S.S., Rastorguev, L.N., Skakov, Yu.A. (1970) *X-ray and electron microscope analysis*. Moscow: Metallurgiya.
- Khejker, D.M., Zevin, L.S. (1963) *X-ray diffractometry*. Moscow: Fizmatgiz.
- Karasevskaya, O.P. (1999) Orientation X-ray experimental method of phase analysis of polycrystals. *Metallofizika i Nov. Tekhnologii*, **21**(8), 34–39.
- Karasevskaya, O.P., Petkov, V.V., Ulshin, S.V. et al. (1995) Specifics of X-ray determination of parameters of single crystal dislocation structure. *Zavod. Laboratoriya*, **61**(3), 18–21.
- Fewster, P.F. (2000) Insight into polycrystalline materials with ultrahigh resolution and reciprocal space mapping. Commission on power diffraction. *Microstructure of Materials*, **23**, 17–19.
- Wilkens, M., Herz, K., Mughrabi, H. (1980) An X-ray diffraction study of cyclically and of unidirectionally deformed copper single crystals. *Z. Metallkund.*, **71**(6), 376–384.
- Ungar, T., Mughrabi, H., Ronnpagel, D. et al. (1984) X-ray line-broadening study of the dislocation cell structure in deformed [001]-oriented copper single crystals. *Acta Met.*, **32**, 333–342.
- Krivoglaz, M.A. (1996) *X-ray and neutron diffraction in nonideal crystals*. Berlin: Springer.
- Karasevskaya, O.P. (2000) Multi-level structures. *Metallofizika i Nov. Tekhnologii*, **22**(11), 44–53.
- Breuer, D., Klimanek, P., Pantleon, W.J. (2000) X-ray determination of dislocation density and arrangement in plasticity deformed copper. *J. Appl. Crystallogr.*, **33**, 1284–1294.
- Barabash, R., Ice, G.E., Larson, B.C. et al. (2001) White microbeam diffraction from distorted crystals. *J. Appl. Phys.*, **79**(6), 749–751.
- Barabash, O.M., Babu, S.S., David, S.A. et al. (2003) Deformation in the heat affected zone during spot welding of a nickel-based single crystal. *Ibid.*, **94**(1), 738–742.
- Zadery, B.A., Smiyan, O.D., Kotenko, S.S. (1995) Distribution of interstitial impurities and structure improvement in single crystal welded joints. *Avtomatich. Svarka*, **4**, 31–36.
- Karasevskaya, O.P., Ivasishin, O.M., Semiatin, S.L. et al. (2003) Deformation behaviour of beta-titanium alloys. *Mater. Sci. and Eng.*, **A354**, 121–132.
- Schmidt, E., Boas, B. (1938) *Plasticity of crystals, and metallic ones in particular*. Moscow-Leningrad: GONTI KKTP SSSR.

TECHNOLOGY FOR EBW OF SHEET STRUCTURES WITH SIMULTANEOUS FEED OF FILLER WIRE TO THE WELD POOL

Semi-finished products in the form of sheet billets constitute a large portion in fabrication of different-application welded structures. Because of specific features of the process of electron beam welding of aluminium alloys, formation of the joints occurs with some lowering of the weld metal surface with respect to the upper plane of the sheets welded.



The technology of EBW with a simultaneous feed of filler wire to the weld pool was developed to avoid the above defect of welded joints in sheet billets. Welding can be performed in different spatial positions using no forming devices. The welds in this case are deposited to form a reinforcement bead, and penetration on the underside of a joint is provided.

Filler wire 0.8–2.6 mm in diameter can be fed during the welding process to the weld pool on any side relative to the melting front. This is particularly important for the case of a simultaneous utilisation of devices providing alignment and guiding of the beam along a joint, where the joint ahead of the beam should not be «closed».

The developed technology and filler wire feeding mechanism can also be employed for performing cladding operations, lining of surfaces and filling of wide gaps in a joint in multipass welding.

Proposals for co-operation. Development of technical documents, transfer of know-how for the technology, technical consultations and engineering services in commercial application of the technology.

Contacts: Prof. Ishchenko A.Ya.
E-mail: office@paton.kiev.ua



EFFECT OF PARAMETERS OF PLASMA DETONATION UNIT DISCHARGE CIRCUIT ON GAS-DYNAMIC CHARACTERISTICS OF PULSED PLASMA FLOWS

M.L. ZHADKEVICH, Yu.N. TYURIN, O.V. KOLISNICHENKO and V.M. MAZUNIN
E.O. Paton Electric Welding Institute, NASU, Kiev, Ukraine

Physical-mathematical model is proposed for description of acceleration of the detonation wave, and calculations of gas-dynamic characteristics of plasma jets generated by a plasma detonation unit were performed. Effect of electric parameters of the discharge circuit on temperature and velocity of plasma behind the detonation wave was analysed. It is established that decrease in inductance leads to a considerable growth of the above plasma characteristics.

Keywords: pulsed plasma flow, amplitude-time characteristics, plasma, parameters of electric circuit

One of the main ways of addressing the problem associated with extension of service life of machine parts or their repair is development and application of technologies of thermochemical treatment and thermal spraying for surfaces of parts using the concentrated heat sources. Methods of continuous treatment and spraying, such as flame, arc and plasma, are widely applied for this purpose. Currently, a special attention is paid to developments of the pulsed plasma technologies using the pulsed plasma units to provide high-enthalpy plasma flows both for treatment of surfaces of solid bodies and for deposition of functional coatings.

The pulsed plasma generator considered in this article uses detonation of a fuel gas mixture (C_3H_8 , O_2 , air) to form conditions for voltage breakdown. Acceleration of plasma in the generator occurs due to a complex impact by the gas-dynamic and electromagnetic forces.

After realisation of conditions of detonation combustion of the fuel gas mixture, the detonation wave propagates through a circular space in channel of the

pulsed detonation unit, which is formed by two coaxial electrodes with a difference of potential induced between them. Schematic diagram of the generator is shown in Figure 1.

The electric current flows through the detonation products behind the detonation wave. As a result of development of the discharge, the detonation wave is followed by the shock-compressed plasma heated by the pulsed discharge. The pulse voltage and current between the coaxial electrodes (Figure 2) are registered using a voltage divider and Rogovsky belt with an integrating link [1]. The double-beam memory oscilloscope S8-17 was used as an instrument registering the above parameters. The major part of the charge of capacitors is consumed for heating and ionisation of the detonation products, and further acceleration of the formed shock-compressed region of plasma. The damping oscillation process occurs at the ionised detonation products until the entire reacted gas leaves the inter-electrode space of the plasma generator. As experimentally found from the damping curves, resistance of the inter-electrode space ranges from 0.04 to 0.10 Ohm.

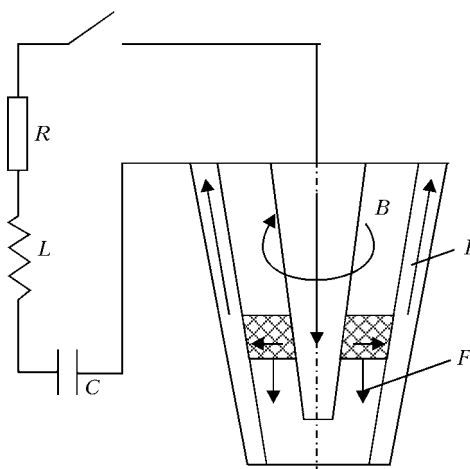


Figure 1. Schematic diagram of pulsed plasma generator: R , L , C — resistance, inductance and capacitance of discharge circuit, respectively; B — induction of magnetic field; I , F — current and magnetic gas-dynamic acceleration force, respectively, formed at discharge of capacitor storage

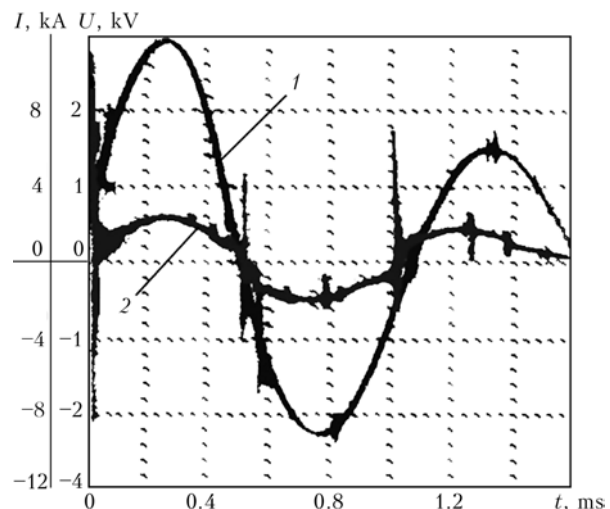


Figure 2. Distribution of current I (1) and voltage U (2) in pulsed plasma generator at discharge of capacitor storage: $C = 800 \mu F$; $U = 2800 V$; $L = 30 \mu H$



The calculation model of acceleration of the detonation wave in the detonation pulsed plasma unit was developed, and parameters of the plasma were evaluated to optimise the pulsed plasma technology and determine the effect of geometry of the coaxial accelerator and electric parameters of the discharge circuit.

The procedure developed allows for the fact that in high-pressure accelerators one of the main roles in acceleration of a working gas is played not only by the electromagnetic interaction forces, but also by the thermodynamic processes of conversion of Joule heat into the kinetic energy. If at a pressure below the atmospheric one it is enough to allow only for the magnetic pressure (used to calculate devices of the plasma focus type [2]) to calculate dynamics of the dense plasma, at a high pressure an important mechanism promoting acceleration of plasma is ohmic heating of the current layer [3]. And in this case it is necessary to take into account the entire inter-electrode volume of the plasma generator passed by the discharge front.

The following simplifications were made to obtain an approximate solution, which would allow for the above main physical mechanisms and be suitable for engineering calculations.

1. The energy behind the detonation wave consumed for dissociation of molecules and ionisation is negligible, compared with energy of the electromagnetic field and chemical energy released in propagation of the detonation wave.

2. The inductance of plasma behind the detonation wave is of an electron character, and it is determined using the Frost formula [4], which is the simplest interpolation between the Lorentz and Spitzer asymptotic forms:

$$\sigma = \frac{n_e e^2}{3kT} \frac{v_e^2}{(v_{ei}/\gamma_S) + v_{ea}}, \quad (1)$$

where n_e is the concentration of electrons; e is the electron charge; k is the Boltzmann constant; T is the temperature of the thermally equilibrium plasma; v_e is the thermal velocity of an electron; $\gamma_S = 0.582$ is the Spitzer factor for the single-ionised plasma [5]; v_{ei} and v_{ea} are the frequencies of collision of electrons with ions and atoms, respectively, determined through the dissipation section [6, 7].

3. The hydraulic approach providing for averaging of parameters of the flow in each section of the inter-electrode channel was used to simplify the problem. In this case the surface of the detonation wave front consists of regions located normal to the electrodes. The vectors of density of the electric current, j , and field intensity, E , are normal to the electrode generating line, while the velocity vector v of the flow is parallel.

Dynamics of the detonation wave was described using the Whitham's method [8], characterising variation in the Mach number of the detonation wave, M_d , depending upon the distance it passed. The problem was solved using the differential equation written down in a dimensionless form for gas-dynamic parameters in propagation of the detonation wave, expressed in M_d [9]:

$$\begin{aligned} (1 + \sqrt{\frac{\gamma}{(\gamma - z)(1 + z)}}) (1 + z + \sqrt{\gamma(\gamma - z)(1 + z)}) \frac{dz}{d\xi} = \\ = k(1 - z)^2 \sqrt{1 - z^2} - \gamma(1 - z^2) \frac{1}{A} \frac{dA}{d\xi}, \end{aligned} \quad (2)$$

where $z = \sqrt{1 - (M_j^2/M_d^2)}$ is the dimensionless value; M_j is the Mach number of the Chapman-Jouguet wave, which characterises the fuel mixture and is determined by the amount of heat released in combustion of unit mass of the initial mixture; $\xi = l/l_c$ is the dimensionless value (here l is the distance along the generating line to a point of initiation of the detonation wave, and l_c is the length of the channel along

the generating line); $k = \frac{\sigma E(t)^2 (\gamma - 1) (\gamma + 1)^2 l_c}{\gamma a_0 p_0 M_j^3}$ is the function characterising the current flowing through the accelerator; γ is the adiabatic exponent of the reaction products; a_0 is the velocity of sound in the detonating mixture; p_0 is the initial pressure; and $A = A(l)$ is the area of the perpendicular section of the circular space along axis l .

Differential equation (2) was solved by the numerical Kutt-Merson method. Dependence $E(t)$ was calculated using experimental data. The initial condition corresponds to $z(0) = 0$. Velocity of the detonation wave and gas-dynamic parameters of the shock-compressed region are determined from the known value of $z(\xi)$ using the following formulae:

velocity of the detonation wave

$$D = \frac{a_0 M_j}{\sqrt{1 - z^2}};$$

density of the detonation products immediately behind the detonation wave

$$\rho = \rho_0 \frac{\gamma + 1}{\gamma - z};$$

averaged value of the velocity of gas behind the detonation wave in a direction of axis l

$$v = \frac{M_j a_0}{\gamma + 1} \sqrt{\frac{1 + z}{1 - z}};$$

pressure of the detonation products immediately behind the detonation wave

$$p = \frac{\gamma p_0 M_j^2}{(\gamma + 1)(1 - z)};$$

velocity of sound in the detonation products immediately behind the detonation wave

$$a = \frac{M_j a_0}{\gamma + 1} \sqrt{\frac{\gamma(\gamma - z)}{1 - z}}.$$

The mathematical model described was used to calculate characteristics of the supersonic flow formed in the plasma detonation unit depending upon the electric parameters of the discharge circuit.

It can be concluded on the basis of analysis of the resulting calculation curves (Figure 3) that the main effect on heating and acceleration of the ionised combustion products at the electric parameters considered



is exerted by the inductance of the electric discharge circuit. Growth of the energy input into a pulse due to a change in voltage and capacitance of the capacitor banks allows the extension of time of the workpiece surface modification process. Increase in the inductance of the electric discharge circuit at constant capacitance and voltage causes a substantial decrease in values of the plasma parameters (velocity, temperature) at the plasma generator output.

As shown in practice, application of the given pulsed plasma detonation generator at low inductance (below 10 μH) of the discharge circuit leads to decrease in service life of the coaxial electrodes, which is caused by a considerable increase (above 25 kA) of the inter-electrode space breakdown current. In this case temperature of the plasma (Figure 3, a) amounts to 20000 K or higher. If the plasma generator is applied to form the pulsed plasma jets for heating and acceleration of powders with subsequent formation of functional coatings, it is recommended to use the following electric parameters: $U = 3000\text{--}3500\text{ V}$, $C = 800\text{--}1000\ \mu\text{F}$, and $L = 15\ \mu\text{H}$. In this case temperature of the plasma is not in excess of 12000 K, and its velocity amounts to 4500 m/s, which is enough for heating and acceleration of powder. Values of the electric parameters depend upon the particle size of a spray powder and thermal-physical properties of its material.

The plasma detonation generators can be efficiently applied for thermochemical treatment of surfaces of tools and machine parts [10]. The process of influence of a high-intensity heat flow formed by the plasma generator provides heating of the surface and its subsequent cooling, the latter being caused by removal of heat both into the environment and into the material. This results in phase transformations occurring in the surface layer. Properties of a heat-hardened layer (thickness, phase composition, physical-mechanical characteristics) are affected, primarily, by the energy of the heat flow and duration of its impact. Duration of the heat flow in pulsed plasma treatment is 0.5–0.8 ms, and it can be adjusted through inductance of the electric discharge circuit ($L = 25\text{--}50\ \mu\text{H}$). Values of the heat flow energy $q = 4 \cdot 10^4\text{--}1.5 \cdot 10^5\text{ W/cm}^2$, which depend upon the temperature and velocity of the plasma jet, are selected on the basis of variations in voltage at plates of the capacitor bank ($U = 2800\text{--}3500\text{ V}$) and its capacitance ($C = 800\text{--}1200\ \mu\text{F}$). The parameters used make it possible to produce the hardened layers up to 70 μm thick on carbon steels. And service life of electrodes of the plasma generator is maintained at a substantial level.

CONCLUSIONS

1. Distributions of current and voltage in the plasma detonation generator operating in the pulsed mode were experimentally found.

2. Analysis of the effect on gas-dynamic characteristics of plasma immediately behind the detonation wave by the electric parameters of the discharge circuit was conducted.

3. The calculation model allowing evaluation of the parameters of plasma required both for calculation of heating and acceleration of powders in the plasma deto-

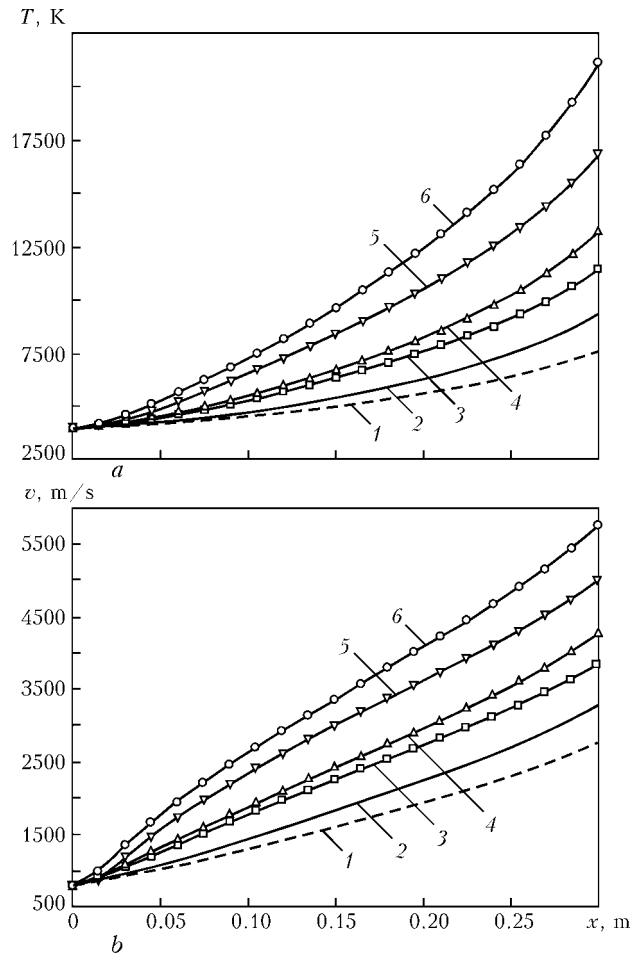


Figure 3. Variations in temperature (a) and velocity (b) of plasma behind the detonation wave as it passes through the inter-electrode space: 1 — $U = 2800\text{ V}$; $C = 1000\ \mu\text{F}$; $L = 30\ \mu\text{H}$; 2 — $U = 3500\text{ V}$; $C = 1000\ \mu\text{F}$; $L = 30\ \mu\text{H}$; 3 — $U = 3200\text{ V}$; $C = 800\ \mu\text{F}$; $L = 15\ \mu\text{H}$; 4 — $U = 3200\text{ V}$; $C = 1000\ \mu\text{F}$; $L = 15\ \mu\text{H}$; 5 — $U = 3200\text{ V}$; $C = 800\ \mu\text{F}$; $L = 7.5\ \mu\text{H}$; 6 — $U = 3500\text{ V}$; $C = 800\ \mu\text{F}$; $L = 7.5\ \mu\text{H}$

nation unit in the case of deposition of coatings, and for evaluation of heat flows into a workpiece in implementation of the technology for pulsed plasma hardening of the surfaces of tools and machine parts was developed using experimental data and theoretical provisions.

- Andelfinger, K. (1971) Methods for investigation of fast processes in plasma physics. In: *Physics of fast processes in plasma physics*. Moscow: Mir.
- Vikhrev, V.V., Braginsky, S.I. (1980) *Problems of plasma theory*. Issue 10. Moscow: Atomizdat.
- Gurovich, B.Ts., Desyatkov, G.A., Spektrov, V.L. (1987) Peculiarities of motion of current shell and shock wave in high pressure pulse accelerator. *Doklady AN SSSR*, 293(5), 1102–1105.
- Tovstopyat-Nelip, I.I., Triger, S.A. (1988) On theory of electrical conductivity of partially ionized plasma. *Teplofizika Vys. Temperatur*, 3(26), 417–435.
- Spitzer, L. (1965) *Physics of fully ionized discharge*. Moscow: Mir.
- Rajzer, Yu.P. (1992) *Physics of gas discharge*. Moscow: Nauka.
- Dresvin, S.V., Donskoj, A.V., Goldfarb, V.M. et al. (1972) *Physics and technique of low-temperature plasma*. Moscow: Atomizdat.
- Whitham, J. (1977) *Linear and non-linear waves*. Moscow: Mir.
- Tyurin, Yu.N. (1977) *Principles of technology for surface hardening of products by electric discharge plasma*: Thesis for Doctor of Sci. (Eng.) Degree.
- Tyurin, Yu.N., Kolisnichenko, O.V., Tsigankov, N.G. (2001) Pulse-plasma hardening of tools. *The Paton Welding J.*, 1, 38–44.

RESISTANCE WELDING OF ALUMINIUM-STEEL TRANSITION PIECES USING DEFORMABLE COMPOSITE INTERLAYERS

V.S. KUCHUK-YATSENKO, A.V. LOZOVSKAYA, A.A. NAKONECHNY and A.G. SAKHATSKY
E.O. Paton Electric Welding Institute, NASU, Kiev, Ukraine

A new technology has been developed for resistance welding of aluminium to steel in fabrication of bimetal transition pieces of large cross-section current-carrying buses used in electrolyzers in aluminium production. The mechanism of pack deformation and welded joint formation has been studied. An experimental set-up and welding process control module have been manufactured.

Keywords: resistance welding, current-carrying buses, bi-metal transition pieces, composite interlayer, technology

Development of technologies of press welding of aluminium to steel is due to the need to apply bimetal current-conducting buses of a large cross-section. Of special interest is resistance welding of a pack of aluminium plates to a solid steel bus, which is difficult to perform by other welding processes.

As shown by experience, high strength of aluminium-steel welded joints is achieved at not more than 6 μm thickness of intermetallic layer. It should be noted that mechanical properties of welded joints are largely dependent on the conditions of formation of intermetallic phases. They preserve a satisfactory level just at the initial stage of the welding process, when transverse growth of the intermetallic phase proceeds. A sound welded joint of the above dissimilar metals can only be obtained by those welding processes, in which the thermal cycle does not exceed the temperature-time conditions of intermetallics formation. Pressure welding meets the above requirements to the greatest degree. Such joining methods as explosion, friction, magnetic-pulse, resistance and flash-butt welding, as well as rolling, became accepted in manufacture of aluminium-steel transition pieces. All these processes are applicable in the case of welding items of limited type-sizes, but are unsuitable for producing bimetal joints of a large cross-section and complex configuration. In addition, essential limitations

are imposed by the high cost of the used equipment and complexity of its operation.

The purpose of this work is development of the technology of producing aluminium-steel transition pieces of large cross-section current-carrying buses, in particular, cathode assemblies of electrolyzers for aluminium production. The following requirements are made of such a component: fracture resistance on the level of base metal --- AD1 aluminium; stable low transition electric resistance; possibility of continuous operation at elevated temperatures and shock mechanical loads under the impact of electromagnetic forces.

Resistance welding was optimized on samples of 120 \times 700 \times 40 mm size, consisting of 20 sheets of AD1 aluminium 1 mm thick and 2 plates of steel 20, 10 mm thick, which were full-scale samples of transition pieces of electrolyzer cathode (Figure 1). Special deformable composite interlayers filled with nonelectrically-conducting flux were placed into the gaps between the aluminium and steel plates. Features of the joint formation were studied on butt samples of 25 mm diameter.

Flux of KF-AlF₃ system was used for protection of the welding zone from oxidation, cleaning it from oxides and activation of the surfaces of metal to be joined. To conduct the experiments upgrading of K602 welding press was performed, specialized modules of welding process control were developed, as well as a fixture, allowing welding of a pack of aluminium and steel plates using the flux.

It is known that application of solid-phase pressure welding will allow reducing or avoiding formation of a continuous intermetallic interlayer. Such a welding process, however, requires high shear deformations and limitation of the weight and size parameters of welding machines, and is used only for welding small-sized parts [1]. Application of welding processes in which surface activation results from wetting by the liquid phase, causes the inevitable formation of intermetallic interlayer, because of a significant heat input into the joint zone, which is related to considerable heat capacity, heat and electrical conductivity of alu-

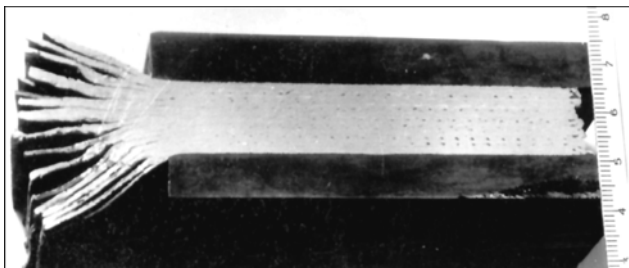


Figure 1. Full-scale sample of an aluminium-steel transition piece of an electrolyzer cathode

minium. For an item of the type of aluminium-steel transition piece of an electrolyzer, in which a pack of aluminium plates are simultaneously lap-welded to each other and to steel plates with a large surface area, one hundred percent weldability can only be achieved in the presence of a liquid phase in the joint zone. It is necessary to limit the welding heat input and temperature, to avoid exceeding the latent period of formation of the intermetallic interlayer.

In the developed welding process, activation of the contact surface of wetting with the liquid phase and plastic deformation occur, this allowing reduction of the welding temperature and time, as well as plastic deformation. This welding process is based on application of finely-dispersed activators, which are added to the welding flux to ensure formation of a liquid eutectic phase at the temperature below that of aluminium melting temperature. An additive of finely dispersed powders of silicon, copper or zinc was used as activators. Butt welded aluminium-steel samples were tested for rupture, and samples welded by overlap joints were tested for shear. Transition electric resistance of the weld was measured.

Figure 2 shows variation of arc voltage U_a , welding current I_w and power Q evolved during time t of welding in abutted samples of 25 mm diameter at the upset force of 10 MPa.

To reveal the features of weld formation and the influence of various activators on strength and electric resistance of the weld, studied were three batches of samples produced in the optimum mode of welding, using activating additives, namely silicon, copper and zinc.

Tensile testing showed that samples produced using the flux with silicon additive fail in the near-weld zone of aluminium at ultimate strength of 55–60 MPa. Ultimate strength of samples with copper additive is equal to 48–52 MPa, and fracture runs in the intermetallic interlayer from the aluminium side. Samples welded with zinc additive have the ultimate strength of 40–43 MPa, and fail in the weld. Measurement of transient resistance of weld metal was conducted using a microohmmeter and ammeter-voltmeter: in samples made with an additive of silicon it was 1.5; copper --- 2; zinc --- 3.7 μOhm .

Features of formation of the structure and nature of phase formation in the welding zone were studied using the methods of optical and analytical electron microscopy. Figure 3 shows the microstructure of welded joint of AD1 aluminium-steel 20, produced using silicon-containing flux.

It is established that no traces of an aluminium composite interlayer used in welding were found. In aluminium structure at the transition zone the eutectic precipitations along the grain boundaries are absent, which is indicative of a complete ousting of the near-eutectic liquid phase from the joint at upsetting.

Transition zone in aluminium-steel joints produced by welding using the above activators, features different structure: when flux with a silicon additive is

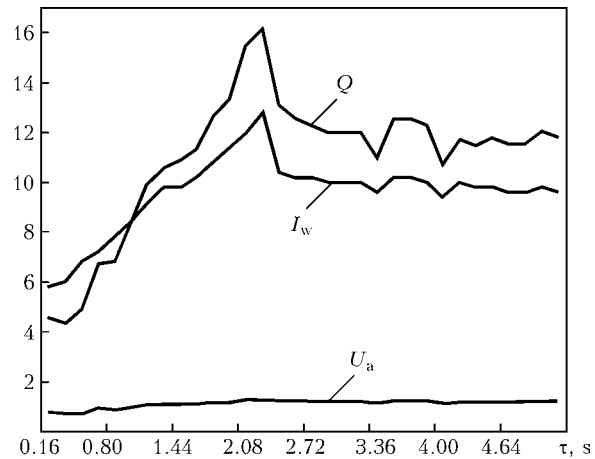


Figure 2. Diagram of the change of the main parameters of the welding process during time τ

used, it is close to a rectilinear one, with copper additive it is wavy, with zinc --- wavy with micropores. A feature of the microstructure shown in Figure 3, is that the forming interlayer consists of layers differing in their etchability. Interlayer thickness is from 3 to 5 μm with a dark layer adjacent directly to aluminium, followed by a thinner intermediate layer and a toothed layer from the steel side. Such a nature of the structure of the transition intermetallic interlayer is indicative of the fact the process of joint formation is accompanied by two-sided diffusion processes, namely iron penetration into aluminium and of aluminium into steel. Usually, in solid-phase welding the intermetallic interlayer does not have a toothed structure, which is characteristic for iron aluminizing by liquid aluminium. This is indicative of the fact that at the initial stage of welding steel is wetted by an aluminium-based alloy. When copper and zinc are used, the weld metal structure forms a developed contact zone, having protrusions and indentations, which is indicative of active dissolution of aluminium in the liquid phase. Intermetallic interlayer thickness from 3 to 6 μm is envisaged in this case. As at the same thermal cycle the temperature of zinc-aluminium eutectic formation is equal to 382 $^{\circ}\text{C}$, of copper-aluminium --- 548 $^{\circ}\text{C}$ (whereas for silicon-aluminium

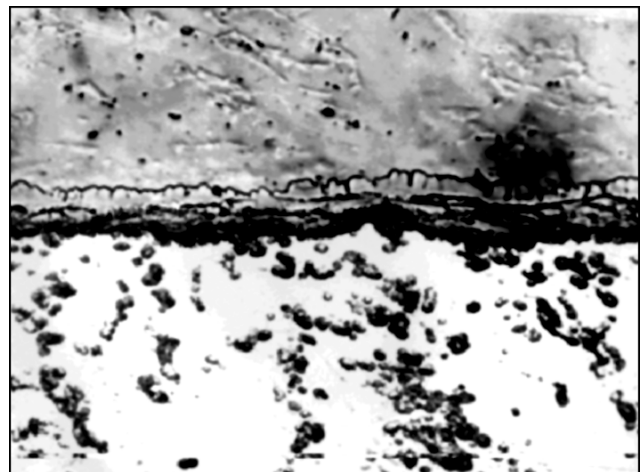


Figure 3. Microstructure of an aluminium-steel welded joint produced when using a flux with silicon ($\times 400$)



it is 577 °C) [2], base metal dilution is much more intensive at the same welding temperature. This leads to formation of a wavy metal structure.

The composition of the joint transition zone was studied, in order to identify the phase components in the zone of steel and aluminium interaction, using X-ray microprobe analysis. Considering that the thickness of the intermetallic interlayer is not more than 5 µm, and that of individual layers — not more than 2 µm, recording was conducted at an angle of 10° to the joint boundary. In addition, structural components of the weld transition zone were determined by irradiation of the object of study by a stationary probe. Analysis of the diagrams of element distribution leads to the conclusion that the intermetallic interlayer formed in the transition zone, has a complex composition, and phases based on Fe₃Al, FeAl₂, FeAl₃ can be found in its individual layers, which are alloyed with silicon, copper and zinc, respectively. According to the published data [3], such alloying prevents further growth of the intermetallic interlayer, this being particularly important in operation of the aluminium-steel transition piece at elevated temperatures.

CONCLUSIONS

1. The proposed technology of resistance welding allows producing sound aluminium-steel joints of a complex configuration with developed surface area. Compared to the technology of the traditional resistance welding, the new technology envisages a lower specific power and upset force, this significantly improving the weight and dimensional parameters of resistance welding machines.

2. The welding process runs in two stages: formation of the liquid metal phase, its wetting of the base metal and ousting of molten flux; and aluminium adhesion to the aluminized layer at solid-phase plastic deformation.

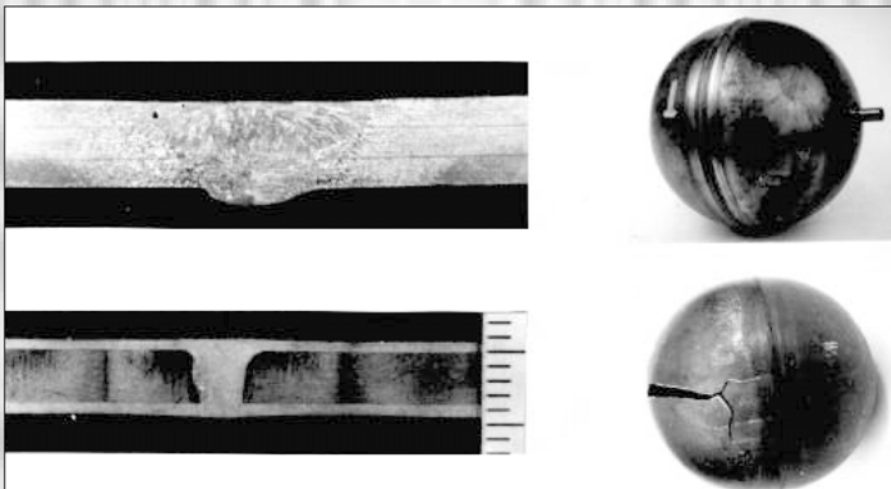
3. An intermetallic interlayer not more than 5 µm thick forms in the zone of aluminium contact with steel, the interlayer being enriched in activating additives, which lower its growth rate.

1. Gelman, A.S. (1970) *Principles of pressure welding*. Moscow: Mashinostroenie.
2. Hansen, M. (1941) *Structure of binary alloys*. Moscow: Mashgiz.
3. Ryabov, V.R. (1983) *Welding of aluminium and its alloys with other metals*. Kiev: Naukova Dumka.

ARGON-ARC WELDING OF JOINTS OF HIGH-STRENGTH MULTI-LAYER STEELS IN SIMILAR AND DISSIMILAR VERSIONS

The high-strength multi-layer steels in similar and dissimilar version of 3–12 mm thickness consist of two and more layers, joined between each other in planes. The high strength is provided by layers of maraging steels and corrosion resistance is provided by external layers of high-alloy chromium-containing steels. The strength of multi-layer corrosion-resistant steels is 1200–2000 MPa depending on the combination of materials and ratio of thicknesses of the layers. The strength of the welded joint of the multi-layer steel made by the offered argon-arc method, reaches 0.87–1 of strength of the parent metal depending on used welding consumables and technological process of welding.

Application. For manufacture of high-pressure vessels and containers, operating under conditions of high loads and corrosion action. Its application is possible in aerospace industry, chemical machine building, for manufacture of navy machinery.



Proposals for co-operation. Creation of multi-layer steels, development of technologies of manufacture and welding, production of experimental batches of these steels and products on contract base.

Contacts: Prof. Savitsky M.M.
E-mail: savitsky@paton.kiev.ua

EFFECT OF SILICON ON PROPERTIES OF LOW-ALLOY CARBON DEPOSITED METAL

A.P. ZHUDRA, S.Yu. KRIVCHIKOV and V.V. PETROV
E.O. Paton Electric Welding Institute, NASU, Kiev, Ukraine

Given are the results of experimental studies of the effect of small additions of silicon on physical-mechanical properties of low-alloy carbon deposited metal in electric arc cladding using self-shielding flux-cored wire. It is shown that increase in the silicon content to 2.3 % leads to decrease in the content of the martensite phase in deposited metal, thus increasing its microcrack resistance.

Keywords: arc cladding, flux-cored wire, deposited metal, crack resistance, silicon alloying, microstructure, microhardness

Main methods for increasing crack resistance of high-carbon low alloys in welding and cladding include the use of expensive nickel-alloyed (up to 80 %) flux-cored wires, preheating, as well as some other approaches of a metallurgical and technological character. The role of comparatively small additions (up to 2–3 %) of such elements as silicon, manganese, aluminium and titanium, is most often evaluated by their participation in the processes of deoxidation of the weld pool and nitride formation, while their effect on some physical-mechanical properties of the deposited metal, e.g. crack resistance, is insufficiently studied as yet.

The purpose of this study was to experimentally investigate the effect of silicon on microstructure, crack resistance and hardness of a carbon alloy in cladding using self-shielding flux-cored wire without preheating.

Flux-cored wires 1.8 mm in diameter were manufactured to conduct investigations. The silicon content of the wires was varied in a discrete manner by varying the ferrosilicium content of the wire core. Constant chemical composition and filling coefficient of the flux-cored wires with increase in the ferrosilicium content were maintained by a corresponding decrease of the amount of an iron powder. Individual beads were deposited under the following conditions: $I_w = 170\text{--}180$ A, $U_a = 19\text{--}21$ V, $v_w = 14$ m/h, and direct current of reverse polarity. Chemical composition of the deposited samples under investigation (in the third layer) was as follows, wt. %: 2.2–2.4 C, 0.7–0.8 Mn, 0.3–0.4 Al, 0.25–0.30 Ti, and 0.58, 1.16, 1.86 and 2.33 Si.

The presence of microcracks in the deposited metal was evaluated visually or using a magnetic flaw detector. Variations in microstructure, quantity and morphology of microcracks were examined by metallographic analysis. To obtain comparable and reliable results, the microsections for metallography were made from specimens of the deposited metal cut at the same distance from the beginning of deposition of each bead, where the technological process was considered the steady-state one.

Microstructure of the deposited metal includes the austenite decomposition products (ferrite-pearlite mixture) and cementite-ledeburite eutectic of a honeycomb structure. It is similar to microstructure of low-alloy foundry hypoeutectic cast iron*.

As shown by experiments, variations in the silicon content within the ranges studied had no effect on formation and quantity of microcracks in the deposited metal. They were formed in all claddings during cooling within a temperature range of 450–250 °C, and accompanied by a substantial sound effect, which allows classifying them as cold cracks.

As proved by metallographic examinations, silicon exerts a high effect on the quantity and length of microcracks in the deposited metal. The maximal quantity of microcracks was detected in a deposited sample containing 0.58 % Si. And they are present both in the deposited metal (Figure 1) and in the fusion zone, the length of the microcracks also being maximal. Increase in the silicon content causes decrease in length of the microcracks. The maximal crack resistance is exhibited by the deposited metal alloyed with silicon in an amount of 2.33 %.



Figure 1. Microstructure of deposited metal at 0.58 % Si content ($\times 600$)

* Bunin, K.P., Malinochka, Ya.N., Taran, Yu.N. (1969) Fundamentals of metallography of cast iron. Moscow: Metallurgia, 416 pp.

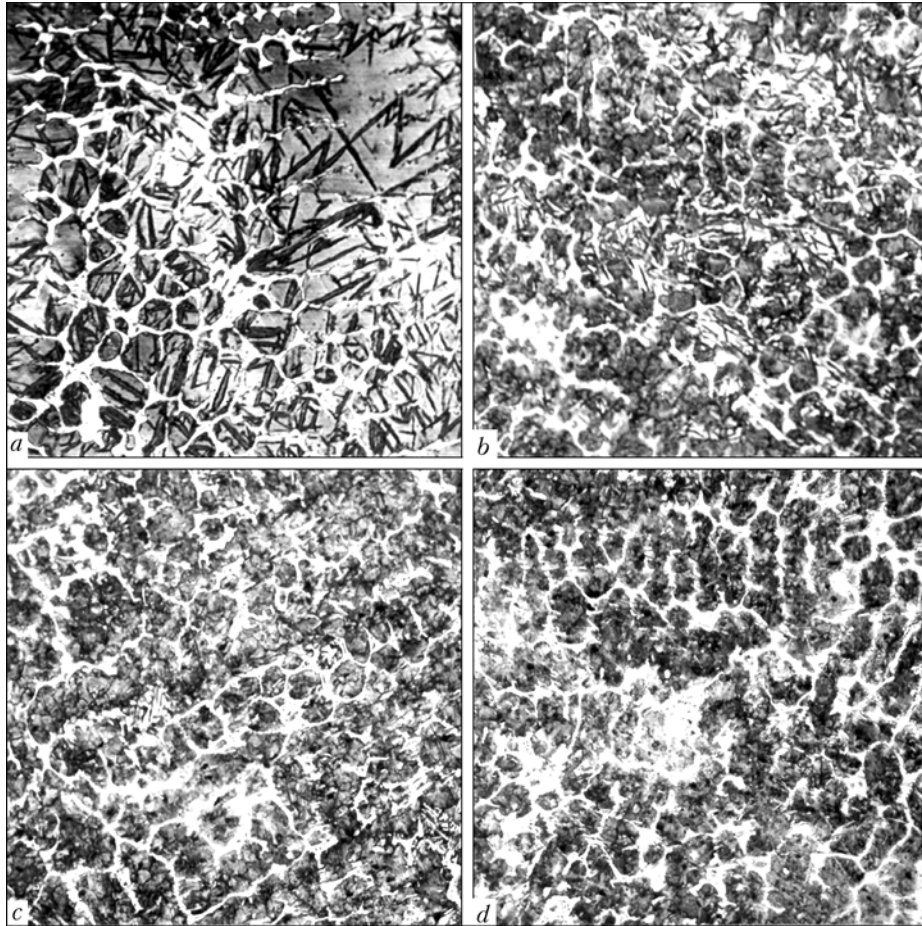


Figure 2. Microstructure of deposited metal at silicon content of 0.58 (a), 1.16 (b), 1.86 (c) and 2.33 (d) % ($\times 320$)

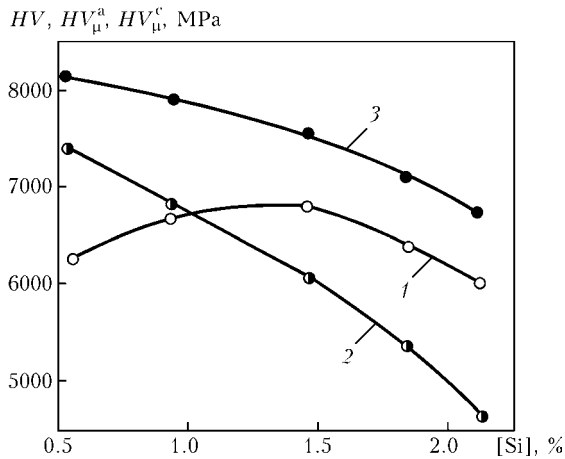


Figure 3. Effect of silicon on hardness HV of deposited metal (1), microhardness H_{μ}^a of solid solution grains (2), and microhardness H_{μ}^c of cementite-ledgeburite eutectic (3)

It is likely that the effect of comparatively small silicon concentrations on formation of microcracks is associated with a variation in quantity, morphology and hardness of martensite. The largest amount of coarse-acicular martensite was detected in claddings containing 0.58 % Si (Figure 2, a). Increase in the silicon concentration is accompanied by decrease in the quantity and length of martensite needles (Figure 2, b, c). The deposited metal with 2.33 % Si contains almost no martensite phase (Figure 2, d).

In addition to structural transformations, alloying with silicon is accompanied by variations in micro-

hardness of the austenite decomposition products, H_{μ}^a (solid solution grains), and carbide eutectic, H_{μ}^c (Figure 3).

Variations in microhardness of structural components of the deposited metal are caused by the fact that increase in the silicon content leads to decrease in the content of pearlitic cementite, and in claddings containing 1.86 and 2.33 % Si the fine (not more than 1 μm in diameter) inclusions of structurally free carbon are detected in the pearlite grains. It leads to decrease in the H_{μ}^a value. The attempts to find the cause of variations in H_{μ}^c by metallography failed. However, it might be in variations of stoichiometric composition of carbide components of the deposited metal with variations in the silicon content.

The presence of maximum at the curve of hardness HV is caused by variations in the amount and hardness of the martensite phase in the deposited metal with a different silicon concentration. Microhardness of martensite in cladding with a minimum silicon content (0.58 %) is relatively low and equals 5000–5200 MPa. Increase in the silicon concentration (claddings with 1.16 and 1.86 % Si) leads to decrease in the amount of martensite, but its microhardness grows to 7000–7400 MPa. In this case, hardness of the deposited metal reaches its maximal value. Further increase in the silicon content causes decrease both in the amount and microhardness (up to 6200–6400 MPa) of martensite, which leads to decrease in the value of hardness of the deposited metal.



«KNOW-HOW» AND HOW TO USE IT

V.S. SIDORUK

E.O. Paton Electric Welding Institute, NASU, Kiev, Ukraine

In the transition economy the «know-how» effectively protects the economic interests of the intellectual product developer. The number of published works and granted patents cannot be taken as the decisive index of the effectiveness of activity of an applied profile research institute. Such indices as the quantity and price of the sold developments and services are important for a successful functioning of an institute. Fulfillment of fundamental research works is important for the long-term perspective. In this case strategic planning is necessary.

Keywords: intellectual activity, know-how, copyright and right of property, features of realization, competitive ability

The term «know-how» is rather often used in publications and discussions, dedicated to industrial-economic (commercial) activity. However, its content still does not have a comprehensive definition. To be precise, it is continuously broadened in connection with scientific-technical progress [1]. For the first time this term was used in the USA in 1916 in Diurand against Brown case. In terms of patent science, know-how is «the object of intellectual property right», although it differs from such «authorized» objects, as a patent and a certificate, in that by its nature it can not have any protecting document.

Know-how is the product of intellectual activity of a human being; information which its owner (seller) keeps confidential with the aim to obtain economic benefit when transferring it to the buyer. As patent attorney V. Kutsevich said: «It can be stated that the manufacturer-seller in the free market can have only one economic aim --- to sell the article manufactured by him at a profit. All the rest is just talk that leads to wasting one's own and others' irretrievable time and often money, materials and energy» [2]. Let us note that he meant exclusively manufacturer-seller and only in the free market. This statement cannot be directly applied to such a specific organization as a scientific research institute. The latter cannot be unambiguously classified as an economic subject, whose only aim is to get profit. The essence of existence of scientific research institute as an organization is solving two dissimilar tasks, the main of which is cognition of the surrounding world, and laws of nature, and the additional one is commercialization of the gained knowledge. However, research institutes have also other socially significant tasks. They promote raising intellectual level of the nation and, therefore, its competitive ability, prevent emigration of intellectual elite to developed countries, offering jobs for its scientists in the home country. The countries with developed scientific sphere are able to develop high-technology, and consequently, highly profitable branches of the national economy. In such countries the level of unemployment is lower.

Knowledge of the laws of nature is not a commodity theoretically, that is why none of the patent offices in the world grants patents for discoveries that assign the monopoly right of property (the right to dispose at one's own discretion) on the subject of discovery. Now, different versions of discoveries application in practical activity with obtaining of the corresponding profit, these already are technical solutions, that can be protected by patents and other protective documents. It should be mentioned that Western civilization («selfish golden milliard») with its sacred right of private property, including the object of intellectual property, does not very consistently follow this fundamental principle --- universality and generality of the right of property to knowledge. Specific «branch» knowledge, obtained in research units of corporations (as well as at universities) becomes the subject of monopoly property, and is realized in their own economic cycle, or sold in the free market as a commodity, and often both are done. Speaking about Ukraine and other republics of the former Soviet Union, until recently, our scientific-technical journals disclosed up to 80 % of know-how in publications (in keeping with the socialist philosophy) [1], and the results of research work of the institutes of the NAS of Ukraine are still exhibited at UkrINTEI with a free access.

Science as a tool for cognition of the surrounding world is unprofitable work, that is why it gets financial support in all the developed countries. Scientific achievements are the intellectual source that provides creative energy for progress of technology.

A customer will buy know-how, if it raises the business efficiency. Know-how is transferred to the buyer under confidentially terms, or is not transferred to anybody at all and is preserved for owner's usage.

Can a research institute have know-how «in-house use»? It is known that by its nature a research institute is «a provider of knowledge», and at the same time generator of new ideas, producer of non-material assets, including know-how. It is not convenient to keep it «in-house use». At the same time, such institutes as the E.O. Paton Electric Welding Institute, which created its own production base --- infrastructure (EDTB, engineering centers, pilot plants etc.) has the possibility to keep some know-how secret, receiving



a lot of benefit from it. This includes the compositions of different types of welding consumables: electrodes, flux-cored wire, etc. Manufacturing them only in-house --- at the Pilot Plant of Welding Consumables, without revealing the composition in the patent (indicating the content of components in a wide range) means securing oneself from unfair competitors and increasing profit by scaling up the production. There are variants, when a small amount of a welding consumable is required for realization of the technology in production --- literally grams per a running meter of the weld (as for example, in nonconsumable electrode arc welding with application of activating fluxes). The research department of the Institute can not disclose the flux composition to anybody, and sell it to the customer together with technology, and manufacture it in its own laboratory or Institute workshops (pilot production).

There is no hurry in sharing one's discoveries with the world also in the field of unique technologies, use of which on the scale of the country is equal to units per year, and realization of which is practically impossible without involvement of employees of the Institute (technology developers). Electroslag welding (ESW) of thick metal can be taken as an example. The E.O. Paton Electric Welding Institute developed the technology of ESW with a consumable nozzle that is effective when used in hard-to-reach places, in particular in site. A consumable nozzle is a plate of metal similar to the welded one, which has a channel inside for feeding electrode wire, and a flux coating outside. Its advantage is that there is no need to use the mechanism for welding head vertical motion. A publication about this method (with a detailed description of all the details, down to the size of the nozzle and wire and flux grades) inspired one American engineer to develop a new variety of the well-known method, who then received a patent for his development not only in the USA, but also in other countries. His development incorporates three innovations:

- manufacturing a plate consumable nozzle from two extruded plates with semi-cylinder spouts on each of the surfaces that together make up a channel;
- using the mechanism for remote wire feed, moving a wire spool from the head of the welding machine to an area removed to a considerable distance (more than 10 m) from the welding site, for which purpose the mechanism for wire feeding is reinforced by additional pushing mechanisms of «push-pull» type;
- process automation, with its simultaneous protocolling in the computer (recording condition parameters in real time).

Now he suggests that the Institute buys the patent from him, or becomes a partner (agent) for application of his invention in the territory of Europe and Asia. There is no doubt, that if the Institute kept this technology secret as know-how and published an article of advertising nature in the journal, without telling the details (as the majority of Western companies do), the American would have to ask the Institute for a

license for using its know-how and sign a prior agreement on non-disclosure of confidential information.

One more example can be given. The Institute designed the technology and equipment for arc welding of butt welds in pipelines in site (butt joining of pipe line sections). Self-shielded flux-cored wire was used, and the weld was formed by movable water-cooled slides. In 1970--1980s many erection organizations in different districts of the Soviet Union became interested in this method. From the first point of view, this process looks very simple: flux-cored wire is fed into the gap between edges, transverse oscillation of the current supplying nozzle from one edge to another is performed, metal pool is formed under the influence of the arc that fills the gap between the edges, and slag pool forms on top. Water cooling slides are pressed to the edges and moved upwards together with the welding head as the gap is filled with filler metal, i.e. with the speed of welding. However, under the real conditions we come across many circumstances that are difficult to foresee in advance: deflection in the abutted pipe diameter, their ellipticity, inaccuracy in edge preparation, unexpected gaps that appear between the slide and welded pipe surfaces through which metal pool can flow out, etc. It is impossible to foresee all the fine points in any technological instructions. That is why welding operations in the above-mentioned organizations were performed with participation and under author's supervision (with scientific-technical support) by the Institute staff. Representative of the E.O. Paton Electric Welding Institute, Mr. A.N. Kutovoj, staff member of Department 10 participated in the work on construction of a drinking water pipeline from Desna to Kiev after Chernobyl NPP accident. The above-mentioned welding method is quite specific, and its mastering without direct transfer («by word of mouth») of the experience, knowledge (know-how) of the developer is not easy work.

What is know-how? International association for protection of industrial property in its resolution 1974 (1) 47 (053B) formulated the definition of know-how as knowledge and experience of technical, commercial, administrative, financial and other origin, that can be used in practice at the time of exploitation in industry or in craftsmanship.

European Union Commission passed special directive document --- Regulation No. 556/89 dated November 30, 1988, about application of Article 85 (3) of Rome Agreement to some categories of license agreements on know-how. In this document know-how is determined as *the total of technical information that is secret, essential and identifiable in any form.*

Experts of the International Chamber of Commerce define know-how as *the body of information, professional knowledge and experience used in production technology of any product.*

Article 10 of the European Council Resolution 1996/240/EC on technology transfer defines know-



how as the main part of technical information that is secret, essential and identifiable in any form [1].

In the Law of Ukraine «On Investment Activity», in Article 1 know-how is characterized as *one of the forms of investment*.

«Technological secrets» that are not disclosed by analysis of goods that are introduced into the market, are typical examples of know-how. Such secrets usually cover the criteria of choosing raw materials, components, charge, technical process conditions, algorithms and control programs of technological processes; knowledge bases, databases, logic and/or mathematic algorithms and programs for computing machines based on them; selection of process equipment and optimum methods for its application in industry. Personal experience and personnel skills are classified as a special kind of know-how, the carriers of which are physical persons. Under the conditions of a developed labor market physical persons --- carriers of know-how are in «use» by the employer along with their inalienable know-how [3]. The following can be the object of know-how:

- any claimed objects of intellectual property that are under the expertise per se --- up to the moment of official publication;

- any patentable solution that it is advantageous not to publish for reasons of preserving high competitive ability of the enterprise (company), but to keep to oneself as secret information for in-house use;

- any patentable decision that is difficult to protect from unauthorized use by unscrupulous persons because of impossibility of legal disclosure of the fact of unauthorized use. The following can be regarded as such solutions: methods of diagnostics, maintenance and repair; methods of measuring physical, chemical and other values without any connection with material (particularly, instrumental) means for measurement; methods for energy conversion not connected with instrumental means for their realization;

- «old, long-forgotten» inventions (preferably, one's own) stored in the archives in the form of authors' certificates, many of which were not even needed for the past period;

- any development that does not «make» a patent in accordance with the legislation of Ukraine, but has commercial appeal. The following can be regarded as such: algorithms and programs for computer (before registration in Ukraine and abroad); layout geometry of integral chips (before registration in Ukraine and abroad); methods of organization and planning of production and/or sale of goods; accounting methods, etc. [3].

Information contained in text and/or graphic technical documentation at any stage of its development and especially as complete working technical documentation also belongs to know-how, for example, in working drawings, formulas (compositions) of manufactured materials; in industrial technological processes (schedules), technological charts, instructions and etc.; in feasibility studies of development

or updating of new processes, materials or devices; in R&D reports prepared for a concrete customer (state authority --- higher echelon, any ministry, department are also concrete customers); in any competition projects, if they contain information about unpatented inventions, useful models, industrial models or other commercially valuable technological solutions; and in any other technological (in the broad sense of the word) information, containing commercially valuable solutions [3].

In welding technology all welding algorithms should be regarded as know-how, especially those that refer to complicated and critical constructions, all the compositions of welding consumables (if they are manufactured at the company's pilot plant), all the designed algorithms of welding devices control, methods of diagnostics and quality control and so on. They should not be disclosed in publications, either.

A typical example of know-how commercialization are agreements for scientific-technical support of construction works and repair of bridges, bridge passes, blast furnaces, gas pipelines and so on. The concentrated vast experience of Institute employees accumulated for decades is realized here. For example, welding of the beams of a bridge load-carrying structure involves so many fine points of such a kind, that overlooking or incorrect following of even one of them may lead to considerable loss of the materials, labor, time, funds. What is the correct way to abut the parts, while preserving the straightness (or preset curvilinear shape) of the construction, while following the specified parameters of the gap between edges. How to fix by welding («to tack-weld») the edges correctly. How to weld correctly, considering that under the real conditions the gap between the edges varies and does not «follow» the design. The size and shape of the run-off tabs, grade and the diameter of welding electrode, its condition (surface quality, its humidity, availability of scale on the rod surface and different contaminations), type and value of welding current, angle of electrode inclination, arc length, weather conditions and many other factors --- all this knowledge and skills are gained over the years, and it is practically impossible to take them into the account in the technological instructions. The above-said also indicates that availability of «old employees» (at the institute or enterprise) is one of the main points for preservation and accumulation of intellectual capital of the staff, just as its replenishment by young employees is a compulsory condition for viability of the organization, and respect for veterans is a pledge of success.

Such an example should also be mentioned. A problem developed at one of Egyptian machine-building plants. A device for obtaining sugar from sugar-cane was manufactured by German company drawings. The device consists of a cylinder vessel of about 2 m diameter and about 10 m length with «filling» from metal strips, welded to inner side of the cylinder wall. The device was sent to the customer to the sugar plant, but it was not accepted there --- German supervisor,



who performed author's supervision, rejected the item because of high deformations in the longitudinal and transverse directions. The plant turned for assistance to the E.O. Paton Electric Welding Institute employees, who worked there as technical advisers. The next item was manufactured already with their participation. The customer representative, who was invited for acceptance, accepted the item, and gave it the «European quality» mark. The problem consisted in the need to strictly follow a certain algorithm of welding operations. In this case, previous experience and accumulated knowledge (know-how) of the E.O. Paton Electric Welding Institute employees proved useful: one of them is a former chief welder of metal fabrication works, the second is a specialist in welding stresses and strains.

Information about properties of the processes, materials and goods hazardous for people and environment, about safety measures, rules of use is not know-how [3]. «Trade secrets» that concern cost price of any goods and credit capacity of enterprises, concrete trade agreements, advertisement content before it is made public, and so on [3] do not belong to know-how.

Know-how is the widest as to its content and nature of information object of intellectual property law in comparison with patents, useful models, industrial specimens taken all together.

Another advantage of know-how is more concrete content suitable for direct application. Its use is easier to supervise and control, because transfer from the seller to the buyer takes place as a confidential procedure. An important function of know-how is indirect secret patent protection from possible unauthorized use. The claims should be formulated so that part of the information vitally important for realization of the patented invention remains with the applicant as his know-how. The latter can be disclosed only to the real buyer of the patent license after reaching a concrete agreement [2].

The main disadvantage of know-how is the imperfection and lack of practice of legal defense from its unauthorized use in the case, for example, of disclosure of the content by the buyer (as a rule, because of indiscretion of the employees of the latter). This is connected with the absence in Ukraine of the law on protection of know-how, because the content of the latter is prohibited to be disclosed.

The procedure of know-how transfer demands high qualifications of the seller. It is important not to disclose its content up to the moment of signing the agreement on transfer.

Where does know-how begin? The sources of know-how origin can be very different: individual and collective experience and knowledge accumulated by the staff; the result of performing ordered research work on assignment of a higher-ranking organization or individual departments, enterprises, companies; «side» result from performing the ordered research work; the result of discretionary research work, performed by the enterprise employees.

The search can be purely intellectual (for example, to study the body of patents from the countries of the world) which may result in one's own ideas appearing «through association» (for example, young A. Einstein experiment in Austria patent department), statistical processing of information of industrial, technical and other nature accumulated at the enterprise, in particular the results of mechanical and other type of testing and so on.

The search can have the form of special experimental work performed by a pre-compiled program.

Copyright and rights of property to know-how. Copyright to know-how is similar to copyright for other objects of intellectual property: inventions, useful models, industrial samples, products of scientific and artistic creative work, integral chips and registered software.

Copyright proprietor can be not only physical persons (single authors or groups of co-authors) whose creative labor produced the know-how.

Co-authorship can be common and separate [3]. In the first case, all the co-authors are regarded to be the owners of intellectual property rights to an equal degree. The second case corresponds to complicated know-how objects: invention with multilink formula, R&D report that includes a few independent sections, draft designs of devices, complexes, etc. that consist of different parts in which each functionally and/or structurally separate part is developed by a certain author or group of co-authors. The fact of co-authorship should be registered in a separate document signed by all the co-authors.

The fact of creation of know-how proper, its substantial part (object) is reflected in the form of information, placed on any of material carrier, suitable for long-time storage and allowing to read all the information. Know-how author's (co-authors') name, family name are also indicated in the accompanying document.

The know-how title is also similar to the rights to other objects of intellectual property rights. They include the right of possession, right of use and right of disposal. If all the components of the right of property to know-how belong to one person (or a group of persons, acting as a collective owner), such rights are usually regarded as exclusive rights of property.

Alongside the above-mentioned information, the full-scale samples of developed goods (which is regarded to be undesirable), material products, manufactured in accordance with concrete know-how [3] can also be the objects of property rights for know-how.

The subjects of the rights of property to know how can be:

- developers (authors, co-authors) in all the cases of know-how development and use;
- physical and/or legal persons --- only in the cases and only to a part of the rights of property (taking into account the part that belongs to the author/co-authors), when they spent money on crea-



tion (development) of know-how and/or taking the know-how to practical application stage. Physical/legal persons can buy the rights of property for know-how on the base of license agreements. They are called conscientious users of rights of property to know-how. This also includes those who independently and single-handedly developed similar know-how.

Persons, who have the right to a part of rights of property for know-how on the basis of expenses incurred in its development, can be:

- citizens of Ukraine or other states, whose *sponsor* (!) participation in the know-how creation is confirmed by corresponding agreements with developers and report documents on the expenses incurred (banking payment documents, documents on supply of materials, power, other material resources and so on) irrespective of whether they have the status of individual legal person;

- legal persons of Ukraine, including joint ventures with foreigners, the state of Ukraine in the person of representatives authorized on the basis of corresponding agreements with know-how developers;

- foreign legal persons who act in the territory of Ukraine in accordance with the legislation of Ukraine on the basis of agreements with know-how developers [3].

The authors (co-authors) may have exclusive rights of property to know-how only in two cases: if they have developed know-how only with their own funds and did not transfer their rights to anybody by agreement neither as a whole, nor even in its part, or, when a person (group of persons) who financed the development of the know-how, of their own will and in writing gave up their part of right of property to know-how in favour of the author (co-authors).

A sufficient reason for accrual of the right of property for know-how is existence of primary objects of these rights in the form of original information carriers that contain information about the essence of know-how and their keeping under the «official secret» conditions.

How to «record» (identify) the subject of know-how? Documented information that forms the subject of know-how, its essence should be kept at the enterprise as a classified document, registered in the proper way. In the case of contingent court examination as to the priority for concrete know-how, it is useful to have the stamp of postal department from the very beginning. The author (authors) mail to themselves the material carrier with the record of the necessary information by registered mail (letter, postal packet, parcel) and keep it, without opening, for indefinitely long time --- till moment «X», when the argument in the court will be required [2]. Post office registers the mail in a proper way, with a clearly distinguishable date of sending on the stamp (in the receipt).

How to sell know-how. One should always bear in mind the law of the market: «the buyer is always right», as well as «the goods are for the buyer and not vice versa». Know-how is commercialized in the

best way [3], if its development has reached the level that is enough for practical use:

- if the enterprise has the necessary space, equipment and personnel for applying the know-how;
- if know-how realization brings considerable profit to the buyer in the short-term.

The buyer is interested in know-how that requires «short» money, i.e. the possibility to do without banking credit with minimum short-term credit. Yet expensive know-how that can guarantee high profit, is also attractive.

The following variants of searching for the buyer (customer) are possible, when [3]:

- the buyer for the ready product is looked for;
- the product is designed by customer inquiry;
- new know-how is developed using internal resources (a brilliant idea has suddenly come!), and a search for a buyer or an investor is performed at the same time.

When contacting a buyer (customer, investor) it is necessary to know his solvency, (wishes do not often correspond to capability), as well as his ability to keep his promises, honesty, and ability to keep know-how in a commercial secret.

When contacting a foreign buyer (customer) it is necessary to take into account the customs of the country of residence and mentality of the people.

In conclusion it should be noted that under our conditions, when economic and legal mechanisms for regulation of market relations are not yet developed or do not work in full measure, know-how is the most effective object of intellectual property right for the developer, owner of know-how, as it gives him an opportunity to follow (and to promote!) «from a short distance» the progress of his development with the highest economic return in the market.

The number of scientific works published by an institute and received patents can not be used as a determinative index from the point of view of competitiveness of a research institute in the market. Furthermore, disclosure of industrial secrets in the papers and patents, which it is not simple to protect legally, results in that the mentioned papers and patents reduce an institute competitiveness, sometimes catastrophically. From this viewpoint, the statements that sometimes appear in press, that the main indication of effectiveness of researchers' work is the index of reference to their works in the world special literature relative to applied science where the largest amount of practical knowledge is generated, which is considered as know-how, can have a provocative nature: «let you, guys, publish more, and we shall carefully study, assimilate and master it!». A more substantial index of an institute competitiveness can be the number of made agreements on development and transfer of scientific products and income from its sale.

Sometimes it is more profitable to keep a patentable technical solution as know-how and to realize it in the market by a proper procedure. Taking a patent on invention is economically profitable only when its



unscrupulous use by an outside organization (enterprise) can be easily revealed by legal means (using such inventions is difficult to conceal), taking into account that commercialization of such an invention will bring certain profit. There is a category of inventions that do not promise obvious material profit, though they promote strengthening of priority and enhance the institute's prestige.

Orientation to the current demand of the market is an utilitarian approach to business that yields an immediate economic effect. However, one should not lose sight of the future trends, which requires strategic planning and active scientific research. Breakthroughs in technology, especially in high technologies, cannot be expected without fundamentally conducted scientific work, including applied sciences.

Reaching the front line in the world market is impossible without strategic planning of the development of science and government support. Economic prosperity of a research institute depends to a great extent on the level of economic development of the state. On the other hand, research institutes proper are an effective tool of economic development of the national economy, that is why the state should be interested in widening and expansion of scientific research and, consequently, in development and strengthening of research institutions.

1. Androshchuk, G. (2004) Legal regulation of know-how. *Intelektualna Vlasnist*, **10**, 29–35.
2. Kutsevich, V. (2004) Inventive act and patenting for market. *Ibid.*, **10**, 45–49.
3. Kutsevich, V. (2005) About know-how. *Ibid.*, **4**, 32–38.

TECHNOLOGY FOR REPAIR OF WAGON AXLES AND OTHER COMPONENTS BY THE PLASMA ARC METALLISING METHOD

The E.O. Paton Electric Welding Institute developed the technology for repair of wagon axles, cast iron shafts, drums and other components by the method of plasma arc metallising of the shot blasted surface using high-carbon wire.

Normal practice of repair of the above components is to employ electric metallising, fuse-spray using self-fluxing materials, and cladding with special flux-cored wires and electrodes. In the case of the fuse-spray method the surface is subjected to high heating to a melting point of consumables, which results in formation of defects of the type of cracks, pores, cavities, chilling of cast iron, etc. In addition, electric metallising fails to provide coatings of a sufficient quality.

To address these problems, the E.O. Paton Electric Welding Institute developed the repair technology by the plasma arc metallising, which comprises melting and spraying of 1–2 mm wire with a high carbon content by the plasma jet in argon atmosphere. The wire sprayed serves as one of the electrodes. With a plasmatron power of up to 24 kW no water cooling is required. Productivity of the unit is 5–7 kg/h of the material sprayed on the prepared surface.

Surface preparation includes degreasing and preliminary shot blasting, which is performed using standard units of the AD-150 type with cut cast iron shots, or using other units of the injection type.

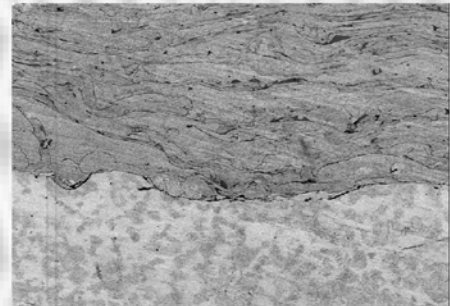
Workpieces in spraying are heated to no more than 200 °C, which excludes any effect of heating on their structures. Adhesion of more than 6 kg/mm of a spraying material to the surface results in a coating up to 20 mm thick with a porosity of not more than 2–5 % and hardness of up to *HRC* 40.

The deposited coatings are subjected to rough machining using lathes and then final grinding using abrasive wheels of the 14A25SM type.

The involved equipment is simple in design and maintenance. The floor area necessary to locate the basic equipment is 150 m².

Application. Repair and reconditioning of parts of railway transport, metallurgical and electrical facilities.

Contacts: Prof. Zhadkevich M.L.
E-mail: office@paton.kiev.ua



Microstructure of coating produced by 65G wire spraying